ฟอร์มแฟกเตอร์แม่เหล็กไฟฟ้าของแบริออนออกเตต
ในแบบจำลองควาร์กเชิงไครัลเพอร์เทอร์เบชัน

นายสัมภาส ฉีดเกตุ

ELECTROMAGNETIC FORM FACTORS OF THE BARYON OCTET IN THE PERTURBATIVE CHIRAL QUARK MODEL

Mr. Sampart Cheedket

ELECTROMAGNETIC FORM FACTORS OF THE BARYON OCTET IN THE PERTURBATIVE CHIRAL QUARK MODEL

Suranaree University of Technology has approved this thesis submitted in partial fulfillment of the requirements for the Degree of Doctor of Philosophy

Thesis Examining Committee

....

(Asst. Prof. Dr. Prasart Suebka)

Chairperson

....

(Assoc. Prof. Dr. Yupeng Yan)

Member (Thesis Advisor)
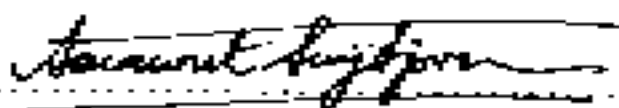
....

(Prof. Dr. Thomas Gutsche)

Member

....

(Assoc. Prof. Dr. Prasart Suebka)

Member

....

(Dr. Wiwat Pchan)

Member

....

(Assoc. Prof. Dr. Saowut Suijluan)   (Assoc. Prof. Dr. Prasart Suebka)

Vice Rector for Academic Affairs   Dean of the Institute of Science

ธันวาฬ ฉันทฤกฤ: ฟอร์มแฟกเตอร์แม่เหล็กไฟฟ้าของแบริออนออกเตตในแบบจำลองควาร์ก
คิงใหวัลเพอร์เกอร์เบชัน (ELECTROMAGNETIC FORM FACTORS OF THE
BARYON OCTET IN THE PERTURBATIVE CHIRAL QUARK MODEL)
อาจารย์ที่ปรึกษา: ASSOC. PROF. DR. YUPENG YAN, 96 หน้า.
ISBN: 974-533-293-3

แบบจำลองควาร์กคิงใหวัลเพอร์เกอร์เกอร์เบชันได้ถูกนำมาประยุกต์เพื่อวิเคราะห์ฟอร์มแฟก
เตอร์แม่เหล็กไฟฟ้าของแบริออนออกเตต สมการเชิงวิเคราะห์สำหรับฟอร์มแฟกเตอร์ของแบริออน
ซึ่งอยู่ในเทอมของพารามิเตอร์พื้นฐานในฟิสิกส์ของคายออน-นิวคลีออนหลังงานต่ำ (ค่าคงตัวการ
สลายตัวแบบอ่อนของพายออน, ค่าคู่ควบแอกเซียลของนิวคลีออน, ฟอร์มแฟกเตอร์แรงอย่างแรง
ของนิวคลีออน) และหลักษณ์ชี้ตัวของโมเมนต์แม่เหล็ก, รัศมีเชิงประจุและเชิงแม่เหล็กของแบ
ริออนได้ถูกนำเสนอ ผลลัพธ์สอดคล้องกับข้อมูลจากการทดลองเป็นอย่างดี

ภาควิชาฟิสิกส์   ลายมือชื่อนักศึกษา..

ปีการศึกษา 2546   ลายมือชื่ออาจารย์ที่ปรึกษา...............................

                                      ลายมือชื่ออาจารย์ที่ปรึกษาร่วม...... A. Faessler

                                      ลายมือชื่ออาจารย์ที่ปรึกษาร่วม.........................

SAMPART CHEEDKET: ELECTROMAGNETIC FORM FAC-
TORS OF THE BARYON OCTET IN THE PERTURBATIVE
CHIRAL QUARK MODEL

THESIS ADVISOR: ASSOC. PROF. YUPENG YAN, Ph.D.
96 PP. ISBN 974-533-293-3

The perturbative chiral quark model is applied to analyze the electromagnetic form factors of the baryon octet. The analytic expressions for baryon form factors, which are given in terms of fundamental parameters of low-energy pion-nucleon physics (weak pion decay constant, axial nucleon coupling, strong pion nucleon form factor), and the numerical results of the magnetic moment, charge and magnetic radii for the baryon octet, are presented. The results are in good agreement with experimental data.

School of Physics

Academic Year 2003

Student's Signature _S. Cheedket_

Advisor's Signature _____

Co-advisor's Signature _____

Co-advisor's Signature _____

Acknowledgements

I am grateful to Assoc. Prof. Dr. Yupeng Yan for being my thesis advisor and for his guidance throughout this work. He set up the research project cooperating with Prof. Faessler's group in Germany that gave me a very good research experience and was the starting point of this work.

I would like to thank Prof. Dr. Amand Faessler, Prof. Dr. Thomas Gutsche and Dr. Valery E. Lyubovitskij for their guidance, consistently helpful advice throughout this work and their kind hospitality during my research start at the Institute for Theoretical Physics, University of Tübingen, Germany for more than two years.

I wish to thank Kem Pumsa-ard and Khanchai Khosonthongkee for their cooperation and discussion to this work. Thanks to Dr. Jessada Tanthanuch for his consistent help, especially in building up the SUT-thesis format in Latex. Special thanks to my officemates Larisa F. Pacearescu and Nopmanee Supanam for their support and good friendship.

Finally, I would especially like to thank my parents, Boontong and Somboon Cheedket for their understanding, support and encouragement over the years of my study.

Sampart Cheedket

Contents

Contents (continued)

Contents (continued)

List of Figures

List of Tables

Chapter I

Introduction

The consistent description of the structure and interactions of hadrons is one of the major research areas in nuclear and particle physics. One of the main research directions is the search for the manifestation of elementary quarks and gluons in strong interaction processes. There is no doubt that Quantum Chromodynamics (QCD) is the fundamental theory of strong interactions, which at least in the perturbative domain, that is for large momentum transfers Q^2, is confirmed in a rather impressive manner. However, in the so-called confinement regime at low momentum transfers Q^2 the properties of QCD are only understood partially in a somewhat qualitative manner. Now perturbative physics dominates and hence traditional approaches in solving QCD cannot be applied. Based on the lack of exact solutions of QCD in the non-perturbative region the main ansatz consists of the development of effective models. The main recipe in constructing these models consists of reducing the elementary degrees of freedom of QCD and introducing effective interactions, characteristic of the fundamental theory.

Our understanding of the structure of hadrons is based to a large extent on the theoretical concept of the constituent quark model. Thereby, quarks and antiquarks form the relevant degrees of freedom, where for example baryons are made up of three of these constituent quarks put together by confinement. In a next step it was realized that chiral symmetry, considered to be one of the best symmetries of the strong interaction, is violated by the quark confinement mechanism.

The problem of chiral symmetry breaking is resolved by introduction of Goldstone boson fields in consistency with chiral symmetry. The Goldstone bosons, like the pion, reflect the presence of the sea quarks, which in addition to the valence quarks, should be present. Modern theories which attempt to describe the structure of baryon should contain both feathers of low-energy QCD, such as confinement and chiral symmetry.

The study of the electromagnetic form factors of baryons is a very important first step in understanding their internal structure. At present, electromagnetic form factors and related properties (magnetic moments, charge and magnetic radii) of the nucleon have been measured precisely, but for the hyperons data rarely exist with the exception of the magnetic moments. Recently, the charge radius of the Σ^- has been measured (Eschrich et al., 2001; Adamovich et al., 1999) and therefore gives a first estimate of the charge form factor of the hyperon at low momentum transfers.

The theoretical description of electromagnetic form factors was performed in detail within approaches of low-energy hadron physics: QCD Sum Rules, Chiral Perturbation Theory, relativistic and non-relativistic quark models, QCD-motivated approaches based on solution of the Schwinger-Dyson/Bethe-Salpeter and Faddeev equations, soliton-type models, etc. Since the early eighties chiral quark models (Théberge, Thomas, and Miller, 1980, 1981; Théberge and Thomas 1983; Thomas, 1984; Oset, Tegen, and Weise, 1984; Tegen, 1990; Chin, 1982; Diakonov, Petrov, and others, 1984, 1986, 1988, 1989; Gutsche, 1987; Gutsche and Robson, 1989), describing the nucleon as a bound system of valence quarks with a surrounding pion cloud, play an important role in the description of low-energy nucleon physics. These models include the two main features of low-energy hadron structure, confinement and chiral symmetry.

With respect to the treatment of the pion cloud, theses approaches fall essentially into two categories. The first type of chiral quark models assumes that the valence quark content dominates the nucleon, thereby treating pion contributions perturbatively (Théberge, Thomas, and Miller, 1980, 1981; Théberge and Thomas 1983; Thomas, 1984; Oset, Tegen, and Weise, 1984; Tegen, 1990; Chin, 1982; Gutsche, 1987; Gutsche and Robson, 1989). Originally, this idea was formulated in the context of the cloudy bag model (Théberge, Thomas, and Miller, 1980, 1981; Théberge and Thomas 1983; Thomas, 1984). By imposing chiral symmetry the MIT bag model (Chodos et al., 1974) was extended to include the interaction of the confined quarks with the pion fields on the bag surface. With the pion cloud treated as a perturbation on the basic features of the MIT bag, pionic effects generally improve the description of nucleon observables. Later, similar perturbative chiral models (Oset, Tegen, and Weise, 1984; Tegen, 1990; Chin, 1982; Gutsche, 1987; Gutsche and Robson, 1989) were developed where the rather unphysical sharp bag boundary is replaced by a finite surface thickness of the quark core. By introducing a static quark potential of general form, these quark models contain a set of free parameters characterizing the confinement (coupling strength) and/or the quark masses. The perturbative technique allows a fully quantized treatment of the pion field up to a given order in accuracy. Although formulated on the quark level, where confinement is put in phenomenologically, perturbative chiral quark models are formally close to chiral perturbation theory which is applied on the hadron level.

Alternatively, when the pion cloud is assumed to dominate the nucleon structure this effect has to be treated non-perturbatively. The non-perturbative approaches are based for example on these Diakonov, Petrov, and others (1984, 1986, 1988, 1989), where the chiral quark soliton model was derived. This model

is based on the concept that the QCD instanton vacuum is responsible for the spontaneous breaking of chiral symmetry, which in turn leads to an effective chiral Lagrangian at low energy as derived from QCD. The classical pion field (the soliton) is described by a trial profile function, which is fixed by minimizing the energy of the nucleon. Further quantization of slow rotations of this soliton field leads to a nucleon state, which is built up from rotational excitations of the classical nucleon. On the phenomenological level the chiral quark soliton model tends to have advantages in the description of the nucleon spin structure, that is for large momentum transfers, but has some problems when compared to the original perturbative chiral quark models in the description of low-energy nucleon properties.

As a further development of chiral quark models with a perturbative treatment of the pion cloud (Théberge, Thomas, and Miller, 1980, 1981; Théberge and Thomas 1983; Thomas, 1984; Oset, Tegen, and Weise, 1984; Tegen, 1990; Chin, 1982; Gutsche, 1987; Gutsche and Robson, 1989), we extended the relativistic quark model suggested by Gutsche (1987) and Gutsche and Robson (1989) for the study of the low-energy properties of the nucleon (Lyubovitskij, Gutsche, Faessler and Drukarev, 2001). Compared to the previous similar models of these Théberge, Thomas and Miller (1980, 1981), Théberge and Thomas (1983), Thomas (1984), Oset, Tegen, and Weise (1984) and Tegen (1990) our current approach contains several new features: i) generalization of the phenomenological confining potential; ii) SU(3) extension of chiral symmetry to include the kaon and eta-meson cloud contributions; iii) consistent formulation of perturbation theory both on the quark and baryon level by use of renormalization techniques and by allowing to account for excited quark states in the meson loop diagrams; iv)fulfillment of the constraints imposed by chiral symmetry (low-energy theorems), including the current quark mass expansion of the matrix elements (for details see Lyubovitskij,

Gutsche, Faessler and Drukarev (2001)); v) possible consistency with chiral perturbation theory. In the following we refer to our model as the Perturbative Chiral Quark Model (PCQM).

The PCQM is based on an effective chiral Lagrangian describing quarks as relativistic fermions moving in a self-consistent field (static potential). The latter is described by a scalar potential S providing confinement of quarks and the time component of a vector potential $\gamma^0 V$ responsible for short-range fluctuations of the gluon field configurations (Lüscher, 1981) (see also recent lattice calculations (Takahashi et al., 2001)). The model potential defines unperturbed wave functions of quarks which are subsequently used in the calculation of baryon properties. Baryons in the the PCQM are described as bound states of valence quarks surrounded by a cloud of Goldstone bosons (π, K, η) as required by chiral symmetry. Interaction of quarks with Goldstone bosons is introduced on the basis of the nonlinear σ-model (Gell-Mann and Lévy, 1960). When considering mesons fields as small fluctuations we restrict ourselves to the linear form of the meson-quark interaction. With the derived interaction Lagrangian we do our perturbation theory in the expansion parameter $1/F$ (where F is the pion leptonic decay constant in the chiral limit). We also treat the mass term of the current quarks as a small perturbation. Dressing the baryon three-quark core by a cloud of Goldstone mesons corresponds to the inclusion of the sea-quark contributions. All calculations are performed at one loop or at order of accuracy $O(1/F^2, \hat{m}, m_s)$. The chiral limit with $\hat{m}, m_s \to 0$ is well defined.

In these Lyubovitskij, Gutsche, and Faessler (2001), Lyubovitskij, Gutsche, Faessler, and Drukarev (2001), Lyubovitskij, Gutsche, Faessler, and Vinh-Mau (2001), Lyubovitskij, Wang, Gutsche, and Faessler (2002), Simkovic et al. (2002) and Pumsa-ard et al. (2003) we developed the PCQM for the study of baryon

properties: electromagnetic form factors of the nucleon, low-energy meson-baryon scattering and σ-terms, electromagnetic excitation of nucleon resonances, etc. In this Lyubovitskij, Gutsche, and Faessler (2001) the PCQM has been applied to study the electromagnetic form factors of the nucleon and the results obtained are in good agreement with experimental data. In this work we extend the PCQM to study the electromagnetic form factors of hyperons and give predictions with respect to future measurements of their magnetic moments, radii and the momentum dependence of form factors.

We proceed as follows. In chapter II we introduce the PCQM and describe the basic notions of our approach. In chapter III we present the analytic expressions for the charge and magnetic form factors of the baryon octet. Chapter IV contains a summary and the discussion of the numerical results for their magnetic moments, charge and magnetic radii, and the momentum dependence of the form factors in comparison to the experimental data.

Chapter II

The Perturbative Chiral Quark Model

2.1 Effective Lagrangian and zeroth order properties

The following considerations are based on the perturbative chiral quark model (PCQM) (Lyubovitskij, Gutsche, and Faessler, 2001; Lyubovitskij, Gutsche, Faessler, and Drukarev, 2001). The PCQM is a relativistic quark model which is based on an effective Lagrangian $\mathcal{L}_{\text{eff}} = \mathcal{L}_{\text{inv}}^{lin} + \mathcal{L}_{\chi SB}$. The Lagrangian includes the linearized chiral invariant term $\mathcal{L}_{\text{inv}}^{lin}$ and a mass term $\mathcal{L}_{\chi SB}$ which explicitly breaks chiral symmetry

$$
\begin{aligned}
\mathcal{L}_{\text{inv}}^{lin} &= \bar{\psi}(x)\left[i\partial\!\!\!/ - \gamma^0 V(r) - S(r)\right]\psi(x) + \frac{1}{2}[\partial_\mu \hat{\Phi}(x)]^2 \\
&\quad - \bar{\psi}(x)S(r)i\gamma^5 \frac{\hat{\Phi}(x)}{F}\psi(x), \hspace{3cm} (2.1) \\
\mathcal{L}_{\chi SB} &= -\bar{\psi}(x)\mathcal{M}\psi(x) - \frac{B}{2}Tr[\hat{\Phi}^2(x)\mathcal{M}], \hspace{2cm} (2.2)
\end{aligned}
$$

where $r = |\vec{x}|$; ψ is the quark field; $\hat{\Phi}$ is the matrix of the pseudoscalar mesons; $S(r)$ and $V(r)$ are scalar and vector components of an effective, static potential providing quark confinement; $\mathcal{M} = \text{diag}\{\hat{m}, \hat{m}, m_s\}$ is the mass matrix of current quarks (we restrict to the isospin symmetry limit with $m_u = m_d = \hat{m}$); B is the quark condensate parameter; and $F = 88$ MeV (Lyubovitskij, Gutsche, and Faessler, 2001; Lyubovitskij, Gutsche, Faessler, and Drukarev, 2001; Gasser, Sainio, and Švarce, 1988) is the pion decay constant in the chiral limit. We rely on the standard picture of chiral symmetry breaking (Weinberg, 1979; Gasser and Leutwyler, 1984, 1985)

and for the masses of pseudoscalar mesons we use the leading term in the chiral expansion (i.e. linear in the current quark mass): $M_\pi^2 = 2\hat{m}B$, $M_K^2 = (\hat{m} + m_s)B$, $M_\eta^2 = \frac{2}{3}(\hat{m} + 2m_s)B$. Meson masses satisfy the Gell-Mann-Oakes-Renner and the Gell-Mann-Okubo relation $3M_\eta^2 + M_\pi^2 = 4M_K^2$. In the evaluation we use the following set of QCD parameters (Gasser and Leutwyler, 1982): $\hat{m} = 7$ MeV, $m_s/\hat{m} = 25$ and B $= M_{\pi^+}^2/(2\hat{m}) = 1.4$ GeV.

To describe the properties of baryons which are modelled as bound states of valence quarks surrounded by a meson cloud we formulate perturbation theory. In our approach the mass (energy) m_N^{core} of the three-quark core of the nucleon is related to the single quark energy $\mathcal{E}_0$ by $m_N^{core} = 3\mathcal{E}_0$. For the unperturbed three-quark state we introduce the notation $|\phi_0>$ with the appropriate normalization $<\phi_0|\phi_0> = 1$. The single quark ground state energy $\mathcal{E}_0$ and wave function (WF) $u_0(\vec{x})$ are obtained from the Dirac equation

$$\left[-i\vec{\alpha} \cdot \vec{\nabla} + \beta S(r) + V(r) - \mathcal{E}_0 \right] u_0(\vec{x}) = 0. \tag{2.3}$$

The quark WF $u_0(\vec{x})$ belongs to the basis of potential eigenstates (including excited quark and antiquark solutions) used for the expansion of the quark field operator $\psi(x)$. Here we restrict the expansion to the ground state contribution with $\psi(x) = b_0 u_0(\vec{x}) \exp(-i\mathcal{E}_0 t)$, where b_0 is the corresponding single quark annihilation operator. In Eq. (2.3) the current quark mass is not included to simplify our calculational technique. Instead, we consider the quark mass term as a small perturbation.

For a given form of the potentials $S(r)$ and $V(r)$ the Dirac equation in Eq. (2.3) can be solved numerically. Here, for the sake of simplicity, we use a variational Gaussian ansatz for the quark wave function given by the analytical

form:

$$u_0(\vec{x}) = N \exp\left[-\frac{\vec{x}^2}{2R^2}\right] \begin{pmatrix} 1 \\ i\rho\vec{\sigma}\cdot\vec{x}/R \end{pmatrix} \chi_s\chi_f\chi_c, \qquad (2.4)$$

where $N = [\pi^{3/2}R^3(1 + 3\rho^2/2)]^{-1/2}$ is a constant fixed by the normalization condition $\int d^3x u_0^\dagger(\vec{x})u_0(\vec{x}) \equiv 1$; χ_s, χ_f, χ_c are the spin, flavor and color quark wave functions, respectively. Our Gaussian ansatz contains two model parameters: the dimensional parameter R and the dimensionless parameter ρ. The parameter ρ can be related to the axial coupling constant g_A calculated in zeroth-order (or 3q-core) approximation (Lyubovitskij, Gutsche, Faessler, and Drukarev, 2001):

$$g_A = \frac{5}{3}\left(1 - \frac{2\rho^2}{1 + \frac{3}{2}\rho^2}\right) = \frac{5}{3}\frac{1 + 2\gamma}{3}, \qquad (2.5)$$

where

$$\gamma = \frac{9g_A}{10} - \frac{1}{2}. \qquad (2.6)$$

The parameter R can be physically understood as the mean radius of the three-quark core and is related to the charge radius $\langle r_E^2 \rangle_{LO}^p$ of the proton in the leading-order (LO) approximation as

$$\langle r_E^2 \rangle_{LO}^p = \frac{3R^2}{2}\frac{1 + \frac{5}{2}\rho^2}{1 + \frac{3}{2}\rho^2} = R^2\left(2 - \frac{\gamma}{2}\right). \qquad (2.7)$$

In our calculations we use the value $g_A = 1.25$ (Gasser, Sainio, and Švarce, 1988) as deduced from chiral perturbation theory in the chiral limit. We therefore have only one free parameter, that is R. In the final numerical evaluation R is varied in the region from 0.55 fm to 0.65 fm, which is sufficiently large to justify perturbation theory.

2.2 Renormalization of the PCQM and perturbation theory

We consider perturbation theory up to one meson loop and up to terms linear in the current quark mass. The formalism utilizes a renormalization technique, which, by introduction of counterterms, effectively reduces the number of Feynman diagrams to be evaluated. For details of this technique we refer to Lyubovitskij, Gutsche, and Faessler (2001) and to appendix B. Here we briefly describe the basic ingredients relevant for the further discussion. We define the renormalized current quark masses, $\hat{m}^r$ and m_s^r and the renormalization constants, $\hat{Z}$ and Z_s as :

$$
\begin{aligned}
\hat{m}^r &= \hat{m} - \frac{3}{400\gamma}\left(\frac{g_A}{\pi F}\right)^2 \int_0^\infty dp\, p^4 F_{\pi NN}(p^2) \\
&\times \left\{ \frac{9}{w_\pi^2(p^2)} + \frac{6}{w_K^2(p^2)} + \frac{1}{w_\eta^2(p^2)} \right\}, \\
m_s^r &= m_s - \frac{3}{400\gamma}\left(\frac{g_A}{\pi F}\right)^2 \int_0^\infty dp\, p^4 F_{\pi NN}(p^2) \left\{ \frac{12}{w_K^2(p^2)} + \frac{4}{w_\eta^2(p^2)} \right\}, \\
\hat{Z} &= 1 - \frac{3}{400}\left(\frac{g_A}{\pi F}\right)^2 \int_0^\infty dp\, p^4 F_{\pi NN}(p^2) \\
&\times \left\{ \frac{9}{w_\pi^3(p^2)} + \frac{6}{w_K^3(p^2)} + \frac{1}{w_\eta^3(p^2)} \right\}, \\
Z_s &= 1 - \frac{3}{400}\left(\frac{g_A}{\pi F}\right)^2 \int_0^\infty dp\, p^4 F_{\pi NN}(p^2) \left\{ \frac{12}{w_K^3(p^2)} + \frac{4}{w_\eta^3(p^2)} \right\}.
\end{aligned}
$$

(2.8)

(2.9)

(2.10)

(2.11)

For a meson with three-momentum $\vec{p}$ the meson energy is $w_\Phi(p^2) = \sqrt{M_\Phi^2 + p^2}$ with $p = |\vec{p}|$ and $F_{\pi NN}(p^2)$ is the πNN form factor normalized to unity at zero recoil $(\vec{p} = 0)$:

$$
F_{\pi NN}(p^2) = \exp\left(-\frac{p^2 R^2}{4}\right)\left\{ 1 + \frac{p^2 R^2}{8}\left(1 - \frac{5}{3g_A}\right) \right\}.
$$

(2.12)

By adding the renormalized current quark mass term to the Dirac equation of Eq. (2.3) we obtain the renormalized quark field ψ^r as :

$$
\psi_i^r(x; m_i^r) = b_0 u_0^r(\vec{x}; m_i^r)\exp[-i\mathcal{E}_0^r(m_i^r)t],
$$

(2.13)

where i is the flavor SU(3) index. The renormalized single quark WF $u_0^r(\vec{x}; m_i^r)$ and energy $\mathcal{E}_0^r(m_i^r)$ are related to the bare expressions $u_0(\vec{x})$ and $\mathcal{E}_0$ as :

$$u_0^r(\vec{x}; m_i^r) \;=\; u_0(\vec{x}) + \delta u_0(\vec{x}; m_i^r), \tag{2.14}$$

$$\mathcal{E}_0^r(m_i^r) \;=\; \mathcal{E}_0 + \delta\mathcal{E}_0^r(m_i^r), \tag{2.15}$$

where

$$\delta u_0(\vec{x}; m_i^r) \;=\; \frac{m_i^r}{2}\frac{\rho R}{1+\frac{3}{2}\rho^2}\left(\frac{\frac{1}{2}+\frac{21}{4}\rho^2}{1+\frac{3}{2}\rho^2} - \frac{\vec{x}^2}{R^2} + \gamma^0\right)u_0(\vec{x}), \tag{2.16}$$

$$\delta\mathcal{E}_0^r(m_i^r) \;=\; \gamma m_i^r. \tag{2.17}$$

Introduction of the electromagnetic field A_μ into the PCQM is accomplished by adding the kinetic energy term and by standard minimal substitution in the Lagrangian of Eq. (2.1) and Eq. (2.2) with

$$\partial_\mu\psi^r \;\longrightarrow\; D_\mu\psi^r = \partial_\mu\psi^r + ie\mathcal{Q}A_\mu\psi^r, \tag{2.18}$$

$$\partial_\mu\Phi_i \;\longrightarrow\; D_\mu\Phi_i = \partial_\mu\Phi_i + e\left[f_{3ij} + \frac{f_{8ij}}{\sqrt{3}}\right]A_\mu\Phi_j, \tag{2.19}$$

where $\mathcal{Q}$ is the quark charge matrix with $\mathcal{Q}$=diag$\{2/3, -1/3, -1/3\}$ and f_{ijk} are the totally antisymmetric structure constants of SU(3). The renormalized effective Lagrangian is obtained from the original one of Eqs. (2.1-2.2) by replacing ψ with ψ^r, adding the counterterms and by standard minimal substitution. From this we derive the renormalized electromagnetic current operator as :

$$j_r^\mu = j_{\psi^r}^\mu + j_\Phi^\mu + \delta j_{\psi^r}^\mu. \tag{2.20}$$

It contains the quark component $j_{\psi^r}^\mu$, the charged meson component j_Φ^μ, and the contribution of the counterterm $\delta j_{\psi^r}^\mu$:

$$j_{\psi^r}^\mu \;=\; \bar{\psi}^r\gamma^\mu\mathcal{Q}\psi^r = \frac{1}{3}\left[2\bar{u}^r\gamma^\mu u^r - \bar{d}^r\gamma^\mu d^r - \bar{s}^r\gamma^\mu s^r\right], \tag{2.21}$$

$$j_\Phi^\mu \;=\; \left[f_{3ij} + \frac{f_{8ij}}{\sqrt{3}}\right]\Phi_i\partial^\mu\Phi_j$$

$$=\; [\pi^-i\partial^\mu\pi^+ - \pi^+i\partial^\mu\pi^- + K^-i\partial^\mu K^+ - K^+i\partial^\mu K^-], \tag{2.22}$$

$$\delta j^\mu_{\psi^r} = \bar{\psi}^r(Z-1)\gamma^\mu \mathcal{Q}\psi^r$$

$$= \frac{1}{3}\left[2\bar{u}^r(\hat{Z}-1)\gamma^\mu u^r - \bar{d}^r(\hat{Z}-1)\gamma^\mu d^r - \bar{s}^r(Z_s-1)\gamma^\mu s^r\right]. \quad (2.23)$$

Following the Gell-Mann and Low theorem (Gell-Mann and Low, 1951) we define the expectation value of an operator $\hat{O}$ for the renormalized PCQM by

$$<\hat{O}> = {}^B<\phi_0|\sum_{n=0}^{\infty}\frac{i^n}{n!}\int d^4x_1...d^4x_n T[\mathcal{L}^{str}_r(x_1)...\mathcal{L}^{str}_r(x_n)\hat{O}]|\phi_0>^B_c. \quad (2.24)$$

In Eq. (2.24) the superscript B indicates that the matrix elements are projected on the respective baryon states, the subscript c refers to contributions from connected graphs only and the renormalized strong interaction Lagrangian $\mathcal{L}^{str}_r$, which is treated as a perturbation, is defined as

$$\mathcal{L}^{str}_r = \mathcal{L}^{str}_I + \delta\mathcal{L}^{str}, \quad (2.25)$$

where

$$\mathcal{L}^{str}_I = -\bar{\psi}^r(x)i\gamma^5\frac{\hat{\Phi}(x)}{F}S(r)\psi^r(x). \quad (2.26)$$

$\delta\mathcal{L}^{str}$ is the strong interaction part of the counterterms (see details in appendix B) at one loop to the order $o(1/F^2)$ using Wick's theorem and the appropriate propagators.

For the quark field we use a Feymann propagator for a fermion in a binding potential.

$$iG_\psi(x,y) = <\phi_0|T\{\psi(x)\psi(y)\}|\phi_0>$$

$$= \Theta(x_0-y_0)\sum_{\alpha}u_\alpha(\vec{x})\bar{u}_\alpha(\vec{y})e^{-i\mathcal{E}_\alpha(x_0-y_0)}$$

$$-\Theta(x_0-y_0)\sum_{\beta}v_\beta(\vec{x})\bar{v}_\beta(\vec{y})e^{i\mathcal{E}_\beta(x_0-y_0)} \quad (2.27)$$

Up to the order of accuracy we are working in, it is sufficient to use $G_\psi(x,y)$ instead of $G_{\psi^r}(x,y)$ where the renormalized quark fields are used. By restricting

the summation over intermediate quark states to the ground state we get

$$iG_\psi(x,y) \quad \longrightarrow \quad iG_\psi^{(0)}(x,y)$$

$$= \quad u_0(\vec{x})\bar{u}_0(\vec{y})\exp[-i\mathcal{E}_0(x_0 - y_0)]\Theta(x_0 - y_0). \qquad (2.28)$$

Such a truncation can be considered as an additional regularization of the quark propagator, where in case of SU(2)-flavor intermediate baryon states in loop-diagrams are restricted to N and Δ.

From our previous works (Lyubovitskij, Gutsche, and Faessler, 2001; Lyubovitskij, Gutsche, Faessler, and Drukarev, 2001; Lyubovitskij, Gutsche, Faessler, and Vinh-Mau, 2001; Lyubovitskij, Wang, Gutsche, and Faessler, 2002; Simkovic et al., 2002; Pumsa-ard et al., 2003) we conclude that the use of a truncated quark propagator leads to a reasonable description of the experiment. In Pumsa-ard et al. (2003) we included for the first time excited quark states in the propagator of Eq. (2.24) and analyzed their influence on the matrix elements for the $N-\Delta$ transition considered. We included the following set of the excited quark states: the first p-states ($1p_{1/2}$ and $1p_{3/2}$ in the non-relativistic notation) and the second excited states ($1d_{3/2}$, $1d_{5/2}$, and $2s_{1/2}$). Again, the Dirac equation is solved analytically for the same form of the effective potential $V_{eff}(r) = S(r) + \gamma^0 V(r)$ as was done for the ground state. The corresponding expressions for the wave functions of the excited quark states are given in appendix A.

In Pumsa-ard et al. (2003) we demontrated that the excited quark states can increase the contribution of the loop diagrams but in comparison to the leading order (three-quark core) diagram this effect was of the order of 10%. In the context of the electromagnetic properties of baryons, we also estimated the effect of excited states, which again is of the order of 10%. However, there are quantities (like, e.g., the charge radius of neutron) which are dominated by higher order effects. Particularly, in the SU(2) flavor limit there is no three-quark core diagram

contributing to this quantity. Only meson-loop diagram contribute to the neutron charge radius in the context of the PCQM and, therefore, the effects of excited states can be essential. In this work (see in chapter IV) we discuss the effects of excited states only for the neutron charge radius. We found that these effects considerably improved our prediction for the neutron charge radius which is close to the experimental result.

For the meson fields we use the free Feymann propagator for a boson with

$$
\begin{aligned}
i\Delta_{ij}(x-y) &= <0|T\{\Phi_i(x)\Phi_j(y)\}|0> \\
&= \delta_{ij}\int \frac{d^4k}{(2\pi)^4 i}\frac{\exp[-ik(x-y)]}{M_\Phi^2 - k^2 - i\epsilon}.
\end{aligned}
\tag{2.29}
$$

Chapter III

Electromagnetic form factors of the baryon octet

We define the electromagnetic form factors of the baryon in the Breit frame, where gauge invariance is fulfilled (Lyubovitskij, Gutsche, and Faessler, 2001; Miller and Thomas, 1997; Lu, Thomas, and Wiiiams, 1998; Ivanov, Locher, and Lyubovitskij, 1996; Ernst, Sachs, and Wali, 1960; Sachs, 1962). In this frame the initial momentum of the baryon is $p = (E, -\vec{q}/2 + \vec{\Delta})$, the final momentum is $p' = (E, \vec{q}/2 + \vec{\Delta})$, and the four-momentum of the photon is $q = (0, \vec{q})$ with $p' = p + q$. For identical baryons we have $\vec{\Delta} = 0$. With the space-like momentum transfer squared given as $Q^2 = -q^2 = \vec{q}^2$, we define the Sachs charge G_E^B and magnetic G_M^B form factors of the baryon as

$$< B'_{s'}(\frac{\vec{q}}{2} + \vec{\Delta})|J^0(0)|B_s(-\frac{\vec{q}}{2} + \vec{\Delta}) > \;=\; \chi^\dagger_{B'_{s'}} \chi_{B_s} G_E^B(Q^2), \tag{3.1}$$

$$< B'_{s'}(\frac{\vec{q}}{2} + \vec{\Delta})|\vec{J}(0)|B_s(-\frac{\vec{q}}{2} + \vec{\Delta}) > \;=\; \chi^\dagger_{B'_{s'}} \frac{i\vec{\sigma}_B \times \vec{q}}{m_B + m'_B} \chi_{B_s} G_M^B(Q^2). \tag{3.2}$$

Here, $J^0(0)$ and $\vec{J}(0)$ are the time and space components of the electromagnetic current operator; χ_{B_s} and $\chi^\dagger_{B'_{s'}}$ are the baryon spin WF in the initial and final states; $\vec{\sigma}_B$ is the baryon spin matrix. Electromagnetic gauge invariance both on the Lagrangian and the baryon level is fulfilled in the Breit frame (Lyubovitskij, Gutsche, and Faessler, 2001).

At zero recoil ($q^2 = 0$) the Sachs form factors satisfy the following normalization conditions:

$$G_E^B(0) = Q_B, \qquad\qquad G_M^B(0) = \mu_B, \tag{3.3}$$

where Q_B and μ_B are charge and magnetic moment of the baryon octet, respectively.

The charge and magnetic radii of baryons are given by

$$\langle r_{E,M}^2 \rangle^B = -\frac{6}{G_{E,M}^B(0)} \frac{d}{dQ^2} G_{E,M}^B(Q^2) \bigg|_{Q^2=0}. \tag{3.4}$$

For neutral particles ($Q_B = 0$) the charge radius is defined by

$$\langle r_E^2 \rangle^B = -6 \frac{d}{dQ^2} G_E^B(Q^2) \bigg|_{Q^2=0}. \tag{3.5}$$

In the PCQM the charge and magnetic form factors of the baryon octet are given as

$$
\begin{aligned}
\chi_{s'}^\dagger \chi_s G_E^B(Q^2) &= \; <\phi_0| \sum_{n=0}^{2} \frac{i^n}{n!} \int \delta(t) d^4x d^4x_1 \ldots d^4x_n e^{-iq \cdot x} \\
&\times \; T[\mathcal{L}_r^{str}(x_1) \ldots \mathcal{L}_r^{str}(x_n) j_r^0(x)]|\phi_0 >_c^B, \tag{3.6} \\
\chi_{s'}^\dagger \frac{i\vec{\sigma}_B \times \vec{q}}{m_B + m'_B} \chi_s G_M^B(Q^2) &= \; <\phi_0| \sum_{n=0}^{2} \frac{i^n}{n!} \int \delta(t) d^4x d^4x_1 \ldots d^4x_n e^{-iq \cdot x} \\
&\times \; T[\mathcal{L}_r^{str}(x_1) \ldots \mathcal{L}_r^{str}(x_n) \vec{j}_r(x)]|\phi_0 >_c^B. \tag{3.7}
\end{aligned}
$$

The relevant diagrams contributing to the charge and magnetic form factors are indicated in Fig. 3.1. In the following we give the analytical expressions for the respective diagrams.

1. Three-quark diagram (3q):

$$G_{E,M}^B(Q^2)\bigg|_{3q} = \; G_{E,M}^B(Q^2)\bigg|_{3q}^{LO} + G_{E,M}^B(Q^2)\bigg|_{3q}^{NLO}, \tag{3.8}$$

where $G_{E,M}^B(Q^2)\bigg|_{3q}^{LO}$ are the leading-order (LO) terms of the three-quark diagram evaluated with the unperturbed quark WF $u_0(\vec{x})$; $G_{E,M}^B(Q^2)\bigg|_{3q}^{NLO}$ is
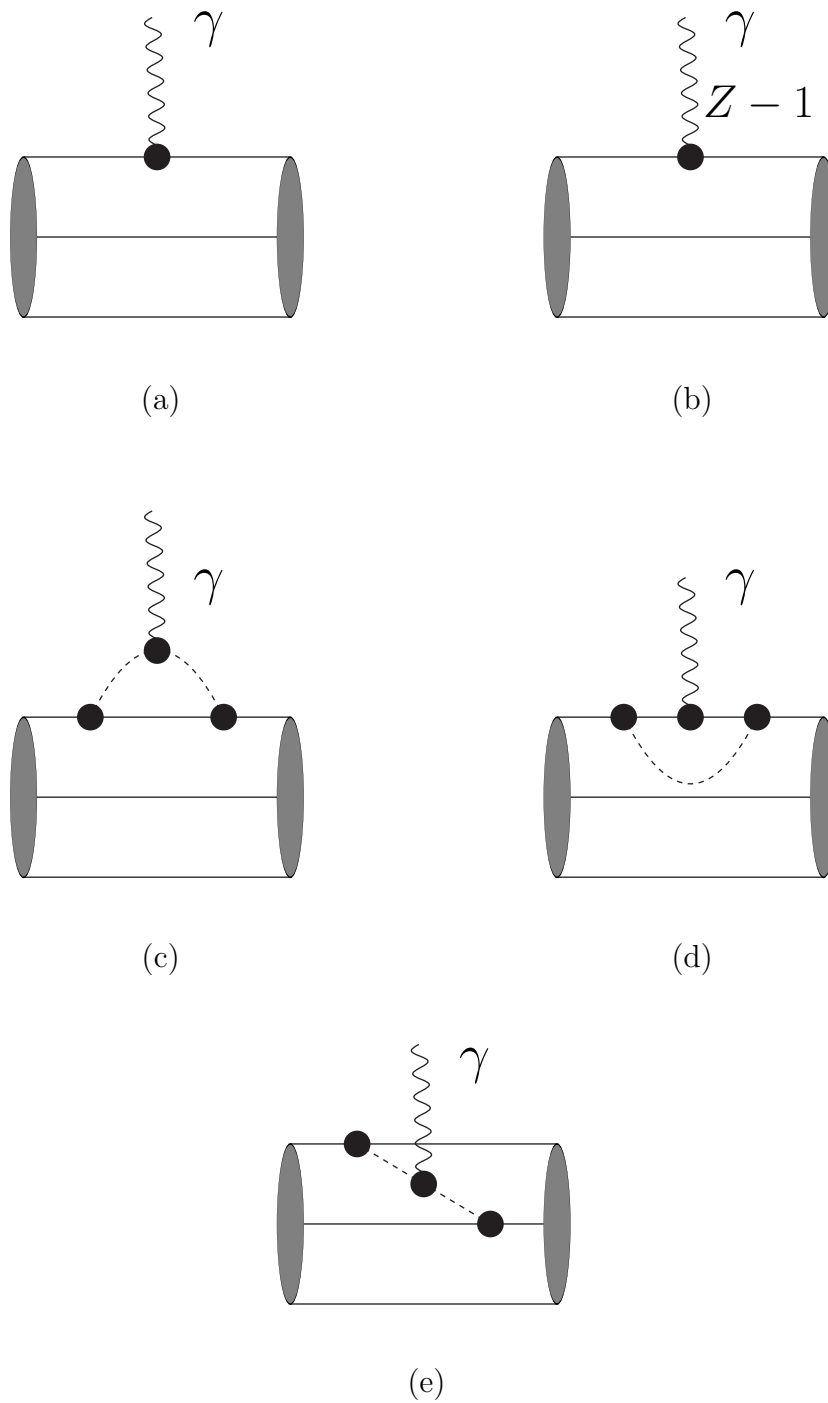
Figure 3.1: Diagrams contributing to the charge and magnetic form factors of the baryon octet: three-quark diagram (a), three-quark counterterm diagram (b), meson-cloud diagram (c), vertex correction diagram (d), and meson-in-flight diagram (e).

a correction due to the modification of the quark WF $u_0(\vec{x}) \rightarrow u_0^r(\vec{x}; m_i^r)$ referred to as next-to-leading order (NLO):

$$G_E^B(Q^2)\Big|_{3q}^{LO} = a_1^B G_E^p(Q^2)\Big|_{3q}^{LO}, \tag{3.9}$$

$$G_M^B(Q^2)\Big|_{3q}^{LO} = b_1^B \frac{m_B}{m_N} G_M^p(Q^2)\Big|_{3q}^{LO}, \tag{3.10}$$

$$G_E^B(Q^2)\Big|_{3q}^{NLO} = \left(a_2^B + a_3^B \varepsilon\right) G_E^p(Q^2)\Big|_{3q}^{NLO}, \tag{3.11}$$

$$G_M^B(Q^2)\Big|_{3q}^{NLO} = \left(b_2^B + b_3^B \varepsilon\right) \frac{m_B}{m_N} G_M^p(Q^2)\Big|_{3q}^{NLO}, \tag{3.12}$$

where

$$G_E^p(Q^2)\Big|_{3q}^{LO} = \exp\left(-\frac{Q^2 R^2}{4}\right)\left(1 - \frac{\rho^2}{1 + \frac{3}{2}\rho^2}\frac{Q^2 R^2}{4}\right), \tag{3.13}$$

$$G_E^p(Q^2)\Big|_{3q}^{NLO} = \exp\left(-\frac{Q^2 R^2}{4}\right)\hat{m}^r \frac{Q^2 R^3 \rho}{4\left(1 + \frac{3}{2}\rho^2\right)^2}$$
$$\times \left(\frac{1 + 7\rho^2 + \frac{15}{4}\rho^4}{1 + \frac{3}{2}\rho^2} - \frac{Q^2 R^2}{4}\rho^2\right), \tag{3.14}$$

$$G_M^p(Q^2)\Big|_{3q}^{LO} = \exp\left(-\frac{Q^2 R^2}{4}\right)\frac{2m_N \rho R}{1 + \frac{3}{2}\rho^2}, \tag{3.15}$$

$$G_M^p(Q^2)\Big|_{3q}^{NLO} = G_M^p(Q^2)\Big|_{3q}^{LO}\frac{\hat{m}^r R \rho}{1 + \frac{3}{2}\rho^2}\left(\frac{Q^2 R^2}{4} - \frac{2 - \frac{3}{2}\rho^2}{1 + \frac{3}{2}\rho^2}\right), \tag{3.16}$$

and $\varepsilon = m_s^r / \hat{m}^r$. The constants a_i^B and b_i^B are given in Table 4.1 and Table 4.2 respectively. When using isospin symmetry we use for m_B, the baryon masses, following values

$$m_N = m_p = m_n = 0.938 \text{ GeV}, \tag{3.17}$$

$$m_\Sigma = m_{\Sigma^\pm} = m_{\Sigma^0} = 1.189 \text{ GeV}, \tag{3.18}$$

$$m_\Lambda = 1.115 \text{ GeV}, \tag{3.19}$$

$$m_\Xi = m_{\Xi^0} = m_{\Xi^-} = 1.321 \text{ GeV}, \tag{3.20}$$

$$m_{\Sigma^0 \Lambda} = \frac{1}{2}\left(m_\Sigma + m_\Lambda\right) = 1.152 \text{ GeV}. \tag{3.21}$$

2. Three-quark counterterm (CT):

$$G_E^B(Q^2)\Big|_{CT} = \left[a_2^B(\hat{Z}-1) + a_3^B(Z_s-1)\right] G_E^p(Q^2)\Big|_{3q}^{LO}, \qquad (3.22)$$

$$G_M^B(Q^2)\Big|_{CT} = \left[b_2^B(\hat{Z}-1) + b_3^B(Z_s-1)\right] \frac{m_B}{m_N} G_M^p(Q^2)\Big|_{3q}^{LO}. \qquad (3.23)$$

3. Meson-cloud diagram (MC):

$$\begin{aligned}
G_E^B(Q^2)\Big|_{MC} &= \frac{9}{400}\left(\frac{g_A}{\pi F}\right)^2 \int_0^\infty dp\, p^2 \int_{-1}^1 dx \left(p^2 + p\sqrt{Q^2}x\right) \\
&\times\ \mathcal{F}_{\pi NN}(p^2, Q^2, x) t_E^B(p^2, Q^2, x)\Big|_{MC}, \qquad (3.24)
\end{aligned}$$

$$\begin{aligned}
G_M^B(Q^2)\Big|_{MC} &= \frac{3}{40} m_B \left(\frac{g_A}{\pi F}\right)^2 \int_0^\infty dp\, p^4 \int_{-1}^1 dx(1-x^2) \\
&\times\ \mathcal{F}_{\pi NN}(p^2, Q^2, x) t_M^B(p^2, Q^2, x)\Big|_{MC}, \qquad (3.25)
\end{aligned}$$

where

$$\mathcal{F}_{\pi NN}(p^2, Q^2, x) = F_{\pi NN}(p^2) F_{\pi NN}(p^2 + Q^2 + 2p\sqrt{Q^2}x), \qquad (3.26)$$

$$t_E^B(p^2, Q^2, x)\Big|_{MC} = a_4^B C_\pi^{11}(p^2, Q^2, x) + a_5^B C_K^{11}(p^2, Q^2, x), \qquad (3.27)$$

$$t_M^B(p^2, Q^2, x)\Big|_{MC} = b_4^B D_\pi^{22}(p^2, Q^2, x) + b_5^B D_K^{22}(p^2, Q^2, x), \qquad (3.28)$$

$$D_\Phi^{n_1 n_2}(p^2, Q^2, x) = \frac{1}{w_\Phi^{n_1}(p^2) w_\Phi^{n_2}(p^2 + Q^2 + 2p\sqrt{Q^2}x)}, \qquad (3.29)$$

$$C_\Phi^{n_1 n_2}(p^2, Q^2, x) = \frac{2 D_\Phi^{n_1 n_2}(p^2, Q^2, x)}{w_\Phi^{n_1}(p^2) + w_\Phi^{n_2}(p^2 + Q^2 + 2p\sqrt{Q^2}x)}. \qquad (3.30)$$

4. Vertex-correction diagram (VC):

$$\begin{aligned}
G_E^B(Q^2)\Big|_{VC} &= G_E^p(Q^2)\Big|_{3q}^{LO} \\
&\times\ \frac{9}{200}\left(\frac{g_A}{\pi F}\right)^2 \int_0^\infty dp\, p^4 F_{\pi NN}^2(p^2) t_E^B(p^2)\Big|_{VC}, \qquad (3.31)
\end{aligned}$$

$$\begin{aligned}
G_M^B(Q^2)\Big|_{VC} &= \frac{m_B}{m_N} G_M^p(Q^2)\Big|_{3q}^{LO} \\
&\times\ \frac{9}{200}\left(\frac{g_A}{\pi F}\right)^2 \int_0^\infty dp\, p^4 F_{\pi NN}^2(p^2) t_M^B(p^2)\Big|_{VC}, \qquad (3.32)
\end{aligned}$$

where

$$t_E^B(p^2)\Big|_{VC} = a_6^B W_\pi(p^2) + a_7^B W_K(p^2) + a_8^B W_\eta(p^2), \qquad (3.33)$$

$$t_M^B(p^2)\Big|_{VC} = b_6^B W_\pi(p^2) + b_7^B W_K(p^2) + b_8^B W_\eta(p^2), \qquad (3.34)$$

$$W_\Phi(p^2) = \frac{1}{w_\Phi^3(p^2)}. \qquad (3.35)$$

5. Meson-in-flight diagram (MF):

$$G_E^B(Q^2)\Big|_{MF} \equiv 0, \qquad (3.36)$$

$$G_M^B(Q^2)\Big|_{MF} = \frac{9}{100} m_B \left(\frac{g_A}{\pi F}\right)^2 \int_0^\infty dp\, p^4 \int_{-1}^1 dx (1-x^2)$$

$$\times \ \mathcal{F}_{\pi NN}(p^2, Q^2, x) t_M^B(p^2, Q^2, x)\Big|_{MF}, \qquad (3.37)$$

where

$$t_M^B(p^2, Q^2, x)\Big|_{MF} = b_9^B D_\pi^{22}(p^2, Q^2, x) + b_{10}^B D_K^{22}(p^2, Q^2, x). \qquad (3.38)$$

The magnetic moments μ_B of the baryon octet are given by the expression (in units of the nucleon magneton μ_N)

$$\mu_B = \mu_B^{LO}\left[1 + \delta\left(b_2^B + b_3^B \varepsilon\right) - \frac{1}{400}\left(\frac{g_A}{\pi F}\right)^2 \int_0^\infty dp\, p^4 F_{\pi NN}(p^2)\left\{\frac{k_1^B}{w_\pi^3} + \frac{k_2^B}{w_K^3} + \frac{k_3^B}{w_\eta^3}\right\}\right]$$

$$+ \ \frac{m_B}{50}\left(\frac{g_A}{\pi F}\right)^2 \int_0^\infty dp\, p^4 F_{\pi NN}(p^2)\left\{\frac{k_4^B}{w_\pi^4} + \frac{k_5^B}{w_K^4}\right\}, \qquad (3.39)$$

where

$$\mu_B^{LO} = b_1^B \frac{m_B}{m_N} G_M^p(0)\Big|_{3q}^{LO} = b_1^B \frac{2 m_B \rho R}{1 + \frac{3}{2}\rho^2} \qquad (3.40)$$

is the leading-order contribution to the baryon magnetic moment. The factor

$$\delta = -\hat{m}^r R \rho \frac{2 - \frac{3}{2}\rho^2}{\left(1 + \frac{3}{2}\rho^2\right)^2} \qquad (3.41)$$

defines the NLO correction to the baryon magnetic moments due to the modification of the quark WF (see Eq. (2.16)). The constants k_i^B are given in Table 4.3.

Chapter IV

Results and Discussion

4.1 Numerical Results

Numerical results for the magnetic moments, charge and magnetic radii of the baryon octet are given in Tables 4.4, 4.5 and 4.6, respectively. The total contributions to the electromagnetic properties are separated into two parts: the leading-order (LO) one due to the three quark core contribution and the next-to-leading order (NLO). The NLO contribution includes the corrections due to the renormalization of the quark WF (NLO;3q), the three-quark counterterm (CT), the meson-cloud diagram (MC), the vertex-correction diagram (VC), and the meson-in-flight diagram. The range of our numerical results is due to variation of the size parameter R in the region 0.55 - 0.65 fm. The mesonic contributions to the baryon magnetic moments are of the order of 20 - 40 % (except for Ξ^- they contribute only 3 %). Hence, meson cloud corrections generate a significant influence on baryon magnetic moments. Our results for the baryon magnetic moments are in good agreement with the experimental data. Mesonic contributions to the charge radii of charged baryons are also of 20 - 40 % (except for Ξ^- where they contribute less than 1 %). We predict that

$$\left\langle r_E^2 \right\rangle^{\Sigma^+} > \left\langle r_E^2 \right\rangle^p > \left\langle r_E^2 \right\rangle^{\Sigma^-} > \left\langle r_E^2 \right\rangle^{\Xi^-} . \tag{4.1}$$

Our result for the proton and Σ^- charge radii squared are in good agreement with the experimental data. In the isospin limit the three-quark core does not contribute to the charge radii of neutral baryons. Only the meson cloud generates a nonvanishing value for the charge radii of these baryons. Since we restrict the quark propagator to the ground state contribution the meson-cloud effects give a small value for the neutron charge radius squared.

We found that the result of the neutron charge radius can be improved by including excited states in the quark propagator. In Table 4.5 we give a comparison of our results for the neutron charge radius squared with the experimental value. The value, where the quark propagator is restricted to the ground state, is indicated by $\langle r_E^2 \rangle^n(\text{GS})$. Contributions from excited states (we have used the $1p^{1/2}$, $1p^{3/2}$, $1d^{3/2}$, $1d^{5/2}$ and $2s^{1/2}$ states) are denoted by $\langle r_E^2 \rangle^n(\text{ES})$. Exemplified for the neutron charge radius, we conclude that excited state contributions can also generate sizable corrections when the LO results are vanishing. In a further effort we intend to improve our calculations to the whole baryon octet by adding the excited states to the quark propagator. For Σ^0, Λ and Ξ^0 we predict that their charge radii squared have a positive sign and follow the pattern

$$\left\langle r_E^2 \right\rangle^{\Xi^0} > \left\langle r_E^2 \right\rangle^{\Sigma^0}, \left\langle r_E^2 \right\rangle^{\Lambda}. \tag{4.2}$$

The mesons also play a very important role for the baryon magnetic radii where they contribute up to 50 %. Our result for the magnetic radius of Ξ^- is quite small compared to the other's because the meson-cloud contribution comes with a negative sign. Results for the magnetic radii squared of the proton and neutron are in good agreement with the experimental data.

The Q^2-dependence of the charge and magnetic form factors are shown in Figs. 4.1, 4.2, 4.3, 4.4 and 4.5. In Fig. 4.2 we compare our result for the neutron charge form factor to the experimental data varying the parameter R. Results are

Table 4.1: The constants a_i^B for the charge form factors G_E^B of the baryon octet.

	p	n	Σ^+	Σ^0	Σ^-	Λ	Ξ^0	Ξ^-	$\Sigma^0\Lambda$
a_1	1	0	1	0	-1	0	0	-1	0
a_2	1	0	4/3	1/3	-2/3	1/3	2/3	-1/3	0
a_3	0	0	-1/3	-1/3	-1/3	-1/3	-2/3	-2/3	0
a_4	1	-1	2	0	-2	0	1	-1	0
a_5	2	1	1	0	-1	0	-1	-2	0
a_6	1/2	1	0	1/2	1	1/2	0	1/2	0
a_7	-1	-1	-1/3	-1/3	-1/3	-1/3	1/3	1/3	0
a_8	1/6	0	0	-1/6	-1/3	-1/6	-1/3	-1/2	0

given for the case, where the quark propagator is restricted to the ground state. We separate the graphs for the charged and neutral baryons by using a proper normalization and compare to the experimental dipole fit, originally obtained for the nucleon given by (Thomas and Weise, 2001)

$$G_D(Q^2) = \frac{1}{\left[1 + \frac{Q^2}{0.71 \text{ GeV}^2}\right]^2}. \tag{4.3}$$

4.2   Summary

We apply the PCQM to calculate the charge and magnetic form factors of the baryon octet up to one loop perturbation theory. Furthermore, we analyze the magnetic moments, charge and magnetic radii. We demonstrated that meson cloud corrections play a sizable and important role in reproducing the experimental values both for magnetic moments and for the charge/magnetic radii. The magnetic moments of the baryon octet can be reproduced rather well. Also, charge and

Table 4.2: The constants b_i^B for the magnetic form factors G_M^B of the baryon octet.

	p	n	Σ^+	Σ^0	Σ^-	Λ	Ξ^0	Ξ^-	$\Sigma^0\Lambda$
b_1	1	-2/3	1	1/3	-1/3	-1/3	-2/3	-1/3	$-\sqrt{3}/3$
b_2	1	-2/3	8/9	2/9	-4/9	0	-2/9	1/9	$-\sqrt{3}/3$
b_3	0	0	1/9	1/9	1/9	-1/3	-4/9	-4/9	0
b_4	1	-1	4/5	0	-4/5	0	-1/5	1/5	$-2\sqrt{3}/5$
b_5	4/5	-1/5	1	3/5	1/5	-3/5	-1	-4/5	$-\sqrt{3}/5$
b_6	1/18	-2/9	0	-1/9	-2/9	0	0	1/18	$-\sqrt{3}/18$
b_7	1/9	1/9	5/27	5/27	5/27	-1/9	-5/27	-5/27	0
b_8	-1/18	1/27	-2/27	-1/27	0	2/27	1/9	5/54	$\sqrt{3}/54$
b_9	1	-1	0	0	0	0	0	0	$-\sqrt{3}/3$
b_{10}	0	0	1	1	1	-1	-1	-1	0

Table 4.3: The constants k_i^B for the magnetic moment μ_B of the baryon octet.

	p	n	Σ^+	Σ^0	Σ^-	Λ	Ξ^0	Ξ^-	$\Sigma^0\Lambda$
k_1	26	21	24	24	24	30	9	-6	24
k_2	16	21	50/3	14	22	0	25	32	18
k_3	4	4	16/3	8	0	16	12	20	4
k_4	11	-11	4	3	-4	-3	-1	1	$-4\sqrt{3}$
k_5	4	-1	11	6	7	-6	-11	-10	$-\sqrt{3}$

Table 4.4: Results for the magnetic moments μ_B of the baryon octet in our model calculation. The total result (Total) consist of the leading-order (LO) contribution due to the three-quark core and the next-to-leading-order (NLO) one due to the summation of the meson-cloud effects. The corresponding experimental data (Hagiwara et al., 2002; Eschrich et al., 2001) are given in the last column (in units of the nucleon magneton μ_N).

	LO	NLO	Total	Exp
μ_p	1.80 ± 0.15	0.80 ± 0.12	2.60 ± 0.03	2.793
μ_n	-1.20 ± 0.10	-0.78 ± 0.12	-1.98 ± 0.02	-1.913
μ_{Σ^+}	2.28 ± 0.19	0.47 ± 0.10	2.75 ± 0.09	2.458 ± 0.010
μ_{Σ^0}	0.76 ± 0.06	0.29 ± 0.07	1.05 ± 0.01	—
μ_{Σ^-}	-0.76 ± 0.06	-0.32 ± 0.02	-1.08 ± 0.05	-1.160 ± 0.025
μ_Λ	-0.71 ± 0.06	-0.18 ± 0.09	-0.89 ± 0.03	-0.613 ± 0.004
μ_{Ξ^0}	-1.69 ± 0.14	-0.05 ± 0.11	-1.74 ± 0.03	-1.250 ± 0.014
μ_{Ξ^-}	-0.85 ± 0.07	0.17 ± 0.07	-0.68 ± 0.01	-0.651 ± 0.003
$|\mu_{\Sigma^0\Lambda}|$	1.28 ± 0.11	0.62 ± 0.09	1.89 ± 0.01	1.61 ± 0.08

Table 4.5: Results for the charge radii squared $\langle r_E^2 \rangle^B$ of the baryon octet. Otherwise, LO and NLO contributions are indicated as in Table 4.4. Experimental data (Hagiwara et al., 2002) are given in the last column (in units of fm^2).

	LO	NLO	Total	Exp
$\langle r_E^2 \rangle^p$	0.60 ± 0.10	0.12 ± 0.01	0.72 ± 0.09	0.76 ± 0.02
$\langle r_E^2 \rangle^n (\text{GS})$	0	-0.043 ± 0.004	-0.043 ± 0.004	
$\langle r_E^2 \rangle^n (\text{ES})$	0	-0.068 ± 0.013	-0.068 ± 0.013	
$\langle r_E^2 \rangle^n (\text{Total})$	0	-0.111 ± 0.014	-0.111 ± 0.014	-0.116 ± 0.002
$\langle r_E^2 \rangle^{\Sigma^+}$	0.60 ± 0.10	0.21 ± 0.004	0.81 ± 0.10	—
$\langle r_E^2 \rangle^{\Sigma^0}$	0	0.050 ± 0.010	0.050 ± 0.010	—
$\langle r_E^2 \rangle^{\Sigma^-}$	0.60 ± 0.10	0.11 ± 0.03	0.71 ± 0.07	0.61 ± 0.21
$\langle r_E^2 \rangle^{\Lambda}$	0	0.050 ± 0.010	0.050 ± 0.010	—
$\langle r_E^2 \rangle^{\Xi^0}$	0	0.14 ± 0.02	0.14 ± 0.02	—
$\langle r_E^2 \rangle^{\Xi^-}$	0.60 ± 0.10	0.02 ± 0.03	0.62 ± 0.07	—
$\langle r_E^2 \rangle^{\Sigma^0 \Lambda}$	0	0	0	—

Table 4.6: Results for the magnetic radii squared $\langle r_M^2 \rangle^B$ of the baryon octet. Total result consists of LO and NLO contributions as in Table 4.4. Experimental data (Simon et al., 1980; Kubon et al., 2002)are given in the last column (in units of fm^2).

	LO	NLO	Total	Exp
$\langle r_M^2 \rangle^p$	0.37±0.09	0.37±0.02	0.74± 0.07	0.74±0.10
$\langle r_M^2 \rangle^n$	0.33±0.08	0.46±0.01	0.79± 0.07	0.76±0.02
$\langle r_M^2 \rangle^{\Sigma^+}$	0.45±0.10	0.19±0.02	0.64± 0.08	—
$\langle r_M^2 \rangle^{\Sigma^0}$	0.39±0.10	0.30±0.03	0.69± 0.07	—
$\langle r_M^2 \rangle^{\Sigma^-}$	0.38±0.08	0.40±0.01	0.78± 0.07	—
$\langle r_M^2 \rangle^{\Lambda}$	0.44±0.12	0.21±0.07	0.65± 0.05	—
$\langle r_M^2 \rangle^{\Xi^0}$	0.52±0.12	0.02±0.05	0.54± 0.06	—
$\langle r_M^2 \rangle^{\Xi^-}$	0.67±0.17	-0.35±0.13	0.32± 0.04	—
$\langle r_M^2 \rangle^{\Sigma^0\Lambda}$	0.36±0.09	0.39±0.02	0.75± 0.07	—
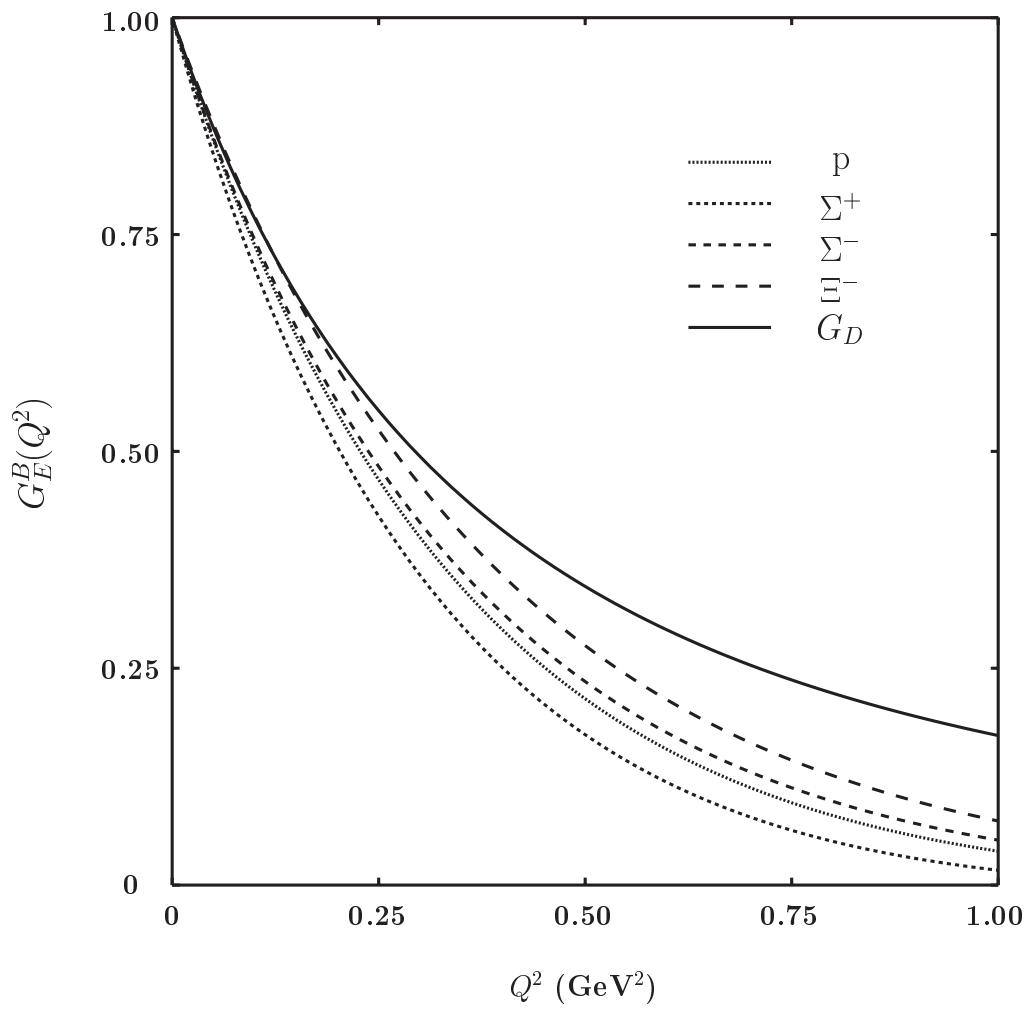
Figure 4.1: The charge form factors $G_E^B(Q^2)$ for B = p, Σ^+, Σ^- and Ξ^- for R = 0.6 fm compared to the dipole fit $G_D(Q^2)$. For Σ^- and Ξ^-, the absolute value of $G_E^B(Q^2)$ is shown.
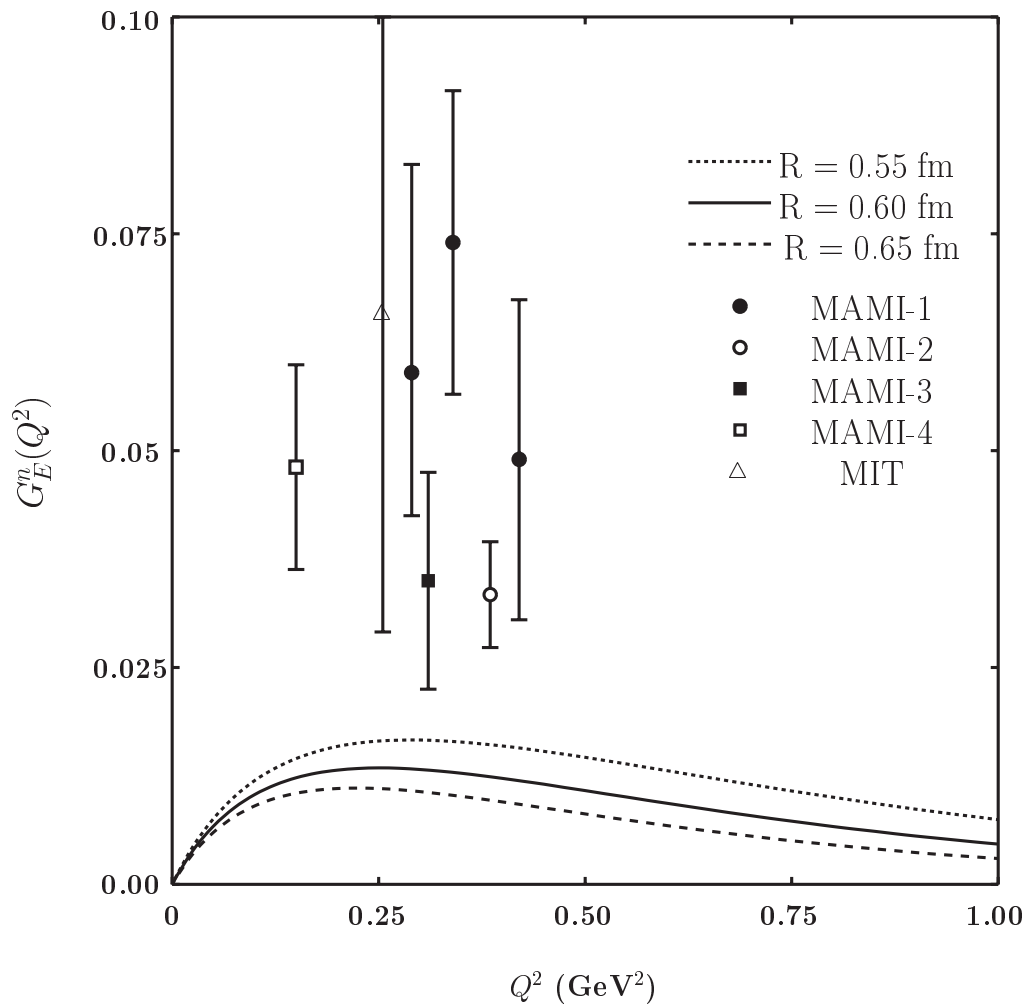
Figure 4.2: The neutron charge form factors $G_E^n(Q^2)$ for different values of R = 0.55, 0.6, and 0.65 fm. Experimental data are taken from Ostrick et al. (1999), Becker et al. (1999), Meyerhoff et al. (1994), Herberg et al. (1999), Eden et al. (1994).
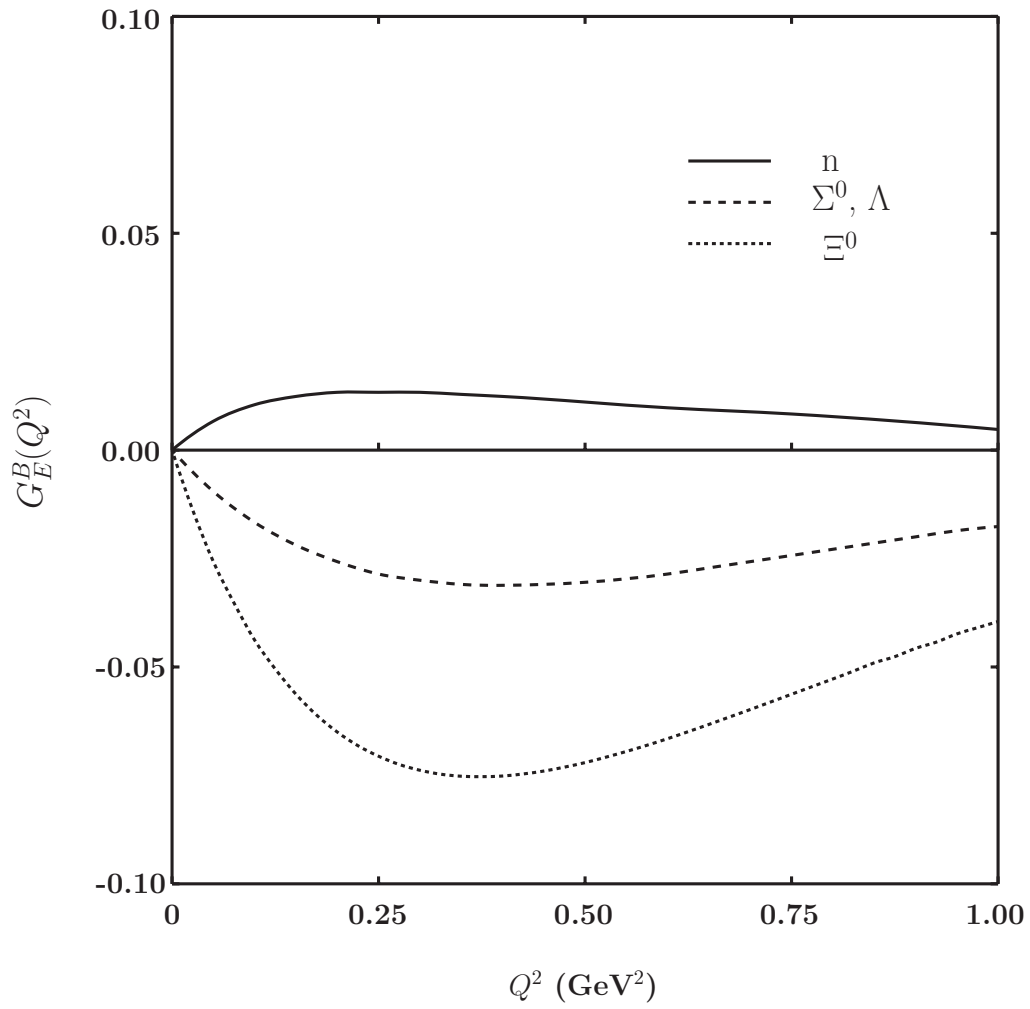
Figure 4.3: The charge form factors $G_E^B(Q^2)$ for B = n, Σ^0, Λ and Ξ^0 at R = 0.6 fm.
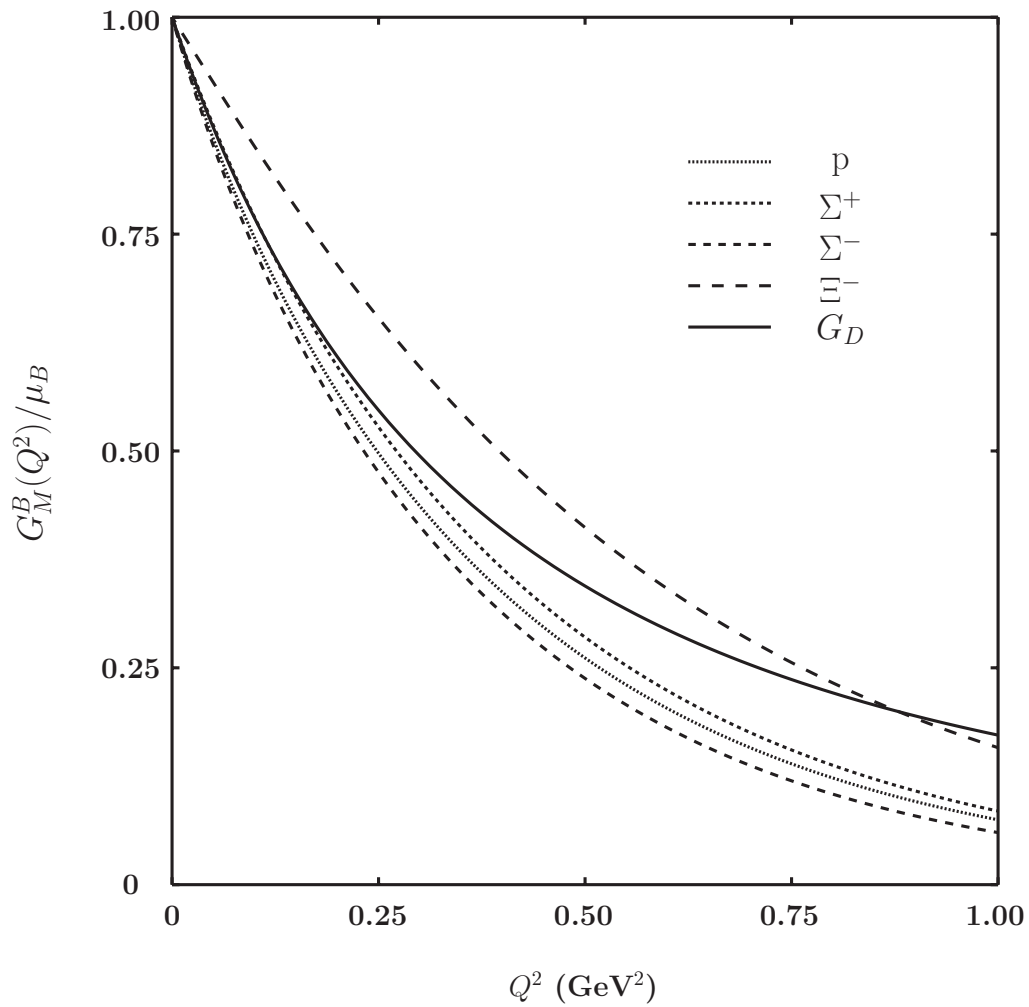
Figure 4.4: The normalized magnetic form factors $G_M^B(Q^2)/\mu_B$ for B = p, Σ^+, Σ^- and Ξ^- at R = 0.6 fm in comparison to the dipole fit $G_D(Q^2)$.
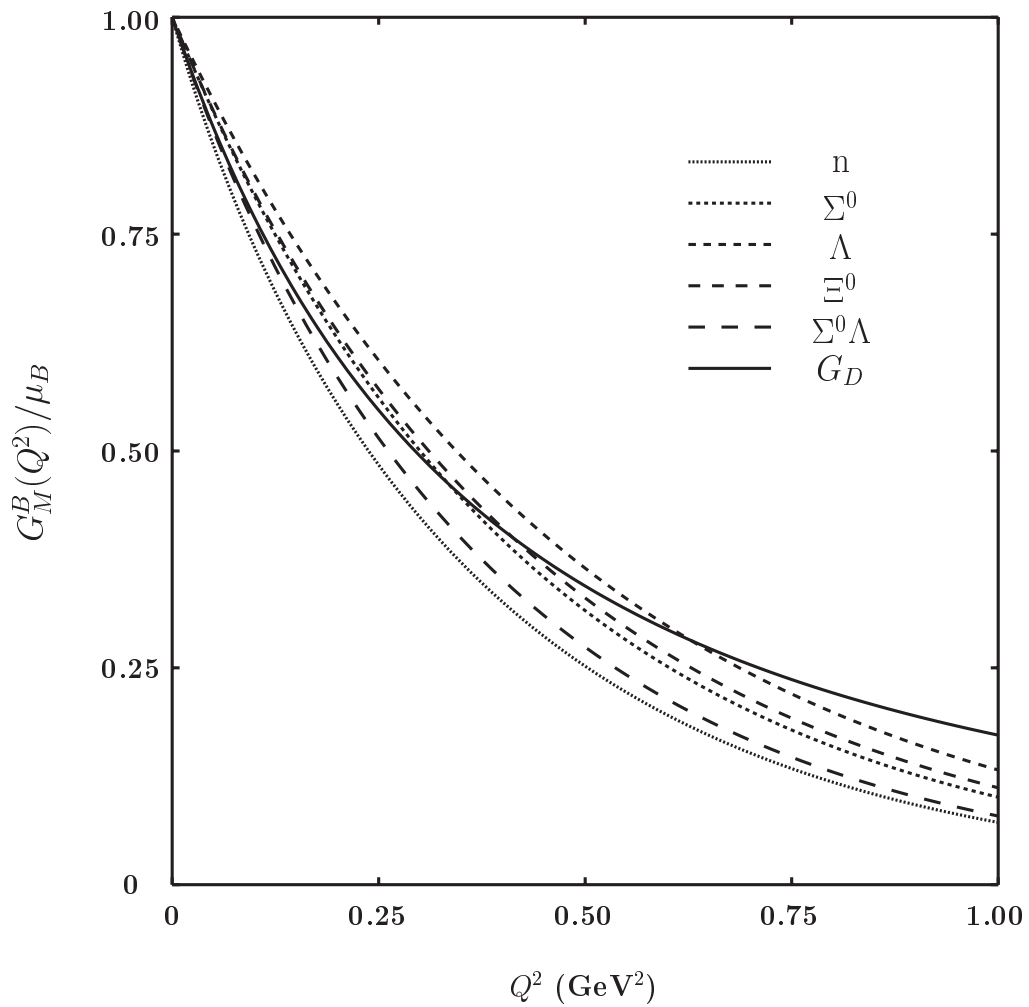
Figure 4.5: The normalized magnetic form factors $G_M^B(Q^2)/\mu_B$ for B = n, Σ^0, Λ and Ξ^0 at R = 0.6 fm as compared to the dipole fit $G_D(Q^2)$.

magnetic radii are explained with the PCQM, when the LO contribution, that is the valence quarks, dominates. As soon as the LO result vanishes, meson cloud corrections which then control the observable tend to be sensitively influenced by the possible contributions of excited states in the loop diagrams. We demonstrated this effect for the case of the neutron charge radius, where inclusion of the excited states tend to improve the model result.

References

References

Adamovich, M., et al. (1999). Charge Asymmetries for D, D_s and Λ_c Production in Σ^- - Nucleus Interactions at 340 GeV/c. **European Physics C** 8: 593.

Becker, J., et al. (1999). Determination of the neutron electric form factor from the reaction $^3H(e, e'n)p$ at medium momentum transfer. **European Physical Journal A** 6: 329.

Chin, S. A., (1982). Many-body theory of confined quarks and excluded pions: A perturbative study of the chiral bag. **Nuclear Physics A** 382: 355.

Chodos, R., Jaffe, R. L., Johnson, K., Thorn, C. B., and Weisskopt, V. F. (1974). New extended model of hadrons. **Physical Review D** 9: 3471.

Close, F. E. (1979). **An Introduction to Quarks and Partons**. Academic Press, New York.

Diakonov, D., and Petrov, V. Yu, (1984). Instanton-based vacuum from the Feynman variational principle. **Nuclear Physics B** 245: 259.

Diakonov, D., and Petrov, V. Yu, (1986). A theory of light quarks in the instanton vacuum. **Nuclear Physics B** 272: 457.

Diakonov, D., Petrov, V. Yu, and Pobilitsa, P. V. (1988). A chiral theory of nucleons. **Nuclear Physics B** 306: 809.

Diakonov, D., Petrov, V. Yu, and Praszalowicz, M. (1989). Nucleon mass and nucleon sigma term. **Nuclear Physics B** 323: 53.

Eden, T., et al. (1994). Electric form factor of the neutron from the $^2H(\vec{e}, e'\vec{n})^1H$ reaction at $Q^2 = 0.255(GeV/c)^2$. **Physical Review C** 50: R1749.

Ernst, F. J., Sachs, R. G., and Wali, K. C. (1960). Electromagnetic Form Factors of the Nucleon. **Physical Review** 119: 1105.

Eschrich, I., et al. (2001). Measurement of the Σ^- Charge Radius by Σ^- - Electron Elastic Scattering. **Physics Letter B** 552: 233.

Gasser, J., Sainio, M. E., and Švarce, A. B., (1988). Nucleons with chiral loops. **Nuclear Physics B** 307: 779.

Gasser, J., and Leutwyler, H. (1982). Quark masses. **Physics Report** 87: 77.

Gasser, J., and Leutwyler, H. (1984). Chiral perturbation theory to one loop. **Annals of Physics** 158: 142.

Gasser, J., and Leutwyler, H. (1985). Chiral perturbation theory: Expansions in the mass of the strange quark. **Nuclear Physics B** 250: 465.

Gell-Mann, M., and Lévy, M. (1960). The axial vector current in beta decay. **Nuovo Cimento** 16: 705.

Gell-Mann, M., and Low, F. (1951). Bound States in Quantum Field Theory. **Physical Review** 84: 350.

Gutsche, Th., and Robson, D. (1989). Positive and convergent self-energy in a chiral potential model. **Physics letter B** 229: 333.

Gutsche, Th. (1987). **A chiral potential model for the light-quark baryons**. Ph. D. Thesis, Florida State University.

Hagiwara, K., et al. (2002). The review of particle physics. **Physical Review D** 66: 010001.

Herberg, C, et al. (1999). Determination of the neutron electric form factor in the $D(e, e'n)p$ reaction and the influence of nuclear binding. **European Physical Journal A** 5: 131.

Ivanov, M. A., Locher, M. P., and Lyubovitskij, V.E. (1996). Nucleon Form Factors in a Relativistic Three-Quark Model. **Few Body System** 21: 131.

Kubon, G., et al. (2002). Precise neutron magnetic form factors. **Physics Letter B** 524: 26.

Lu, D. H., Thomas, A. W., and Williams, A. G. (1997). Electromagnetic form factors of the nucleon in an improved quark model. **Physical Review C** 57: 2628.

Lüscher, M. (1981). Symmetry-breaking aspects of the roughening transition in gauge theories. **Nuclear Physics B** 180: 317.

Takahashi, T. T., Matsufuru, H., Nemoto, Y., and Suganuma, H. (2001). Three-Quark Potential in SU(3) Lattice QCD. **Physical Review Letter B** 86: 18.

Lyubovitskij, V.E., Gutsche, Th., and Faessler, A. (2001). Electromagnetic Structure of the Nucleon in the Perturbative Chiral Quark Model .**Physical Review C** 64: 065203.

Lyubovitskij, V.E., Gutsche, Th., Faessler, A., and Drukarev, D. (2001). Sigma-term physics in the perturbative chiral quark model .**Physical Review D** 63: 054026.

Lyubovitskij, V.E., Gutsche, Th., Faessler, A., and Vinh-Mau, R. (2001). πN scattering and electromagnetic corrections in the perturbative chiral quark model . **Physics Letter B** 520: 204.

Lyubovitskij, V.E., Gutsche, Th., Faessler, A. and Vinh-Mau, R. (2002). Electromagnetic couplings of the ChPT Lagrangian from the perturbative chiral quark model. **Physical Review C** 65: 025202.

Lyubovitskij, V.E., Wang, P., Gutsche, Th., and Faessler, A. (2002). Strange nucleon form factors in the perturbative chiral quark model. **Physical Review C** 66: 055204.

Mayerhoff, M., et al. (1994). First measurement of the electric form factor of neutron in the exclusive quasielastic scattering of polarized electrons from polarized ^3He. **Physics Letter B** 327: 201.

Oset, E., Tegen, R., Weise, W. (1984). Nucleon charge form factors and chiral quark models. **Nuclear Physics A** 426: 456.

Ostrick, M., et al. (1999). Measurement of the neutron electric form factor $G_{E,n}$ in the quasifree $^2H(\vec{e}, e'\vec{n})p$ reaction. **Physical Review Letter** 83: 276.

Pumsa-ard, K., Lyubovitskij, V.E., Gutsche, Th., Faessler, A., and Cheedket, S. (2003). Electromagnetic nucleon-delta transition in the perturbative chiral quark model. **Physical Review C** 68: 015205.

Sachs, R. G. (1962). High-Energy Behavior of Nucleon Electromagnetic Form Factors. **Physical Review** 126: 2256.

Simkovic, F., Lyubovitskij, V.E., Gutsche, Th., Faessler, A., and Kovalenko, S. (2002). Neutrino mediated μ^--electron conversion in nuclei revisited . **Physics Letter B** 544: 121.

Simon, G. G., Borkowski, F., Schmitt, Ch., and Walther, V. H. (1980). The Structure of the Nucleons. **Zeitschrift für Naturforschung** 35a: 1.

Tegen, R., (1990). Relativistic harmonic oscillator potential for quarks in the nucleon. **Annals of Physics** 197: 439.

Théberge, S., Thomas, A. W., and Miller, G. A. (1980). Pionic corrections to the MIT bag model: The (3,3) resonance. **Physical Review D** 22: 2838.

Théberge, S., Thomas, A. W., and Miller, G. A. (1981). Cloudy bag model of the nucleon. **Physical Review D** 24: 216.

Théberge, S. and Thomas, A. W. (1983). Magnetic moments of the nucleon octet calculated in the cloudy bag model. **Nuclear Physics A** 393: 252.

Thomas, A. W. (1984). Chiral symmetry and the bag model: A new starting point for nuclear physics. **Advanced in Nuclear Physics** 13: 1.

Thomas, A. W., and Weise, W. (2001). **The structure of the nucleon**. WILEY-VCH Verlag, Berlin.

Weinberg, S. (1979). Phenomenological Lagrangians. **Physica A** 96: 327.

Appendices

Appendix A

Solutions of the Dirac equation

We start with the static potential of the form $V_{eff} = S(r) + \gamma^0 V(r)$ where $S(r)$ and $V(r)$ are given by

$$
\begin{aligned}
S(r) &= \frac{1-3\rho^2}{2\rho R} + \frac{\rho}{2R^3}r^2 \\
V(r) &= \mathcal{E}_0 - \frac{1+3\rho^2}{2\rho R} + \frac{\rho}{2R^3}r^2
\end{aligned}
\tag{A.1}
$$

The quark wave function $u_\alpha(\vec{x})$ in the state α with the eigen-energy $\mathcal{E}_\alpha$ satisfies the Dirac equation

$$
[-i\vec{\alpha} \cdot \vec{\nabla} + \beta S(r) + V(r) - \mathcal{E}_\alpha]u_\alpha(\vec{x}) = 0
\tag{A.2}
$$

where $r = |\vec{x}|$ and $u_\alpha(\vec{x})$ is in the form

$$
u_\alpha(\vec{x}) = N_\alpha \begin{pmatrix} g_\alpha(r) \\ i\vec{\sigma} \cdot \hat{r} f_\alpha(r) \end{pmatrix} \mathcal{Y}_\alpha(\hat{r})\chi_f\chi_c
\tag{A.3}
$$

where $\hat{r} = \vec{x}/|\vec{x}|$ and

$$
g_\alpha(r) = \left(\frac{r}{R_\alpha}\right)^l L_{n-1}^{l+1/2}(\frac{r^2}{R_\alpha^2})e^{-\frac{r^2}{2R_\alpha^2}}.
\tag{A.4}
$$

For $j = l + 1/2$

$$
f_\alpha(r) = \rho_\alpha \left(\frac{r}{R_\alpha}\right)^{l+1} \left[L_{n-1}^{l+3/2}(\frac{r^2}{R_\alpha^2}) + L_{n-2}^{l+3/2}(\frac{r^2}{R_\alpha^2})\right] e^{-\frac{r^2}{2R_\alpha^2}},
\tag{A.5}
$$

and for $j = l - 1/2$

$$
f_\alpha(r) = -\rho_\alpha \left(\frac{r}{R_\alpha}\right)^{l-1} \left[(n+l-\frac{1}{2})L_{n-1}^{l-1/2}(\frac{r^2}{R_\alpha^2}) + nL_n^{l-1/2}(\frac{r^2}{R_\alpha^2})\right] e^{-\frac{r^2}{2R_\alpha^2}},
\tag{A.6}
$$

$\alpha = (nljm)$ is the state with the quantum number n, l, j, and m with $n = 1, 2, 3, \ldots; l = 0, 1, 2, \ldots; j = l \pm \frac{1}{2}$ and $m = -j, -j + 1, \ldots, j - 1, j$ represent the principle, the orbital angular momentum, the total angular momentum and its projection in the z-direction, respectively. $L_n^k(x)$ is the associated Laguerre polynomial

$$L_n^k(x) = \sum_{m=0}^{n} (-1)^m \frac{(n+k)!}{(n-m)!(k+m)!m!} x^m. \qquad (A.7)$$

The angular dependence of the wave function, $\mathcal{Y}_\alpha(\hat{r}) \equiv \mathcal{Y}_{lmj}(\hat{r})$, is

$$\mathcal{Y}_{lmj}(\hat{r}) = \sum_{m_l, m_s} (lm_l \frac{1}{2} m_s | jm) Y_{lm_l}(\hat{r}) \chi_{\frac{1}{2}m_s} \qquad (A.8)$$

where $\mathcal{Y}_{lmj}(\hat{r})$ is the usual spherical harmonic. The coupling between the orbital, $Y_{lm_l}(\hat{r})$ and the spin $\chi_{\frac{1}{2}m_s}$ angular momentum are determined with the help of the Clebsch-Gordan coefficients $(lm_l \frac{1}{2} m_s | jm)$. The flavor and the color part of the wave function are represent by χ_f and χ_c, respectively. The normalization constant is obtained from the condition

$$\int_0^\infty d^3 x u_\alpha^\dagger(\vec{x}) u_\alpha(\vec{x}) = 1 \qquad (A.9)$$

which gives

$$N_\alpha = \left[2^{-2(n+l+1/2)} \pi^{1/2} R_\alpha^3 \frac{(2n+2l)!}{(n+l)!(n-1)!} \{ 1 + \rho_\alpha^2 (2n + l - \frac{1}{2}) \} \right]^{-1/2} \qquad (A.10)$$

The other two parameters R_α and ρ_α are in the form

$$R_\alpha = R(1 + \Delta\mathcal{E}_\alpha \rho R)^{-1/4}, \qquad (A.11)$$

$$\rho_\alpha = \rho \left(\frac{R_\alpha}{R} \right)^3 \qquad (A.12)$$

which are related to the Gausian ansatz parameters ρ, R, and $\Delta\mathcal{E}_\alpha$ is the difference between an energy in the state α and the ground state energy, $\Delta\mathcal{E}_\alpha = \mathcal{E}_\alpha - \mathcal{E}_0$.

$\Delta\mathcal{E}_\alpha$ depends on the quantum numbers n and l and is related to the parameters ρ and R by

$$(\Delta\mathcal{E}_\alpha + \frac{3\rho}{R})^3(\Delta\mathcal{E}_\alpha + \frac{1}{\rho R}) = \frac{\rho}{R^3}(4n + 2l - 1)^2. \qquad \text{(A.13)}$$

The ground state $(1s^{1/2})$, we label as $\alpha = 0 \longrightarrow (n = 1, l = 0, j = 1/2)$. The ground state energy is $\mathcal{E}_0$ and the ground state wave function, $u_0(\vec{x})$, is given by

$$
\begin{aligned}
u_0(\vec{x}) &= N e^{-\frac{\vec{x}^2}{2R^2}} \begin{pmatrix} 1 \\ i\rho\vec{\sigma}\cdot\vec{x}/R \end{pmatrix} \chi_s\chi_f\chi_c, \\
N &= \left[\pi^{3/2}R^3(1 + \frac{3\rho^2}{2})\right]^{-1/2}
\end{aligned}
\qquad \text{(A.14)}
$$

Appendix B

Renormalized PCQM Lagrangian

B.1 Perturbation theory and nucleon mass

Before setting out to present the renormalization scheme of the PCQM, we first define and discuss the quantities, relevant for mass and wave function renormalization. Following the Gell-Mann and Low theorem (Gell-Mann and Low, 1951) we define the mass shift of the nucleonic three-quark ground state Δm_N due to the interaction with Goldstone mesons as

$$\Delta m_N = {}^N\!<\phi_0| \sum_{n=1}^{\infty} \frac{i^n}{n!} \int i\delta(t_1)d^4x_1...d^4x_n T\left[\mathcal{L}_I(x_1)...\mathcal{L}_I(x_n)\right]|\phi_0>_c^N . \quad \text{(B.1)}$$

In Eq.(B.1) the strong interaction Lagrangian $\mathcal{L}_I$ treated as a perturbation is defined as

$$\mathcal{L}_I(x) = -\bar{\psi}(x)i\gamma^5\frac{\hat{\Phi}(x)}{F}S(r)\psi(x) \quad \text{(B.2)}$$

and subscript c refers to contributions from connected graphs only. We evaluate Eq.(B.1) at one loop to order $o(1/F^2)$ using Wick's theorem and the appropriate propagators. For the quark field we use a Feymann propagator for a fermion in a binding potential. By restricting the summation over intermediate quark states to the ground state we get

$$\begin{aligned} iG_\psi(x,y) &= <\phi_0|T\left\{\psi(x)\bar{\psi}(y)\right\}|\phi_0> \\ &= u_0(\vec{x})\bar{u}_0(\vec{y})\exp\left[-i\mathcal{E}_0(x_0-y_0)\right]\Theta(x_0-y_0). \end{aligned} \quad \text{(B.3)}$$

For meson fields we use the free Feynman propagator for a boson field with

$$i\Delta_{ij}(x-y) = < 0|T\Phi_i(x)\Phi_j(y)|0 > = \delta_{ij} \int \frac{d^4k}{(2\pi)^4 i} \frac{\exp[-ik(x-y)]}{M_\Phi^2 - k^2 - i\epsilon}. \qquad (B.4)$$

Superscript N in Eq.(B.1) indicates that the matrix elements are projected on the respective nucleon states. The nucleon wave function $|N>$ is conventionally set up by the product of the SU(6) spin-flavor WF and $SU(3)_c$ color WF (Close, 1979), where the nonrelativistic single quark spin w.f. is replaced by the relativistic ground state solution of Eq.(2.4). Projection of one-body diagrams on the nucleon state refers to

$$\chi_{f'}^\dagger \chi_{s'}^\dagger I^{f'f} J^{s's} \chi_f \chi_s \quad \longrightarrow \quad < N| \sum_{i=1}^3 (IJ)^{(i)} |N > \qquad (B.5)$$

where the single particle matrix element of the opertors I and J, acting in flavor and spin space, is replaced by the one embedded in the nucleon state. For two-body diagrams with two independent quark indices i and j the projection precription reads as

$$\chi_{f'}^\dagger \chi_{s'}^\dagger I_1^{f'f} J_1^{s's} \chi_f \chi_s \otimes \chi_{k'}^\dagger \chi_{\sigma'}^\dagger I_2^{k'k} J_2^{\sigma'\sigma} \chi_f \chi_s \quad \longrightarrow \quad < N| \sum_{i \neq j}^3 (I_1 J_1)^{(i)} \otimes (I_2 J_2)^{(j)} |N > .$$
$$(B.6)$$

The total nucleon mass is given by $m_N^r = m_N^{core} + \Delta m_N$. Superscript r refers to the renormalized value of the nucleon mass at one loop, that is the order of accuracy we are working in. The diagrams that contribute to the nucleon mass shift Δm_N at one loop are shown in Fig.B.1: meson cloud (Fig.B.1a) and meson exchange diagrams (Fig.B.1b). The explicit expression for the nucleon mass including one-loop corrections is given by

$$m_N^r = m_N^{core} + \Delta m_N = 3(\mathcal{E}_0 + \gamma \hat{m}) + \sum_{\Phi=\pi,K,\eta} d_N^\Phi \Pi(M_\Phi^2) \qquad (B.7)$$

$$\text{with} \quad d_N^\pi = \frac{171}{400}, \qquad d_N^K = \frac{6}{19} d_N^\eta = \frac{1}{57} d_N^\pi, \qquad (B.8)$$
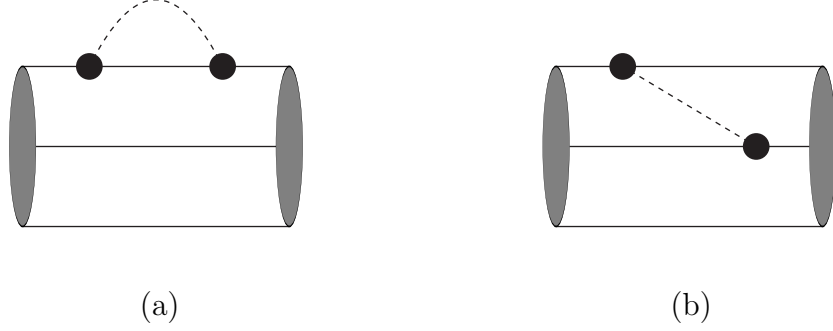
(a)   (b)

Figure B.1: Diagrams contributing to the nucleon mass: meson-cloud diagram (a), meson exchange diagram (b).

where d_N^Φ are the recoupling coefficients defining the partial contribution of the π, K, and η-meson cloud to the mass shift of the nucleon. For the following it is also useful to separately indicate the contributions to d_N^Φ from the meson cloud, $d_N^{\Phi;MC}$ and the meson exchange diagrams, $d_N^{\Phi;EX}$:

$$
\begin{aligned}
d_N^{\pi;MC} &= \frac{81}{400}, & d_N^{K;MC} \equiv d_N^K &= \frac{54}{400}, & d_N^{\eta;MC} &= \frac{9}{400} \\
\text{and } d_N^{\pi;EX} &= \frac{90}{400}, & d_N^{K;EX} &= 0, & d_N^{\eta;EX} &= -\frac{6}{400}.
\end{aligned}
\tag{B.9}
$$

The self-energy operators $\Pi(M_\Phi^2)$, corresponding to meson cloud contributions with definite flavor, differ only in their value for the meson mass and are given by

$$
\Pi(M_\Phi^2) = -\left(\frac{g_A}{\pi F}\right)^2 \int_0^\infty \frac{dp\, p^4}{w_\Phi^2(p^2)} F_{\pi NN}^2(p^2).
\tag{B.10}
$$

For a meson with three-momentum $\vec{p}$ the meson energy is $w_\Phi(p^2) = \sqrt{M_\Phi^2 + p^2}$ with $p = |\vec{p}|$ and $F_{\pi NN}(p^2)$ is the πNN form factor normalized to unity at zero recoil ($p^2 = 0$):

$$
F_{\pi NN}(p^2) = \exp\left(-\frac{p^2 R^2}{4}\right)\left\{1 + \frac{p^2 R^2}{8}\left(1 - \frac{5}{3g_A}\right)\right\}.
\tag{B.11}
$$

Finally, the effect of a finite current quark mass $\hat{m}$ on the nucleon mass shift is taken into account perturbatively (Lyubovitskij, Gutsche, Faessler, and Drukarev, 2001), resulting in the linear term $3\gamma\hat{m}$ in Eq. (B.7)

B.2 Renormalization of the PCQM

To redefine our perturbation series up to a given order in terms of renormalized quantities a set of counterterms $\delta\mathcal{L}$ has to be introduced in the Lagrangian. Thereby, the counterterms play a dual role: i) to maintain the proper definition of physical parameters, such as nucleon mass and, in particular, the nucleon charge and ii) to effectively reduce the number of Feynman diagrams to be evaluated.

B.2.1 Renormalization of the quark field

First, we introduce the renormalized quark field ψ^r with renormalized mass $\mathcal{M}^r$, substituting the original field ψ. Again, we restrict the expansion of the renormalized quark field to the ground state with

$$\psi_i^r(x; m_i^r) = b_0 u_0^r(\vec{x}; m_i^r) \exp\left(-i\mathcal{E}_0^r(m_i^r)t\right), \tag{B.12}$$

where i is the SU(3) flavor index; $\mathcal{E}_0^r(m_i^r)$ is the renormalized energy of the quark field in the ground state obtained from the solution of the Dirac equation

$$\left[-i\vec{\alpha}\cdot\vec{\nabla} + \beta m_i^r + \beta S(r) + V(r) - \mathcal{E}_0^r(m_i^r)\right] u_0^r(m_i^r) = 0. \tag{B.13}$$

Using the derivations of the Eq. (B.7), the renormalized mass m_i^r of the quark field is given by

$$\begin{aligned} m_u^r &= m_d^r = \hat{m}^r = \hat{m} - \delta m = \hat{m} + \frac{1}{3\gamma}\sum_{\Phi=\pi,K,\eta} d_N^{\Phi;MC}\Pi(M_\Phi^2), \\ m_s^r &= m_s - \delta m_s = m_s + \frac{2}{3\gamma}\left[d_N^{K;MC}\Pi(M_K^2) + 2d_N^{\eta;MC}\Pi(M_\eta^2)\right], \quad \text{(B.14)} \end{aligned}$$

The meson exchange contribution will be included when introducing nucleon renormalization. For the quark mass we will use in the following compact notation:

$$\mathcal{M}^r = diag\{\hat{m}^r, \hat{m}^r, m_s^r\} \quad \text{and} \quad \delta\mathcal{M} = diag\{\delta\hat{m}, \delta\hat{m}, \delta m_s\}. \quad \text{(B.15)}$$

The solutions of Eq.(B.13), $\mathcal{E}_0^r(m_i^r)$ and $u_0^r(\vec{x}; m_i^r)$, are functions of m_i^r. Obviously, the difference between nonstrange and strange quark solutions is solely due to the flavor dependent quark mass m_i^r. In the limit $m_i^r \to 0$ the solutions for nonstrange and strange quarks are degenerate: $\mathcal{E}_0^r(0) \equiv \mathcal{E}_0$ and $u_0^r(\vec{x}; 0) \equiv u_0(\vec{x})$. For the renormalized wave function $u_0^r(\vec{x}; m_i^r)$ we again consider the Gaussian ansatz

$$u_0^r(\vec{x}; m_i^r) = N(m_i^r) \exp\left[-c(m_i^r)\frac{\vec{x}^2}{2R^2}\right] \begin{pmatrix} 1 \\ i\rho(m_i^r)\vec{\sigma} \cdot \vec{x}/R \end{pmatrix} \chi_s \chi_f \chi_c \quad \text{(B.16)}$$

with normalization

$$\int d^3x u_0^{r\dagger}(\vec{x}; m_i^r) u_0^r(\vec{x}; m_i^r) \equiv 1. \quad \text{(B.17)}$$

In Eq.(B.16) the functions $N(m_i^r)$, $c(m_i^r)$ and $\rho(m_i^r)$ are normalized at the point $m_i^r = 0$ as follows:

$$N(0) = N, \qquad c(0) = 1, \qquad \rho(0) = \rho \quad \text{(B.18)}$$

The product $\rho(m_i^r)c(m_i^r)$ can be shown to be m_i^r-invariant and we therefore obtain the additional condition

$$\rho(m_i^r)c(m_i^r) \equiv \rho \quad \text{(B.19)}$$

Treating m_i^r as a small perturbation, Eq.(B.13) can be solved perturbatively, resulting in:

$$\mathcal{E}_0^r(m_i^r) = \mathcal{E}_0 + \delta\mathcal{E}_0(m_i^r) \quad \text{and} \quad u_0^r(\vec{x}; m_i^r) = u_0(\vec{x}) + \delta u_0(\vec{x}; m_i^r) \quad \text{(B.20)}$$

where

$$
\begin{aligned}
\delta\mathcal{E}_0(m_i^r) &= \gamma m_i^r \mathcal{E}_0 + \delta\mathcal{E}_0(m_i^r) \ \ \text{and} \\
\delta u_0^r(\vec{x}; m_i^r) &= \frac{m_i^r}{2}\frac{\rho R}{1+\frac{3}{2}\rho^2}\left(\frac{\frac{1}{2}+\frac{21}{4}\rho^2}{1+\frac{3}{2}\rho^2} - \frac{\vec{x}^2}{R^2} + \gamma^0\right)u_0(\vec{x}).
\end{aligned} \tag{B.21}
$$

For our set of model parameters the ground state quark energy $\mathcal{E}_0$ is about 400 MeV and for the energy corrections $\delta\mathcal{E}_0$ relative to $\mathcal{E}_0$ we obtain

$$
\left|\frac{\delta\mathcal{E}_0(\hat{m}^r)}{\mathcal{E}_0}\right| \approx 14\% \ \ \text{and} \ \ \left|\frac{\delta\mathcal{E}_0(m_s^r)}{\mathcal{E}_0}\right| \approx 18\%. \tag{B.22}
$$

Given the small corrections expressed in Eq.(B.22), the perturbative treatment of a finite (renormalized) quark mass is a meaningful procedure.

B.2.2 Renormalized effective Lagrangian

Having set up renormalized fields and masses for the quarks we are in the position to rewrite the original Lagrangian. The renormalized effective Lagrangian including the photon field A_μ is now written as

$$
\mathcal{L}_{full}^r = \mathcal{L}_\psi^r + \mathcal{L}_\Phi + \mathcal{L}_{ph} + \mathcal{L}_{int}^r. \tag{B.23}
$$

The renormalized quark Lagrangian $\mathcal{L}_\psi^r$ defines free nucleon dynamics at one-loop with

$$
\begin{aligned}
\mathcal{L}_\psi^r &= \mathcal{L}_{\bar\psi\psi}^r + \mathcal{L}_{(\bar\psi\psi)^2}^r, \\
\mathcal{L}_{\bar\psi\psi}^r &= \bar\psi^r(x)[i\slashed{\partial} - \mathcal{M}^r - S(r) - \gamma^0 V(r)]\psi^r(x) \\
\mathcal{L}_{(\bar\psi\psi)^2}^r &= c_\pi \sum_{i=1}^{3}[\bar\psi^r(x)i\gamma^5\lambda_i\psi^r(x)]^2 + c_K \sum_{i=4}^{7}[\bar\psi^r(x)i\gamma^5\lambda_i\psi^r(x)]^2 \\
&\quad + c_\eta[\bar\psi^r(x)i\gamma^5\lambda_8\psi^r(x)]^2.
\end{aligned} \tag{B.24}
$$

The parameters $\delta\mathcal{M}$ of Eq.(B.15) guarantee the proper nucleon mass renormalization due to the meson cloud diagrams of Fig.(B.1a). The terms contained in $\mathcal{L}_{(\bar\psi\psi)^2}^r$

are introduced for the purpose of nucleon mass renormalization due to the meson exchange diagram of Fig.(B.1b). The corresponding renormalization parameters c_π, c_K and c_η are deduced from Eqs.(B.7) and (B.9) as

$$c_\Phi = -\frac{9}{200}\frac{(2\pi R^2)^{3/2}}{(1-\gamma^2)}\Pi(M_\Phi^2). \tag{B.25}$$

The free meson Lagrangian $\mathcal{L}_\Phi$ is written as

$$\mathcal{L}_\Phi = -\frac{1}{2}\sum_{i,j=1}^{8}\Phi_i(x)(\delta_{ij}\square + M_{ij}^2)\Phi_j(x) \tag{B.26}$$

where $\square = \partial^\mu\partial_\mu$ and M_{ij}^2 is the diagonal meson mass matrix with

$$
\begin{aligned}
M_{11}^2 &= M_{22}^2 = M_{33}^2 = M_\pi^2, & M_{44}^2 = M_{55}^2 = M_{66}^2 = M_{77}^2 = M_K^2, \\
M_{88}^2 &= M_\eta^2.
\end{aligned} \tag{B.27}
$$

For the photon field A_μ we have the kinetic term

$$\mathcal{L}_{ph} = -\frac{1}{4}F_{\mu\nu}(x)F^{\mu\nu}(x) \;\; \text{with} \;\; F_{\mu\nu} = \partial_\nu A_\mu(x) - \partial_\mu A_\nu. \tag{B.28}$$

The renormalized interaction Lagrangian $\mathcal{L}_{int}^r = \mathcal{L}_{str}^r + \mathcal{L}_{em}^r$ contains a part due to the strong

$$\mathcal{L}_{str}^r = \mathcal{L}_I^{str} + \delta\mathcal{L}^{str} \tag{B.29}$$

and the electromagnetic interaction

$$\mathcal{L}_{em}^r = \mathcal{L}_I^{em} + \delta\mathcal{L}^{em}. \tag{B.30}$$

The strong interaction term $\mathcal{L}_I^{str}$ is given by

$$\mathcal{L}_I^{str} = -\bar{\psi}^r(x)i\gamma^5\frac{\hat{\Phi}(x)}{F}S(r)\psi^r(x) \tag{B.31}$$

The interaction of mesons and quarks with the electromagnetic field is described by

$$
\begin{aligned}
\mathcal{L}_I^{em} &= -eA_\mu(x)\bar{\psi}^r(x)\gamma^\mu Q\psi^r(x) - eA_\mu(x)\sum_{i,j=1}^{8}\left[f_{3ij} + \frac{f_{8ij}}{\sqrt{3}}\right]\Phi_i(x)\partial^\mu\Phi_j(x) \\
&+ \frac{e^2}{2}A_\mu^2(x)\sum_{i=1,2,4,5}\Phi_i^2(x).
\end{aligned} \tag{B.32}
$$

The term $\mathcal{L}_I^{em}$ is generated by minimal substitution with

$$\partial_\mu \psi^r \to D_\mu \psi^r = \partial_\mu \psi^r + ie\mathcal{Q}A_\mu \psi^r,$$

$$\partial_\mu \Phi_i \to D_\mu \Phi_i = \partial_\mu \Phi_i + e\left[f_{3ij} + \frac{f_{8ij}}{\sqrt{3}}\right]A_\mu \Phi_j. \tag{B.33}$$

The set of counterterms, denoted by $\delta\mathcal{L}^{str}$ and $\delta\mathcal{L}^{em}$, is explicitly given by

$$\delta\mathcal{L}^{str} = \delta\mathcal{L}_1^{str} + \delta\mathcal{L}_2^{str} + \delta\mathcal{L}_3^{str},$$

with

$$\delta\mathcal{L}_1^{str} = \bar{\psi}^r(x)(Z-1)\left[i\not{\partial} - \mathcal{M}^r - S(r) - \gamma^0 V(r)\right]\psi^r(x),$$

$$\delta\mathcal{L}_2^{str} = -\bar{\psi}^r(x)\delta\mathcal{M}^r \psi^r(x),$$

$$\delta\mathcal{L}_3^{str} = -c_\pi \sum_{i=1}^{3}[\bar{\psi}^r(x)i\gamma^5\lambda_i\psi^r(x)]^2 - c_K \sum_{i=4}^{7}[\bar{\psi}^r(x)i\gamma^5\lambda_i\psi^r(x)]^2$$
$$-c_\eta[\bar{\psi}^r(x)i\gamma^5\lambda_8\psi^r(x)]^2,$$

and

$$\delta\mathcal{L}^{em} = -eA_\mu(x)\bar{\psi}^r(x)(Z-1)\gamma^\mu Q\psi^r(x). \tag{B.34}$$

Here, $Z = diag\{\hat{Z}, \hat{Z}, Z_s\}$ is the diagonal matrix of renormalization constants ($\hat{Z}$ for u,d-quark and Z_s for s-quark). The values of $\hat{Z}$ and Z_s are determined by the charge conservation condition. The simplest way to fix $\hat{Z}$ and Z_s is on the quark level. The same set of values for $\hat{Z}$ and Z_s is also obtained when requiring charge conservation on baryon level. Results for $\hat{Z}$ and Z_s will be discussed below.

Now we briefly explain the role of each counterterm and why the set of constants $\hat{Z}$ and Z_s is identical in $\delta\mathcal{L}_1^{str}$ and $\delta\mathcal{L}^{em}$. The counterterm $\delta\mathcal{L}^{em}$ is introduced to guarantee charge conservation. The counterterm $\delta\mathcal{L}_1^{str}$, containing the same renormaliztion constants $\hat{Z}$ and Z_s as in $\delta\mathcal{L}^{em}$, is added to fulfil electromagnetic local gauge invariance on the Lagrangian level. The same term also leads to conservation of the vector current (baryon number conservation). Alternatively, $\delta\mathcal{L}^{em}$ can also be deduced from $\delta\mathcal{L}_1^{str}$ by minimal substitution. In covariant the-

ories the equality of the renomalization constants in $\delta\mathcal{L}_1^{str}$ and $\delta\mathcal{L}^{em}$ is known as the Ward identity. The counterterms $\delta\mathcal{L}_2^{str}$ and $\delta\mathcal{L}_3^{str}$ compensate the contributions of the meson cloud (Fig.B.1a) and meson exchange diagrams (Fig.B.1b) to the nucleon mass m_N^r (The contribution of meson cloud and exchange diagrams is already taken into account in the renormalized quark Lagrangian $\mathcal{L}_\psi^r$).

B.2.3   Renormalization of nucleon mass and charge

Now we illustrate the explicit role of the counterterms when performing the calculation of the nucleon mass and the nucleon charge. The renormalized nucleon mass m_N^r is defined by the expectation value of the Hamiltonian $\mathcal{H}_\psi^r$ (as derived from the Lagrangian $\mathcal{L}_\psi^r$) averaged over state $|\phi_0>$ and projected on the respective nucleon states:

$$m_N^r \equiv {}^N\!\!<\phi_0|\int \delta(t)d^4x \mathcal{H}_\psi^r(x)|\phi_0>^N,\qquad(\text{B.35})$$

By inclusion of the counterterms the strong interaction Lagrangian $\mathcal{L}_\psi^r$ should give a zero contribution to the shift of the renormalized nucleon mass at one loop, that is

$$
\begin{aligned}
\delta m_N^r &= {}^N\!\!<\phi_0|\sum_{n=1}^2 \frac{i^n}{n!}\int \delta(t_1)d^4x_1\ldots d^4x_n T[\mathcal{L}_r^{str}(x_1)\ldots\mathcal{L}_r^{str}(x_n)]|\phi_0>_c^N,\\
&= {}^N\!\!<\phi_0|-\frac{i}{2}\int \delta(t_1)d^4x_1 d^4x_2 T[\mathcal{L}_r^{str}(x_1)\mathcal{L}_r^{str}(x_2)]|\phi_0>_c^N,\\
&\quad -{}^N\!\!<\phi_0|\int \delta(t)d^4x \sum_{i=1}^3 \delta\mathcal{L}_i^{str}(x)|\phi_0>^N\equiv 0.\qquad(\text{B.36})
\end{aligned}
$$

The propagator of the renormalized quark field ψ^r is given by

$$
\begin{aligned}
iG_{\psi^r}(x,y) &= <\phi_0|T\{\psi^r(x)\bar\psi^r(y)\}|\phi_0>\\
&= u_0^r(\vec{x})\bar u_0^r(\vec{y})\exp[-i\mathcal{E}_0^r(x_0-y_0)]\theta(x_0-y_0).\qquad(\text{B.37})
\end{aligned}
$$

It differs from the unperturbed quark propagator $iG_{\psi^r}(x,y)$ by terms of order $\hat m^r$, which in turn only contribute to the two-loop calculations. Thus, to the order of

accuracy we are working in (up to one-loop perturbation theory) it is sufficient to use the unperturbed quark propagator $iG_\psi(x,y)$ instead of the renormalized one.

To prove Eq.(B.36), we first note that the contribution of the counterterm $\delta\mathcal{L}_1^{str}$ is equal to zero due to the equation of motion Eq.(B.13), that is

$$^N\!\!< \phi_0| \int \delta(t)d^4x\delta\mathcal{L}_1^{str}(x)|\phi_0 >^N \equiv 0. \tag{B.38}$$

The counterterms $\delta\mathcal{L}_2^{str}$ and $\delta\mathcal{L}_3^{str}$ compensate the contribution of the meson cloud (Fig.B.1a) and exchange diagrams (Fig.B.1b), respectively, with

$$^N\!\!< \phi_0| -\frac{i}{2} \int \delta(t_1)d^4x_1 d^4x_2 T[\mathcal{L}_r^{str}(x_1)\mathcal{L}_r^{str}(x_2)]|\phi_0 >_c^N$$
$$-^N\!\!< \phi_0| \int \delta(t)d^4x[\delta\mathcal{L}_2^{str}(x) + \delta\mathcal{L}_3^{str}(x)]|\phi_0 >^N \equiv 0, \tag{B.39}$$

hence Eq.(B.36) is fulfilled. The calculation of the nucleon mass m_N^r at one-loop can then either be done with the unrenormalized Lagrangian $\mathcal{L}_{eff}$ or with the renormalized version $\mathcal{L}_{full}^r$ Eq.(B.23). Both results for m_N^r are identical and are given by Eq.(B.7).

Now we consider the nucleon charge and prove that the properly introduced counterterms guarantee charge conservation. Using Noether's theorem we first derive from the renormalized Lagrangian Eq.(B.23) the electromagnetic, renormalized current operator:

$$j_r^\mu = j_{\psi^r}^\mu + j_\Phi^\mu + \delta j_{\psi^r}^\mu. \tag{B.40}$$

It contains the quark component $j_{\psi^r}^\mu$, the charged meson component j_Φ^μ and the

contribution of the counterterm $\delta j^{\mu}_{\psi^r}$:

$$
\begin{aligned}
j^{\mu}_{\psi^r} &= \bar{\psi}^r \gamma^{\mu} \mathcal{Q} \psi^r \equiv \frac{1}{3}[2\bar{u}^r \gamma^{\mu} u^r - \bar{d}^r \gamma^{\mu} d^r - \bar{s}^r \gamma^{\mu} s^r], \\
j^{\mu}_{\Phi} &= \left[f_{3ij} + \frac{f_{8ij}}{\sqrt{3}}\right] \Phi_i \partial^{\mu} \Phi_j \equiv [\pi^- i\partial^{\mu}\pi^+ - \pi^+ i\partial^{\mu}\pi^- + K^- i\partial^{\mu}K^+ - K^+ i\partial^{\mu}K^-],
\end{aligned}
$$

and

$$
\delta j^{\mu}_{\psi^r} = \bar{\psi}^r (Z-1)\gamma^{\mu} \mathcal{Q} \psi^r \equiv \frac{1}{3}[2(\hat{Z}-1)\bar{u}^r \gamma^{\mu} u^r - (\hat{Z}-1)\bar{d}^r \gamma^{\mu} d^r - (Z_s-1)\bar{s}^r \gamma^{\mu} s^r].
$$

$$(B.41)$$

The renormalized nucleon charge Q^r_N at one loop is defined as

$$
Q^r_N = {}^N\!\!< \phi_0| \sum_{n=1}^{2} \frac{i^n}{n!} \int \delta(t_1) d^4x_1 \ldots d^4x_n T[\mathcal{L}^{str}_r(x_1) \ldots \mathcal{L}^{str}_r(x_n) j^0_r(x)]|\phi_0 >^N_c
$$

$$. \qquad (B.42)$$

Charge conservation requires that the nucleon charge is not changed after renormalization, that is

$$
Q^r_N \equiv Q_N = \begin{cases} 1 & \text{for} \quad N = p \quad \text{(proton)} \\ 0 & \text{for} \quad N = n \quad \text{(neutron)} \end{cases}
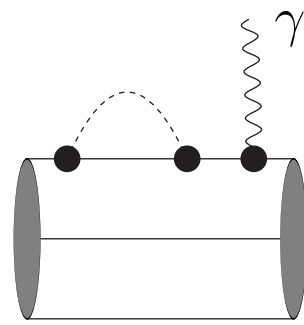$$

$$(B.43)$$

Thereby, Q_N is the nucleon charge in the three-quark core approximation, which is defined as the expectation value of the quark charge operator $\hat{Q}_{\psi} = \int d^3x j^0_{\psi}(x)$ taken between the unperturbed 3q-states $|\phi_0 >$:

$$
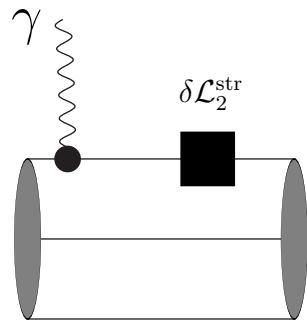Q_N = {}^N\!\!< \phi_0| \int \delta(t_1) d^4x j^0_{\psi}(x)|\phi_0 >^N .
$$

$$(B.44)$$

Eqs.(B.42) - (B.44) completely define *the charge conservation condition* within our approach.
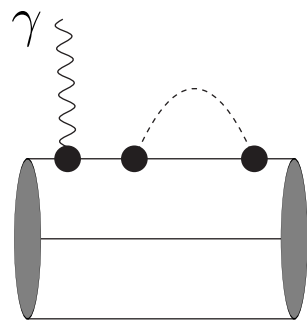
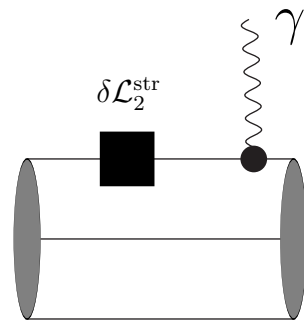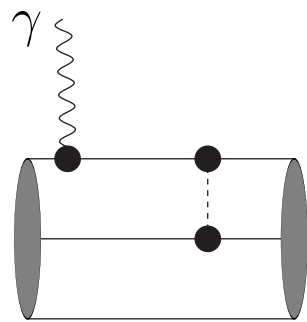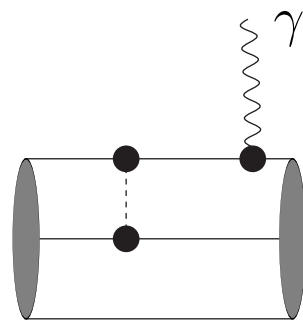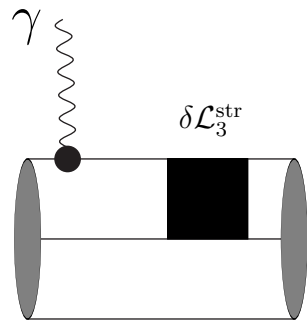Figure B.2: The self-energy diagrams, (a) - (b) and diagrams produced by the counterterm $\delta\mathcal{L}_2^{\mathrm{str}}$, (c) - (d)
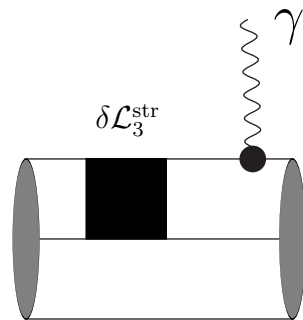
Figure B.3: The meson exchange current diagrams, (a) - (b) and diagrams produced by the counterterm $\delta\mathcal{L}_3^{\mathrm{str}}$, (c) - (d)

From nucleon charge conservation at one loop we obtain a condition on the renormalization constant $\hat{Z}$. To fix the constant Z_s we should consider the charge conservation of baryons containing s-quarks, e.g. Σ^+-baryon. In the one-loop approximation following diagrams contribute to the nucleon charge Q_N^r (see Fig.3.1): three-quark diagram (Fig.3.1a) with insertion of the quark current $j_{\psi^r}^\mu$, three-quark diagram (Fig.3.1b) with the counterterm $\delta j_{\psi^r}^\mu$ (three-quark counterterm diagram), meson-cloud diagram (Fig.3.1c) with the meson current j_Φ^μ, vertex correction diagram (Fig.3.1d) with the quark current $j_{\psi^r}^\mu$, self-energy diagrams (Figs. B.2a and B.2b) and exchange current diagrams (Figs. B.3a and B.2b) with insertion of the quark current $j_{\psi^r}^\mu$. We also obtain a set of diagrams (Figs. B.2a, B.2b, B.3a, and B.3b) generated by the counterterms $\delta\mathcal{L}_2^{str}(x)$ and $\delta\mathcal{L}_3^{str}(x)$. The contribution of the counterterm $\delta\mathcal{L}_1^{str}(x)$ is equal to zero due to the equation of motion (B.13). By definition of the counterterms $\delta\mathcal{L}_2^{str}(x)$ and $\delta\mathcal{L}_3^{str}(x)$, the self-energy and the meson exchange current diagrams of Figs. B.2a , B.2b, B.3a, and B.2b are compensated by the counterterm diagrams of Figs. B.2c , B.2d, B.3c , and B.3d respectively.

The contribution of the three-quark diagram (Fig.3.1a) to the nucleon charge is trivially given by

$$Q_N^{r;a} = {}^N\!\!< \phi_0| \int \delta(t)d^4x j_{\psi^r}^0(x)|\phi_0 >^N \equiv Q_N. \qquad (B.45)$$

The three-quark counterterm diagram (Fig.3.1b) is simply related to the one of Fig.3.1a with:

$$Q_N^{r;b} = (\hat{Z} - 1)^N\!\!< \phi_0| \int \delta(t)d^4x j_{\psi^r}^0(x)|\phi_0 >^N \equiv (\hat{Z} - 1)Q_N. \qquad (B.46)$$

The meson cloud diagram (Fig.3.1c) generates the term

$$Q_N^{r;c} = \frac{27}{400}\left(\frac{g_A}{\pi F}\right)^2 \int_0^\infty dp\, p^4 F_{\pi NN}^2(p^2) \sum_{\Phi=\pi,K} \frac{q_N^{\Phi;c}}{w_\Phi^3(p^2)} \qquad (B.47)$$

where

$$
q_N^{\pi;c} = \begin{cases} \frac{2}{3} & \text{for} \;\; N = p \\[2em] -\frac{2}{3} & \text{for} \;\; N = n \end{cases} \;\;,\;\;\; q_N^{K;c} = \begin{cases} \frac{4}{3} & \text{for} \;\; N = p \\[2em] \frac{2}{3} & \text{for} \;\; N = n \end{cases} \;\;.
$$

The contribution of the vertex correction diagram (Fig.3.1d) is given by

$$
Q_N^{r;d} = \frac{27}{400} \left(\frac{g_A}{\pi F} \right)^2 \int_0^\infty dp\, p^4 F_{\pi NN}^2(p^2) \sum_{\Phi = \pi, K, \eta} \frac{q_N^{\Phi;d}}{w_\Phi^3(p^2)} \tag{B.48}
$$

where

$$
q_N^{\pi;d} = \begin{cases} \frac{1}{3} & \text{for} \;\; N = p \\[2em] \frac{2}{3} & \text{for} \;\; N = n \end{cases} \;,\;\; q_N^{K;d} = \begin{cases} -\frac{2}{3} & \text{for} \;\; N = p \\[2em] -\frac{2}{3} & \text{for} \;\; N = n \end{cases} \;,\;\; q_N^{\eta;d} = \begin{cases} \frac{1}{9} & \text{for} \;\; N = p \\[2em] 0 & \text{for} \;\; N = n \end{cases} \;.
$$

To guarantee charge conservation, the sum of meson-cloud and vertex correction diagrams

$$
Q_N^{r;b} + Q_N^{r;c} + Q_N^{r;d} \equiv 0. \tag{B.49}
$$

The last requirement fixes the value of the renormalization constant $\hat{Z}$ at one loop to

$$
\hat{Z} = 1 - \frac{27}{400} \left(\frac{g_A}{\pi F} \right)^2 \int_0^\infty dp\, p^4 F_{\pi NN}^2(p^2) \left\{ \frac{1}{w_\pi^3(p^2)} + \frac{2}{3 w_K^3(p^2)} + \frac{1}{9 w_\eta^3(p^2)} \right\}. \tag{B.50}
$$

In the two-flavor picture, that is when we restrict to the pion cloud contribution only, we obtain a value of $\hat{Z} = 0.9 \pm 0.02$ for our set of parameters. The contribution of kaon and η-meson loops to the constant $\hat{Z}$ is strongly suppressed due to the energy denominators in Eq.(B.50). In the three-flavor picture we get $\hat{Z} = 0.88 \pm 0.03$, which deviates only slightly from two-flavor result. The minor role of kaon and η-meson loop contributions to nucleon properties was also found in our

previous analysis of meson-nucleon sigma-terms (Lyubovitskij, Gutsche, Faessler and Drukarev, 2001). As already mentioned, the renormalization constant Z_s is fixed from the charge conservation of baryons containing strange quarks (e.g. Σ^+-baryon). Here we obtain the analytical result:

$$Z_s = 1 - \frac{27}{400} \left(\frac{g_A}{\pi F}\right)^2 \int_0^\infty dp\, p^4 F_{\pi NN}^2(p^2) \left\{ \frac{4}{3w_K^3(p^2)} + \frac{4}{9w_\eta^3(p^2)} \right\}. \qquad (B.51)$$

In the SU(3) flavor symmetry limit ($m_u = m_d = m_s$) both renormalization constants $\hat{Z}$ and Z_s are degenerate. Again, charge conservation within our approach is fulfilled both on the quark level (when we directly calculate the charge of u, d or s-quark at one loop) and on the baryon level. With the value of $\hat{Z}$ being close to unity for our set of parameters the perturbative treatment of the meson cloud is also justified.

Appendix C

The electromagnetic form factors in Breit frame

We use the kinematic notation $p' = (E, \vec{q}/2)$, $p = (E, -\vec{q}/2)$, $q = p' - p = (0, \vec{q})$ and $Q^2 = -q^2 = \vec{q}^2$. The electromagnetic current operator for the baryon J^μ can be written as

$$\langle B'(p')|J^\mu(0)|B(p)\rangle = \bar{u}_{B'}(p') \left[\gamma^\mu F_1^B(q^2) + \frac{i\sigma^{\mu\nu} q_\nu}{2m_B} F_2^B(q^2) \right] u_B(p)$$

$$= \bar{u}_{B'}(p')[\gamma^\mu F_1^B(q^2) + \{\gamma^\mu - \frac{1}{2m_B}(p' + p)^\mu\} F_2^B(q^2)] u_B(p)$$

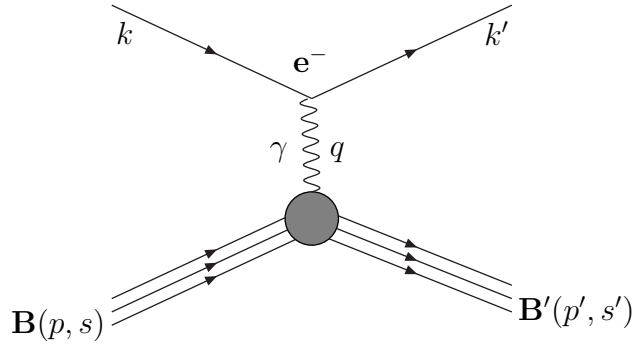$$= \bar{u}_{B'}(p')[\gamma^\mu \{F_1^B(q^2) + F_2^B(q^2)\} - \frac{1}{2m_B}(p' + p)^\mu F_2^B(q^2)] u_B \qquad \text{(C.1)}$$

Figure C.1: The elastic electron-baryon interaction

where

$$\bar{u}_{B'}(p')i\sigma^{\mu\nu}q_\nu u_B(p)$$

$$= \bar{u}_{B'}(p') \left[-\frac{1}{2}(\gamma^\mu\gamma^\nu - \gamma^\mu\gamma^\nu)(p'-p)_\nu \right] u_B(p)$$

$$= -\frac{1}{2}\bar{u}_{B'}(p')[\{(2g^{\mu\nu} - \gamma^\nu\gamma^\mu) - \gamma^\nu\gamma^\mu\}\, p'_\nu -$$

$$\{\gamma^\mu\gamma^\nu - (2g^{\mu\nu} - \gamma^\mu\gamma^\nu)\}\, p_\nu]u_B(p)$$

$$= -\frac{1}{2}\bar{u}_{B'}(p') \left[2p'^\mu - 2\gamma^\nu p'_\nu\gamma^\mu + 2p^\mu - 2\gamma^\mu\gamma^\nu p_\nu \right] u_B(p)$$

$$= -\bar{u}_{B'}(p') \left[p'^\mu - m_B\gamma^\mu + p^\mu - \gamma^\mu m_B \right] u_B(p)$$

$$= \bar{u}_{B'}(p') \left[2m_B\gamma^\mu - (p'+p)^\mu \right] u(p) \tag{C.2}$$

with

$$\bar{u}_{B'}(\gamma^\nu p_\nu - m_B) = 0 \rightarrow \bar{u}_{B'}\gamma^\nu p_\nu = m_B\bar{u}_{B'} \tag{C.3}$$

$$(\gamma^\nu p_\nu - m_B)u_B = 0 \rightarrow \gamma^\nu p_\nu u_B = m_B u_B \tag{C.4}$$

We define the Sachs form factors following

$$G_E^B(Q^2) \equiv F_1^B(q^2) + \frac{q^2}{4m_B^2}F_2^B(q^2) \tag{C.5}$$

$$G_M^B(Q^2) \equiv F_1^B(q^2) + F_2^B(q^2) \tag{C.6}$$

$G_E^B(Q^2)$ and $G_M^B(Q^2)$ are given separately as

$$\langle B'(p')|J^0(0)|B(p)\rangle = \{F_1^B(q^2) + F_2^B(q^2)\}\bar{u}_{B'}(p')\gamma^0 u_B(p)$$

$$-\frac{E}{m_B}F_2^B(q^2)]\bar{u}_{B'}(p')u_B(p)$$

$$= \{F_1^B(q^2) + F_2^B(q^2)\}\chi_{s'}^\dagger\chi_s - \frac{E}{m_B}F_2^B(q^2)\frac{E}{m_B}\chi_{s'}^\dagger\chi_s$$

$$= \{F_1^B(q^2) + (1 - \frac{E^2}{m_B^2})F_2^B(q^2)\}\chi_{s'}^\dagger\chi_s$$

$$= \{F_1^B(q^2) + \frac{q^2}{4m_B^2}F_2^B(q^2)\}\chi_{s'}^\dagger\chi_s$$

$$= G_E^B(Q^2)\chi_{s'}^\dagger\chi_s \qquad (C.7)$$

$$\langle B'(p')|\vec{J}(0)|B(p)\rangle = \{F_1^B(q^2) + F_2^B(q^2)\}\bar{u}_{B'}(p')\vec{\gamma}u_B(p)$$

$$= \{F_1^B(q^2) + F_2^B(q^2)\}\chi_{s'}^\dagger\frac{i\vec{\sigma}_B \times \vec{q}}{2m_B}\chi_s$$

$$= G_M^B(Q^2)\chi_{s'}^\dagger\frac{i\vec{\sigma}_B \times \vec{q}}{2m_B}\chi_s \qquad (C.8)$$

Here we have used the free solutions of the Dirac equation

$$u_B(p) = N \begin{pmatrix} 1 \\ \frac{\vec{\sigma} \cdot (-\vec{q}/2)}{E+m_B} \end{pmatrix} \chi_s, \qquad N = \sqrt{\frac{E+m_B}{2m_B}} \qquad (C.9)$$

$$\bar{u}_B(p) = N\chi_{s'}^{\dagger} \left(1, -\frac{\vec{\sigma} \cdot \vec{q}/2}{E+m_B}\right) \qquad (C.10)$$

$$\bar{u}_{B'}(p')\gamma^0 u_B(p) = N^2 \chi_{s'}^{\dagger} \left(1, -\frac{\vec{\sigma} \cdot \vec{q}/2}{E+m_B}\right) \begin{pmatrix} 1 & 0 \\ 0 & -1 \end{pmatrix}$$

$$\times \begin{pmatrix} 1 \\ \frac{\vec{\sigma} \cdot (-\vec{q}/2)}{E+m_B} \end{pmatrix} \chi_s$$

$$= \frac{E+m_B}{2m_B} \chi_{s'}^{\dagger} \left(1 - \frac{(\vec{\sigma} \cdot \vec{q}/2)^2}{(E+m_B)^2}\right) \chi_s$$

$$= \frac{m_B^2 + 2Em_B + (E^2 - \frac{\vec{q}^2}{4})}{2m_B(E+m_B)} \chi_{s'}^{\dagger} \chi_s$$

$$= \frac{m_B^2 + 2Em_B + m_B^2}{2m_B(E+m_B)} \chi_{s'}^{\dagger} \chi_s$$

$$= \chi_{s'}^{\dagger} \chi_s \qquad (C.11)$$

$$\bar{u}_{B'}(p')u_B(p) = N^2 \chi_{s'}^{\dagger} \left(1, -\frac{\vec{\sigma} \cdot \vec{q}/2}{E+m_B}\right) \begin{pmatrix} 1 \\ \frac{\vec{\sigma} \cdot (-\vec{q}/2)}{E+m_B} \end{pmatrix} \chi_s$$

$$= \frac{E+m_B}{2m_B} \chi_{s'}^{\dagger} \left(1 + \frac{(\vec{\sigma} \cdot \vec{q}/2)^2}{(E+m_B)^2}\right) \chi_s$$

$$= \frac{E^2 + 2Em_B + (m_B^2 + \frac{\vec{q}^2}{4})}{2m_B(E+m_B)} \chi_{s'}^{\dagger} \chi_s$$

$$= \frac{E}{m_B} \chi_{s'}^{\dagger} \chi_s \qquad (C.12)$$

$$\bar{u}_{B'}(p')\gamma^i u_B(p) = N^2\chi_{s'}^\dagger\left(1,-\frac{\vec{\sigma}\cdot\vec{q}/2}{E+m_B}\right)\begin{pmatrix} 0 & \sigma^i \\ -\sigma^i & 0 \end{pmatrix}$$

$$\times\begin{pmatrix} 1 \\ \frac{\vec{\sigma}\cdot(-\vec{q}/2)}{E+m_B} \end{pmatrix}\chi_s$$

$$= N^2\chi_{s'}^\dagger\left\{\sigma^i\frac{\vec{\sigma}\cdot(-\vec{q}/2)}{E+m_B}+\frac{\vec{\sigma}\cdot\vec{q}/2}{E+m_B}\sigma^i\right\}\chi_s$$

$$= \frac{1}{4m_B}\chi_{s'}^\dagger\left\{-\sigma^i(\vec{\sigma}\cdot\vec{q})+(\vec{\sigma}\cdot\vec{q})\sigma^i\right\}\chi_s$$

$$= \frac{1}{4m_B}\chi_{s'}^\dagger\left\{-\sigma^i\sigma^j q_j+\sigma^j q_j\sigma^i\right\}\chi_s$$

$$= \frac{1}{4m_B}\chi_{s'}^\dagger\left(-\sigma^i\sigma^j+\sigma^j\sigma^i\right)q_j\chi_s$$

$$= \frac{1}{4m_B}\chi_{s'}^\dagger\left(-i\epsilon^{ijk}\sigma^k+i\epsilon^{jik}\sigma^k\right)q_j\chi_s$$

$$= \frac{1}{4m_B}\chi_{s'}^\dagger\left(-i\epsilon^{ijk}\sigma^k+i\epsilon^{jik}\sigma^k\right)q_j\chi_s$$

$$= \frac{-i}{2m_B}\chi_{s'}^\dagger\epsilon^{ijk}\sigma^k q_j\chi_s$$

$$= \frac{1}{2m_B}\chi_{s'}^\dagger i(\vec{\sigma}\times\vec{q})^i\chi_s \qquad\text{(C.13)}$$

Appendix D

Calculation of the diagrams for the charge form factor

D.1 Three-quark diagram

$$\chi_{s'}^{\dagger}\chi_s G_E^B(Q^2)\Big|_{3q} = \langle\phi_0|\int \delta(t)d^4x e^{-iq\cdot x} : \mathcal{Q}\bar{\psi}^r(x)\gamma^0\psi^r(x): |\phi_0\rangle^B$$

$$= \langle\phi_0|b_0^{\dagger}\int \delta(t)d^4x e^{-iq\cdot x}\mathcal{Q}\bar{u}_0{}^r(\vec{x};m_i^r)e^{i\mathcal{E}_0^r t}\gamma^0 u_0^r(\vec{x};m_i^r)e^{-i\mathcal{E}_0^r t}b_0|\phi_0\rangle^B$$

$$= \langle\phi_0|b_0^{\dagger}\mathcal{Q}\left[\int d^3x u_0^{r\dagger}(\vec{x};m_i^r)u_0^r(\vec{x};m_i^r)e^{i\vec{q}\cdot\vec{x}}\right]b_0|\phi_0\rangle^B \tag{D.1}$$

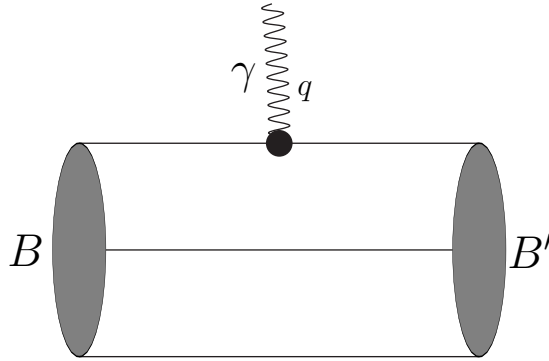

Figure D.1: The three-quark diagram

where

$$\psi^r(x; m_i^r) = b_0 u_0^r(\vec{x}; m_i^r) \exp[-i\mathcal{E}_0^r(m_i^r)t], \tag{D.2}$$

$$u_0^r(\vec{x}; m_i^r) = [1 + z(m_i^r)] \, u_0(\vec{x}) \tag{D.3}$$

$$z(m_i^r) = \frac{m_i^r}{2} \frac{\rho R}{1 + \frac{3}{2}\rho^2} \left(\frac{\frac{1}{2} + \frac{21}{4}\rho^2}{1 + \frac{3}{2}\rho^2} - \frac{\vec{x}^2}{R^2} + \gamma^0 \right) \tag{D.4}$$

$$u_0^{r\dagger}(\vec{x}; m_i^r) u_0^r(\vec{x}; m_i^r) = u_0^\dagger(\vec{x}) \left[1 + z(m_i^r) \right]^2 u_0(\vec{x})$$

$$= u_0^\dagger(\vec{x}) u_0(\vec{x}) + 2 u_0^\dagger(\vec{x}) z(m_i^r) u_0(\vec{x}) + o(m_i^{r2}) \tag{D.5}$$

D.1.1 Leading order term (LO)

$$\chi_{s'}^\dagger \chi_s G_E^B(Q^2) \Big|_{3q}^{LO} = \langle \phi_0 | b_0^\dagger \mathcal{Q} \left[\int d^3 x \, u_0^\dagger(\vec{x}) u_0(\vec{x}) e^{i\vec{q}\cdot\vec{x}} \right] b_0 | \phi_0 \rangle^B \tag{D.6}$$

By choosing the initial and the final state as the spin-up state, $G_E^B(Q^2) \Big|_{3q}^{LO}$ is obtained as:

$$G_E^B(Q^2) \Big|_{3q}^{LO} = a_1^B G_E^p(Q^2) \Big|_{3q}^{LO} \tag{D.7}$$

where

$$\int d^3x u_0^\dagger(\vec{x})u_0(\vec{x})e^{i\vec{q}\cdot\vec{x}} = \chi_{f'}^\dagger\chi_f G_E^p(Q^2)\Big|_{3q}^{LO}$$

$$= \exp\left(-\frac{Q^2R^2}{4}\right)\left(1 - \frac{\rho^2}{1+\frac{3}{2}\rho^2}\frac{Q^2R^2}{4}\right) \quad \text{(D.8)}$$

$$a_1^B = \langle\phi_0|b_0^\dagger\chi_{f'}^\dagger \mathcal{Q}\chi_f b_0|\phi_0\rangle^B$$

$$= \langle B(\uparrow)|\sum_{i=1}^{3}\mathcal{Q}(i)|B(\uparrow)\rangle \quad \text{(D.9)}$$

$$\mathcal{Q} = \begin{pmatrix} 2/3 & 0 & 0 \\ 0 & -1/3 & 0 \\ 0 & 0 & -1/3 \end{pmatrix} \quad \text{(D.10)}$$

D.1.2 Next-to-leading-order term (NLO)

$$\chi_{s'}^\dagger\chi_s G_E^B(Q^2)\Big|_{3q}^{NLO} = \langle\phi_0|b_0^\dagger\mathcal{Q}_i\left[2\int d^3x u_0^\dagger(\vec{x})z(m_i^r)u_0(\vec{x})e^{i\vec{q}\cdot\vec{x}}\right]b_0|\phi_0\rangle^B \quad \text{(D.11)}$$

$$G_E^B(Q^2)\Big|_{3q}^{NLO} = (a_2^B + a_3^B\varepsilon)G_E^p(Q^2)\Big|_{3q}^{NLO} \quad \text{(D.12)}$$

where

$$2\int d^3x u_0^\dagger(\vec{x})z(\hat{m}^r)u_0(\vec{x})e^{i\vec{q}\cdot\vec{x}} = \chi_{f'}^\dagger\chi_f G_E^p(Q^2)\Big|_{3q}^{NLO}$$

$$= \exp\left(-\frac{Q^2R^2}{4}\right)\hat{m}^r\frac{Q^2R^3\rho}{4(1+\frac{3}{2}\rho^2)^2}$$

$$\times\left(\frac{1+7\rho^2+\frac{15}{4}\rho^4}{1+\frac{3}{2}\rho^2}-\frac{Q^2R^2}{4}\rho^2\right) \quad (D.13)$$

$$\varepsilon = \frac{m_s^r}{\hat{m}^r} \quad (D.14)$$

$$a_2^B = \langle\phi_0|b_0^\dagger\chi_{f'}^\dagger\hat{\mathcal{Q}}\chi_f b_0|\phi_0\rangle^B$$

$$= \langle B(\uparrow)|\sum_{i=1}^{3}\hat{\mathcal{Q}}(i)|B(\uparrow)\rangle \quad (D.15)$$

$$a_3^B = \langle\phi_0|b_0^\dagger\chi_{f'}^\dagger\mathcal{Q}_s\chi_f b_0|\phi_0\rangle^B$$

$$= \langle B(\uparrow)|\sum_{i=1}^{3}\mathcal{Q}_s(i)|B(\uparrow)\rangle \quad (D.16)$$

$$\hat{\mathcal{Q}} = \begin{pmatrix} 2/3 & 0 & 0 \\ 0 & -1/3 & 0 \\ 0 & 0 & 0 \end{pmatrix} \quad (D.17)$$

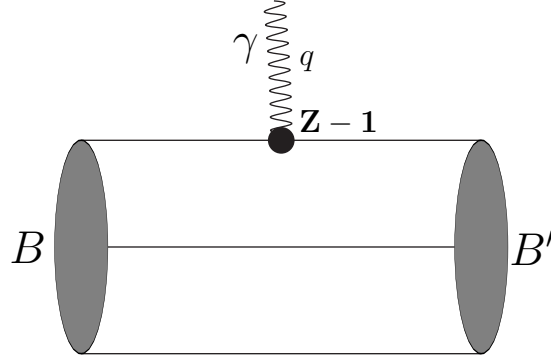$$\mathcal{Q}_s = \begin{pmatrix} 0 & 0 & 0 \\ 0 & 0 & 0 \\ 0 & 0 & -1/3 \end{pmatrix} \quad (D.18)$$

Figure D.2: The three-quark counterterm diagram

D.2 Three-quark counterterm

$$\chi_{s'}^{\dagger}\chi_s G_E^B(Q^2)\Big|_{CT} = \langle\phi_0| \int \delta(t)d^4x e^{-iq\cdot x} : \bar{\psi}(x)(Z-1)\gamma^0 \mathcal{Q}\psi(x) : |\phi_0\rangle^B$$

$$= \langle\phi_0|b_0^{\dagger}(Z_i-1)\mathcal{Q}_i \left[\int d^3x u_0^{\dagger}(\vec{x})u_0(\vec{x})e^{i\vec{q}\cdot\vec{x}}\right] b_0|\phi_0\rangle^B \tag{D.19}$$

$$G_E^B(Q^2)\Big|_{CT} = \left[a_2^B(\hat{Z}-1) + a_3^B(Z_s-1)\right] G_E^p(Q^2)\Big|_{3q}^{LO} \tag{D.20}$$
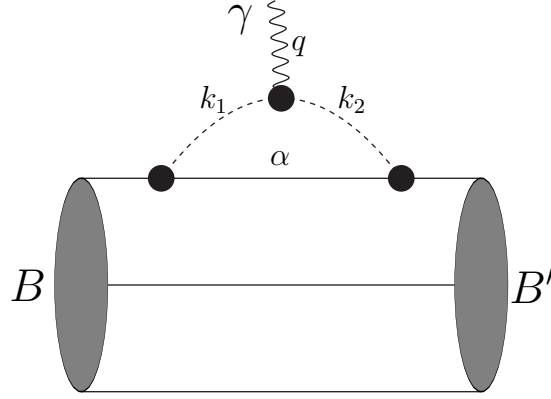
D.3 Meson cloud diagram

Figure D.3: The meson cloud diagram

$$\chi_{s'}^{\dagger}\chi_s G_E^B(Q^2)\Big|_{MC} = 4\langle\phi_0|\frac{i^2}{2!}\int \delta(t)d^4x d^4x_1 d^4x_2 e^{-iq\cdot x}$$

$$\times : [-\bar{\psi}i\gamma^5\frac{\lambda_k}{F}\Phi_k S\psi]_{x_1}[-\bar{\psi}i\gamma^5\frac{\lambda_l}{F}\Phi_l S\psi]_{x_2}[(f_{3ij}+\frac{f_{8ij}}{\sqrt{3}})\Phi_i\partial_t\Phi_j]_x :$$

$$\times |\phi_0\rangle^B \tag{D.21}$$

We use the wave function and the Feymann propagator for fermion and for boson following:

$$\psi_\alpha(x) = b_\alpha u_\alpha(\vec{x})e^{-i\mathcal{E}_\alpha t} \tag{D.22}$$

$$iG_\psi(x,y) = \langle\phi_0|T\{\psi(x)\bar{\psi}(y)\}|\phi_0\rangle$$

$$= \sum_\alpha u_\alpha(\vec{x})\bar{u}_\alpha(\vec{y})e^{-i\mathcal{E}_\alpha(x_0-y_0)}\Theta(x_0-y_0) \tag{D.23}$$

$$i\Delta_{ij}(x-y) = \langle 0|T\{\Phi_i(x)\Phi_j(y)\}|0\rangle$$

$$= \delta_{ij}\int\frac{d^4k}{(2\pi)^4 i}\frac{\exp[-ik(x-y)]}{M_\Phi^2-k^2-i\epsilon} \tag{D.24}$$

$$\chi_{s'}^{\dagger}\chi_s G_E^B(Q^2)\Big|_{MC}^{\alpha} = -\frac{2}{F^2}\langle\phi_0|b_0^{\dagger}\int\delta(t)d^4x d^4x_1 d^4x_2 e^{-iq\cdot x}$$

$$\times\bar{u}_0(\vec{x}_1)e^{i\mathcal{E}_0 t_1}i\gamma^5\lambda_l S(r_1)u_\alpha(\vec{x}_1)\bar{u}_\alpha(\vec{x}_2)e^{-i\mathcal{E}_\alpha(t_1-t_2)}\Theta(t_1-t_2)$$

$$\times i\gamma^5\lambda_m S(r_2)u_0(\vec{x}_2)e^{-i\mathcal{E}_0 t_2}(f_{3ij}+\frac{f_{8ij}}{\sqrt{3}})\delta_{il}\int\frac{d^4k_1}{(2\pi)^4 i}\frac{e^{-ik_1(x_1-x)}}{M_\Phi^2-k_1^2-i\epsilon}$$

$$\times\partial_t\{\delta_{jm}\int\frac{d^4k_2}{(2\pi)^4 i}\frac{e^{-ik_2(x-x_2)}}{M_\Phi^2-k_2^2-i\epsilon}\}b_0|\phi_0\rangle^B$$

$$=\frac{-2i}{(2\pi)^8 F^2}\langle\phi_0|b_0^{\dagger}\int d^3x d^4x_1 d^4x_2 d^4k_1 d^4k_2\Theta(t_1-t_2)e^{-i(\mathcal{E}_\alpha-\mathcal{E}_0)(t_1-t_2)}$$

$$\times\int dt\delta(t)e^{-ik_2^0(t-t_2)-ik_1^0(t_1-t)-iq^0 t}\left[\bar{u}_0(\vec{x}_1)i\gamma^5\lambda_i S(r_1)u_\alpha(\vec{x}_1)\right]$$

$$\times\left[\bar{u}_\alpha(\vec{x}_2)i\gamma^5\lambda_j S(r_2)u_0(\vec{x}_2)\right](f_{3ij}+\frac{f_{8ij}}{\sqrt{3}})$$

$$\times\frac{k_2^0 e^{-i\vec{q}\cdot\vec{x}+i\vec{k}_1\cdot(\vec{x}_1-\vec{x})+i\vec{k}_2\cdot(\vec{x}-\vec{x}_2)}}{[M_\Phi^2+\vec{k}_1^2-(k_1^0)^2-i\epsilon][M_\Phi^2+\vec{k}_2^2-(k_2^0)^2-i\epsilon]}b_0|\phi_0\rangle^B \tag{D.25}$$

$$
\chi_{s'}^{\dagger}\chi_s G_E^B(Q^2)\Big|_{MC}^{\alpha} = \frac{-2i}{(2\pi)^8 F^2}\langle\phi_0|b_0^{\dagger}\int d^3x_1 d^4x_2 d^4k_1 d^4k_2\left[\int d^3x e^{i(\vec{q}-\vec{k}_1+\vec{k}_2)\cdot\vec{x}}\right]
$$

$$
\times\left[\int dt_1 e^{-i(k_1^0+\Delta\mathcal{E}_\alpha)t_1}\Theta(t_1-t_2)\right]\left[\bar{u}_0(\vec{x}_1)i\gamma^5\lambda_i S(r_1)u_\alpha(\vec{x}_1)\right]
$$

$$
\times\left[\bar{u}_\alpha(\vec{x}_2)i\gamma^5\lambda_j S(r_2)u_0(\vec{x}_2)\right]e^{i(k_2^0+\Delta\mathcal{E}_\alpha)t_2}(f_{3ij}+\frac{f_{8ij}}{\sqrt{3}})
$$

$$
\times\frac{e^{i\vec{k}_1\cdot\vec{x}_1}}{\left[M_\Phi^2+\vec{k}_1^2-(k_1^0)^2-i\epsilon\right]}\frac{k_2^0 e^{-i\vec{k}_2\cdot\vec{x}_2}}{\left[M_\Phi^2+\vec{k}_2^2-(k_2^0)^2-i\epsilon\right]}b_0|\phi_0\rangle^B
$$

$$
= \frac{-2}{(2\pi)^5 F^2}\langle\phi_0|b_0^{\dagger}\int d^3x_1 d^3x_2 d^4k_2 dk_1^0\left[\int dt_2 e^{i(k_2^0-k_1^0)t_2}\right]
$$

$$
\times\left[\bar{u}_0(\vec{x}_1)i\gamma^5\lambda_i S(r_1)u_\alpha(\vec{x}_1)\right]\left[\bar{u}_\alpha(\vec{x}_2)i\gamma^5\lambda_j S(r_2)u_0(\vec{x}_2)\right]
$$

$$
\times(f_{3ij}+\frac{f_{8ij}}{\sqrt{3}})\left[\int d^3k_1\frac{\delta^{(3)}(\vec{q}-\vec{k}_1+\vec{k}_2)e^{i\vec{k}_1\cdot\vec{x}_1}}{M_\Phi^2+\vec{k}_1^2-(k_1^0)^2-i\epsilon}\right]
$$

$$
\times\frac{1}{[k_1^0+\Delta\mathcal{E}_\alpha-i\eta]}\frac{k_2^0 e^{-i\vec{k}_2\cdot\vec{x}_2}}{\left[M_\Phi^2+\vec{k}_2^2-(k_2^0)^2-i\epsilon\right]}b_0|\phi_0\rangle^B
$$

$$
= \frac{-2}{(2\pi)^4 F^2}\langle\phi_0|b_0^{\dagger}\int d^3k_2\left[\int d^3x_1\bar{u}_0(\vec{x}_1)i\gamma^5 S(r_1)u_\alpha(\vec{x}_1)e^{i\vec{k'}_2\cdot\vec{x}_1}\right]
$$

$$
\times\left[\int d^3x_2\bar{u}_\alpha(\vec{x}_2)i\gamma^5 S(r_2)u_0(\vec{x}_2)e^{-i\vec{k}_2\cdot\vec{x}_2}\right](f_{3ij}+\frac{f_{8ij}}{\sqrt{3}})\lambda_i\lambda_j
$$

$$
\times\int dk_2^0\frac{k_2^0}{[k_2^0+\Delta\mathcal{E}_\alpha-i\eta][(k_2^0)^2-\omega_\Phi^2(\vec{k}_2^2)+i\epsilon][(k_2^0)^2-\omega_\Phi^2(\vec{k'}_2^2)+i\epsilon]}
$$

$$
\times b_0|\phi_0\rangle^B,\text{where}\ \ \omega_\Phi(\vec{k}^2)=\sqrt{M_\Phi^2+\vec{k}^2}\ \ \text{and}\ \ \vec{k'}_2=\vec{q}+\vec{k}_2 \qquad (D.26)
$$

$$\chi_{s'}^{\dagger}\chi_s G_E^B(Q^2)\Big|_{MC}^{\alpha} = \frac{1}{(2\pi)^3 F^2}\langle\phi_0|b_0^{\dagger}\chi_{f'}^{\dagger}\chi_{s'}^{\dagger}$$

$$\times \int d^3k_2 \frac{R_{\alpha}^{\dagger}(\vec{k'}_2)R_{\alpha}(\vec{k}_2)[-i(f_{3ij}+\frac{f_{8ij}}{\sqrt{3}})\lambda_i\lambda_j]\vec{\sigma}\cdot\vec{k'}_2\vec{\sigma}\cdot\vec{k}_2}{[\omega_{\Phi}(\vec{k}_2^2)+\Delta\mathcal{E}_{\alpha}][\omega_{\Phi}(\vec{k'}_2^2)+\Delta\mathcal{E}_{\alpha}][\omega_{\Phi}(\vec{k}_2^2)+\omega_{\Phi}(\vec{k'}_2^2)]}$$

$$\times \chi_f\chi_s b_0|\phi_0\rangle^B \tag{D.27}$$

where

$$\int d^3x \bar{u}_{\alpha}(\vec{x})i\gamma^5 S(r)u_0(\vec{x})e^{-i\vec{k}\cdot\vec{x}} = R_{\alpha}(k)\chi_{f'}^{\dagger}\chi_{s'}^{\dagger}\vec{\sigma}\cdot\vec{k}\chi_f\chi_s, \quad k=|\vec{k}| \tag{D.28}$$

To simplify our expression , we define $x=\cos\theta=\frac{\vec{q}\cdot\vec{k}_2}{|\vec{q}||\vec{k}_2|}$, $p=|\vec{k}_2|$, $Q=|\vec{q}|$ and

$$y = |\vec{q}+\vec{k}_2| = \sqrt{p^2+Q^2+2pQx}, \tag{D.29}$$

$$\int d^3k_2 = \int_0^{\infty} p^2 dp \int_{-1}^{1} dx \int_0^{2\pi} d\phi, \tag{D.30}$$

$$\vec{\sigma}\cdot\vec{k'}_2\vec{\sigma}\cdot\vec{k}_2 = \vec{\sigma}\cdot(\vec{q}+\vec{k}_2)\vec{\sigma}\cdot\vec{k}_2$$

$$= (\vec{q}+\vec{k}_2)\cdot\vec{k}_2 + i\vec{\sigma}\cdot(\vec{q}\times\vec{k}_2), \tag{D.31}$$

$$C_{\alpha,\Phi}^{n_1 n_2}(p^2,Q^2,x) = \frac{2D_{\alpha,\Phi}^{n_1 n_2}}{\omega_{\Phi}(p^2)+\omega_{\Phi}(p^2+Q^2+2pQx)}, \tag{D.32}$$

$$D_{\alpha,\Phi}^{n_1 n_2}(p^2,Q^2,x) = \frac{1}{[\omega_{\Phi}(p^2)+\Delta\mathcal{E}_{\alpha}]^{n_1}[\omega_{\Phi}(y^2)+\Delta\mathcal{E}_{\alpha}]^{n_2}}. \tag{D.33}$$

The integration over the ϕ-angle makes the second term on the right hand side of

Eq.(D.31) vanish, so we keep only the first term that equals p^2+pQx. We also

define the following symbols

$$t_E^B(p^2, Q^2, x)\Big|_{MC}^{\alpha} = \langle\phi_0|b_0^\dagger\chi_{f'}^\dagger\chi_{s'}^\dagger[-\frac{i}{2}(f_{3ij} + \frac{f_{8ij}}{\sqrt{3}})\lambda_i\lambda_j]C_{\alpha,\Phi}^{11}(p^2, Q^2, x)\chi_f\chi_s b_0|\phi_0\rangle^B$$

$$= \sum_{i,j=1}^{8} C_{\alpha,\Phi_{i,j}}^{11}(p^2, Q^2, x)\langle B|\sum_{k=1}^{3}[-\frac{i}{2}(f_{3ij} + \frac{f_{8ij}}{\sqrt{3}})\lambda_i(k)\lambda_j(k)]|B\rangle,$$

$$= a_4^B C_{\alpha,\pi}^{11}(p^2, Q^2, x) + a_5^B C_{\alpha,K}^{11}(p^2, Q^2, x) \tag{D.34}$$

and

$$V_\alpha(p^2, Q^2, x) = R_\alpha^\dagger(y)R_\alpha(p). \tag{D.35}$$

The final expression is obtained by

$$G_E^B(Q^2)\Big|_{MC}^{\alpha} = \frac{1}{(2\pi F)^2}\int_0^\infty dp p^2 \int_{-1}^1 dx(p^2 + pQx)$$

$$\times V_\alpha(p^2, Q^2, x)t_E(p^2, Q^2, x)\Big|_{MC}^{\alpha}. \tag{D.36}$$

If we restrict the quark propagator to just only the ground state($\alpha = 0$), we have

$$R_0(p) = i\frac{3g_A}{10}F_{\pi NN}(p^2),$$

$$F_{\pi NN}(p^2) = \exp\left(-\frac{p^2 R^2}{4}\right)\left\{1 + \frac{p^2 R^2}{8}\left(1 - \frac{5}{3g_A}\right)\right\}, \tag{D.37}$$

and the charge form factor from the meson-cloud diagram $G_E^B(Q^2)\Big|_{MC}^{\alpha=0}$ is given by

$$G_E^B(Q^2)\Big|_{MC}^{\alpha=0} = \frac{9}{400}\left(\frac{g_A}{\pi F}\right)^2\int_0^\infty dp p^2 \int_{-1}^1 dx(p^2 + pQx)$$

$$\times\mathcal{F}_{\pi NN}(p^2, Q^2, x)t_E(p^2, Q^2, x)\Big|_{MC}^{\alpha=0} \tag{D.38}$$

where

$$\mathcal{F}_{\pi NN}(p, Q, x) = F_{\pi NN}(p^2)F_{\pi NN}(y^2). \tag{D.39}$$
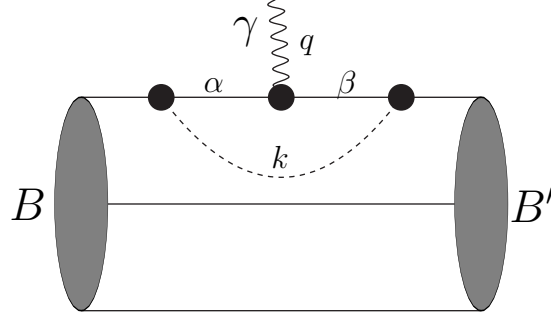
Figure D.4: The vertex correction diagram

D.4 Vertex correction diagram

$$
\chi_{s'}^{\dagger}\chi_s G_E^B(Q^2)\Big|_{VC}^{\alpha\beta} = 2\langle\phi_0|\frac{i^2}{2!}\int \delta(t)d^4x\,d^4x_1\,d^4x_2\,e^{-iq\cdot x}
$$

$$
\times : [-\bar{\psi}i\gamma^5\frac{\lambda_i}{F}\Phi_k S\psi]_{x_1}[-\bar{\psi}i\gamma^5\frac{\lambda_j}{F}\Phi_l S\psi]_{x_2}[\mathcal{Q}\bar{\psi}\gamma^0\psi]_x : |\phi_0\rangle^B
$$

$$
(D.40)
$$

$$\chi_{s'}^\dagger \chi_s G_E^B(Q^2)\Big|_{VC}^{\alpha\beta} = \frac{-1}{F^2} \langle\phi_0| \int \delta(t) d^4x\, d^4x_1\, d^4x_2\, e^{-iq\cdot x} : b_0^\dagger$$

$$\times \bar{u}_0(\vec{x_1}) e^{i\mathcal{E}_0 t_1} i\gamma^5 \lambda_i S(r_1) u_\alpha(\vec{x_1}) \bar{u}_\alpha(\vec{x}) e^{-i\mathcal{E}_\alpha(t_1-t)} \Theta(t_1 - t)$$

$$\times \mathcal{Q}\gamma^0 u_\beta(\vec{x}) \bar{u}_\beta(\vec{x_2}) e^{-i\mathcal{E}_\beta(t-t_2)} \Theta(t - t_2) i\gamma^5 \lambda_j S(r_2)$$

$$\times b_0 u_0(\vec{x_2}) e^{-i\mathcal{E}_0 t_2} \delta_{ij} \int \frac{d^4k}{(2\pi)^4 i} \frac{e^{-ik\cdot(x_1-x_2)}}{[M_{\Phi_j}^2 - k^2 - i\epsilon]} : |\phi_0\rangle^B$$

$$= \frac{i}{(2\pi)^4 F^2} \langle\phi_0| b_0^\dagger \int dt_1 dt_2 d^4k \int \delta(t) e^{-i(q^0 + \Delta\mathcal{E}_{\alpha\beta})t} \Theta(t_1 - t)$$

$$\times \Theta(t - t_2) \left[\int d^3x_1 \bar{u}_0(\vec{x_1}) i\gamma^5 S(r_1) u_\alpha(\vec{x_1} e^{i\vec{k}\cdot\vec{x_1}} \right]$$

$$\times \frac{\lambda_i \mathcal{Q} \lambda_i e^{-i(\Delta\mathcal{E}_{\alpha 0} + k^0)t_1} e^{i(\Delta\mathcal{E}_{\beta 0} + k^0)t_2}}{[M_{\Phi_i}^2 - k^2 - i\epsilon]} \left[\int d^3x \bar{u}_\alpha(x) \gamma^0 u_\beta(x) e^{i\vec{q}\cdot\vec{x}} \right]$$

$$\times \left[\int d^3x_2 \bar{u}_0(\vec{x_2}) i\gamma^5 S(r_2) u_\beta(\vec{x_2} e^{-i\vec{k}\cdot\vec{x_2}} \right] b_0 |\phi_0\rangle$$

$$= \frac{i}{(2\pi)^4 F^2} \langle\phi_0| b_0^\dagger \chi_{s'}^\dagger \chi_{f'}^\dagger \int d^4k \left[\int dt_1 e^{-i(\Delta\mathcal{E}_\alpha + k^0)t_1} \Theta(t_1) \right]$$

$$\times \left[\int dt_2 e^{i(\Delta\mathcal{E}_\beta + k^0)t_2} \Theta(-t_2) \right] R_\alpha^\dagger(\vec{k}) v_{\alpha\beta}(\vec{q}^2) R_\beta(\vec{k})$$

$$\times \frac{\lambda_i \mathcal{Q} \lambda_i}{[M_{\Phi_i}^2 + \vec{k}^2 - (k^0)^2 - i\epsilon]} \chi_s \chi_f b_0 |\phi_0\rangle^B \tag{D.41}$$

$$\chi_{s'}^\dagger \chi_s G_E^B(Q^2)\Big|_{VC}^{\alpha\beta} = \frac{1}{(2\pi)^4 F^2}\langle\phi_0|b_0^\dagger\chi_{s'}^\dagger\chi_{f'}^\dagger\int d^3k R_\alpha^\dagger(\vec{k})v_{\alpha\beta}(\vec{q}^2)R_\beta(\vec{k})\int dk^0$$

$$\times\frac{i\lambda_i\mathcal{Q}\lambda_i}{[k^0+\Delta\mathcal{E}_\alpha-i\eta'][k^0+\Delta\mathcal{E}_\beta-i\eta][(k^0)^2-\omega_\Phi(\vec{k}^2)^2-i\epsilon]}$$

$$\times\chi_s\chi_f b_0|\phi_0\rangle^B$$

$$= \frac{1}{2\pi^2 F^2}\int_0^\infty dp p^2 R_\alpha^\dagger(p)v_{\alpha\beta}(Q^2)R_\beta(p)t_E^B(p^2)\Big|_{VC}^{\alpha\beta} \tag{D.42}$$

where

$$v_{\alpha\beta}(\vec{k}^2) = \int d^3x \bar{u}_\alpha(x)\gamma^0 u_\beta(x)e^{i\vec{k}\cdot\vec{x}} \tag{D.43}$$

$$t_E^B(p^2)\Big|_{VC}^{\alpha\beta} = \langle\phi_0|b_0^\dagger\chi_{f'}^\dagger\chi_{s'}^\dagger\mathcal{Q}\lambda_i\lambda_j W_\Phi^{\alpha\beta}(p^2)\chi_f\chi_s b_0|\phi_0\rangle^B$$

$$= \sum_{i,j=1}^{8} W_{\Phi_{i,j}}^{\alpha\beta}(p^2)\langle B|\sum_{k=1}^{3}\mathcal{Q}\lambda_i(k)\lambda_j(k)|B\rangle,$$

$$= a_6^B W_\pi^{\alpha\beta}(p^2) + a_7^B W_K^{\alpha\beta}(p^2) + a_8^B W_\eta^{\alpha\beta}(p^2), \tag{D.44}$$

$$W_\Phi^{\alpha\beta}(p^2) = \frac{1}{\omega_\Phi(p^2)[\omega_\Phi(p^2)+\Delta\mathcal{E}_\alpha][\omega_\Phi(p^2)+\Delta\mathcal{E}_\beta]} \tag{D.45}$$

If we restrict the quark propagator just only to the ground state($\alpha = 0,\ \beta = 0$),

$$v_{00}(Q^2) = \int d^3x u_0^\dagger(x)u_0(x)e^{i\vec{q}\cdot\vec{x}}$$

$$= G_E^p(Q^2)\Big|_{3q}^{LO}, \tag{D.46}$$

and the contribution to the charge form factor from the vertex correction diagram
$G_E^B(Q^2)\big|_{VC}^{00}$ is given by

$$G_E^B(Q^2)\bigg|_{VC}^{00} = G_E^p(Q^2)\bigg|_{3q}^{LO} \cdot \frac{9}{200} \left(\frac{g_A}{\pi F}\right)^2 \int_0^\infty dp\, p^4 F_{\pi NN}^2(p^2) t_E^B(p^2)\bigg|_{VC}^{00} \quad (\text{D.47})$$

Appendix E

Calculation of the diagrams for the magnetic form factor

The diagrams contributing to the magnetic form factor are the same ones as for the case of the charge form factor and the meson-in-flight diagram in addition.

E.1 Three-quark diagram

$$\chi_{s'}^{\dagger} \frac{i\vec{\sigma}_B \times \vec{q}}{2m_B} \chi_s G_M^B(Q^2)\Big|_{3q} = \langle \phi_0| \int \delta(t) d^4x e^{-iq \cdot x} : \mathcal{Q}\bar{\psi}^r(x)\vec{\gamma}\psi^r(x) : |\phi_0\rangle^B$$

$$= \langle \phi_0|b_0^{\dagger} \int \delta(t) d^4x e^{-iq \cdot x} \mathcal{Q}\bar{u}_0^r(\vec{x}; m_i^r) e^{i\mathcal{E}_0^r t}\vec{\gamma}u_0^r(\vec{x}; m_i^r)e^{-i\mathcal{E}_0^r t}b_0|\phi_0\rangle^B$$

$$= \langle \phi_0|b_0^{\dagger} \int \delta(t) d^4x e^{-iq \cdot x} \mathcal{Q}u_0^{\dagger}(\vec{x}) \left[1 + \frac{m_i^r}{2} \frac{\rho R}{1 + \frac{3}{2}\rho^2} \left(\frac{\frac{1}{2} + \frac{21}{4}\rho^2}{1 + \frac{3}{2}\rho^2} - \frac{\vec{x}^2}{R^2} + \gamma^0\right)\right]$$

$$\times \gamma^0 \vec{\gamma} \left[1 + \frac{m_i^r}{2} \frac{\rho R}{1 + \frac{3}{2}\rho^2} \left(\frac{\frac{1}{2} + \frac{21}{4}\rho^2}{1 + \frac{3}{2}\rho^2} - \frac{\vec{x}^2}{R^2} + \gamma^0\right)\right] u_0(\vec{x})b_0|\phi_0\rangle^B$$

$$= \langle \phi_0|b_0^{\dagger} \int d^3x e^{-i\vec{q}\cdot\vec{x}} \mathcal{Q}u_0^{\dagger}(\vec{x})\gamma^0\vec{\gamma}u_0(\vec{x})$$

$$\times \left[1 + m_i^r \frac{\rho R}{1 + \frac{3}{2}\rho^2} \left(\frac{\frac{1}{2} + \frac{21}{4}\rho^2}{1 + \frac{3}{2}\rho^2} - \frac{\vec{x}^2}{R^2}\right) + o(m_i^{r2})\right] b_0|\phi_0\rangle^B \tag{E.1}$$

where

$$u_0^\dagger(\vec{x})\gamma^0\vec{\gamma}u_0(\vec{x}) = \chi_{f'}^\dagger\chi_{s'}^\dagger N^2 e^{-\frac{\vec{x}^2}{R^2}}\left(1, \frac{i\rho}{R}\vec{\sigma}\cdot\vec{x}\right)\begin{pmatrix} 0 & \vec{\sigma} \\ -\vec{\sigma} & 0 \end{pmatrix}$$

$$\times \begin{pmatrix} 1 \\ \frac{i\rho}{R}\vec{\sigma}\cdot\vec{x} \end{pmatrix}\chi_s\chi_f$$

$$= \chi_{f'}^\dagger\chi_{s'}^\dagger N^2 e^{-\frac{\vec{x}^2}{R^2}}\frac{\rho}{R}\left[\vec{\sigma}(\vec{\sigma}\cdot\vec{x}) - (\vec{\sigma}\cdot\vec{x})\vec{\sigma}\right]\chi_s\chi_f$$

$$= \chi_{f'}^\dagger\chi_{s'}^\dagger\frac{2\rho}{R}N^2 e^{-\frac{\vec{x}^2}{R^2}}\left(\vec{\sigma}\times\vec{x}\right)\chi_s\chi_f \qquad \text{(E.2)}$$

E.1.1 Leading order term (LO)

$$\chi_{s'}^\dagger\frac{i\vec{\sigma}_B\times\vec{q}}{2m_B}\chi_s G_M^B(Q^2)\bigg|_{3q}^{LO} = \langle\phi_0|b_0^\dagger\int d^3x\, e^{-i\vec{q}\cdot\vec{x}}\mathcal{Q}u_0^\dagger(\vec{x})\gamma^0\vec{\gamma}u_0(\vec{x})b_0|\phi_0\rangle^B$$

$$= \langle\phi_0|b_0^\dagger\chi_{f'}^\dagger\chi_{s'}^\dagger\mathcal{Q}\frac{2\rho}{R}N^2\int d^3x\, e^{-iq\cdot x}e^{-\frac{\vec{x}^2}{R^2}}\left(\vec{\sigma}\times\vec{x}\right)\chi_s\chi_f b_0|\phi_0\rangle^B$$

$$= \langle\phi_0|b_0^\dagger\chi_{f'}^\dagger\chi_{s'}^\dagger\mathcal{Q}\frac{2\rho}{R}N^2(-i\vec{\sigma}\times\vec{q})\frac{1}{q}\frac{\partial}{\partial q}\int d^3x\, e^{-iq\cdot x}e^{-\frac{\vec{x}^2}{R^2}}\chi_s\chi_f b_0|\phi_0\rangle^B$$

$$= -i\langle\phi_0|b_0^\dagger\chi_{f'}^\dagger\chi_{s'}^\dagger\mathcal{Q}(\vec{\sigma}\times\vec{q})\chi_s\chi_f b_0|\phi_0\rangle^B\left\{\frac{2\rho N^2}{qR}\frac{\partial}{\partial q}\frac{\exp\left(-\frac{Q^2R^2}{4}\right)}{N^2(1+\frac{3}{2}\rho^2)}\right\}$$

$$= i\langle B|\sum_{i=1}^{3}\mathcal{Q}(i)\vec{\sigma}(i)\times\vec{q}|B\rangle\frac{\rho R}{1+\frac{3}{2}\rho^2}\exp\left(-\frac{Q^2R^2}{4}\right). \qquad \text{(E.3)}$$

By choosing $\vec{q} = q\hat{j} \longrightarrow \vec{\sigma} \times \vec{q} = -\sigma_3 q\hat{i} + \sigma_1 q\hat{k}$, then

$$
\begin{aligned}
\langle B| \sum_{i=1}^{3} \mathcal{Q}(i)\vec{\sigma}(i) \times \vec{q}|B\rangle &= -q\langle B| \sum_{i=1}^{3} \mathcal{Q}(i)\sigma_3(i)|B\rangle\hat{i} + q\langle B| \sum_{i=1}^{3} \mathcal{Q}(i)\sigma_1(i)|B\rangle\hat{k} \\
&= -q\langle B| \sum_{i=1}^{3} \mathcal{Q}(i)\sigma_3(i)|B\rangle\hat{i} \quad\quad\quad\quad\quad\quad (\text{E.4})
\end{aligned}
$$

σ_1 is spin-flip operator and in our case the final state and initial state are the same spin state, so that the second term on the right-hand side vanishes. By the same way we get

$$
\begin{aligned}
\chi_{s'}^{\dagger} \frac{i\vec{\sigma}_B \times \vec{q}}{2m_B} \chi_s &= -\frac{iq}{2m_B}\chi_{s'}^{\dagger}\sigma_3\chi_s\hat{i} + \frac{iq}{2m_B}\chi_{s'}^{\dagger}\sigma_1\chi_s\hat{k} \\
&= -\frac{iq}{2m_B}\chi_{s'}^{\dagger}\sigma_3\chi_s\hat{i} \quad\quad\quad\quad\quad\quad\quad (\text{E.5})
\end{aligned}
$$

Usually, we choose the final state and initial state as the spin-up state so that the expression is written as.

$$
G_M^B(Q^2)\Big|_{3q}^{LO} = b_1^B \frac{m_B}{m_N} G_M^p(Q^2)\Big|_{3q}^{LO} \quad\quad\quad\quad\quad\quad (\text{E.6})
$$

where

$$
G_M^p(Q^2)\Big|_{3q}^{LO} = \frac{2m_N\rho R}{1 + \frac{3}{2}\rho^2} \exp\left(-\frac{Q^2 R^2}{4}\right) \quad\quad\quad\quad (\text{E.7})
$$

$$
b_1^B = \langle B(\uparrow)| \sum_{i=1}^{3} \mathcal{Q}(i)\sigma_3(i)|B(\uparrow)\rangle \quad\quad\quad\quad\quad (\text{E.8})
$$

E.1.2 Next-to-leading-order term (NLO)

From Eq.(E.1) and Eq.(E.3), the next-to-leading-order-three-quark contribution for the magnetic form factor is obtained as

$$
\chi_{s'}^{\dagger} \frac{i\vec{\sigma}_B \times \vec{q}}{2m_B} \chi_s G_M^B(Q^2)\Big|_{3q}^{NLO} = \Omega_1 + \Omega_2 \quad\quad\quad\quad (\text{E.9})
$$

where

$$\Omega_1 = i\langle B|\sum_{i=1}^{3} m_i^r \mathcal{Q}(i)\vec{\sigma}(i) \times \vec{q}|B\rangle \frac{\rho^2 R^2(1+\frac{21}{2}\rho^2)}{2(1+\frac{3}{2}\rho^2)^2}e^{-\frac{Q^2R^2}{4}} \qquad (E.10)$$

$$\Omega_2 = -\langle\phi_0|b_0^\dagger\chi_{f'}^\dagger\chi_{s'}^\dagger\mathcal{Q}\frac{2m_i^r N^2\rho^2}{(1+\frac{3}{2}\rho^2)R^2}\int d^3x e^{-iq\cdot x}e^{-\frac{\vec{x}^2}{R^2}}(\vec{\sigma}\times\vec{x})\,\vec{x}^2\chi_s\chi_f b_0|\phi_0\rangle^B$$

$$= -\langle\phi_0|b_0^\dagger\chi_{f'}^\dagger\chi_{s'}^\dagger\mathcal{Q}\frac{2m_i^r N^2\rho^2}{(1+\frac{3}{2}\rho^2)R^2}(-i\vec{\sigma}\times\vec{q})\frac{1}{q}\frac{\partial}{\partial q}\int d^3x\vec{x}^2 e^{-iq\cdot x}e^{-\frac{\vec{x}^2}{R^2}}\chi_s\chi_f b_0|\phi_0\rangle^B$$

$$= i\langle\phi_0|b_0^\dagger\chi_{f'}^\dagger\chi_{s'}^\dagger m_i^r\mathcal{Q}(\vec{\sigma}\times\vec{q})\chi_s\chi_f b_0|\phi_0\rangle^B\frac{2\rho^2}{q(1+\frac{3}{2}\rho^2)^2}\frac{\partial}{\partial q}\left[e^{-\frac{Q^2R^2}{4}}\left(\frac{3}{2}-\frac{Q^2R^2}{4}\right)\right]$$

$$= -i\langle B|\sum_{i=1}^{3} m_i^r\mathcal{Q}(i)\vec{\sigma}(i)\times\vec{q}|B\rangle\frac{\rho^2 R^2}{(1+\frac{3}{2}\rho^2)^2}e^{-\frac{Q^2R^2}{4}}\left(\frac{5}{2}-\frac{Q^2R^2}{4}\right) \qquad (E.11)$$

$$\chi_{s'}^\dagger\frac{i\vec{\sigma}_B\times\vec{q}}{2m_B}\chi_s G_M^B(Q^2)\Big|_{3q}^{NLO} = i\langle B|\sum_{i=1}^{3} m_i^r\mathcal{Q}(i)\vec{\sigma}(i)\times\vec{q}|B\rangle$$

$$\times\frac{\rho^2 R^2}{(1+\frac{3}{2}\rho^2)^2}e^{-\frac{Q^2R^2}{4}}\left(\frac{1+\frac{21}{2}\rho^2}{2(1+\frac{3}{2}\rho^2)}-\frac{5}{2}+\frac{Q^2R^2}{4}\right)$$

$$= i\langle B|\sum_{i=1}^{3} m_i^r\mathcal{Q}(i)\vec{\sigma}(i)\times\vec{q}|B\rangle\frac{\rho^2 R^2 e^{-\frac{Q^2R^2}{4}}}{(1+\frac{3}{2}\rho^2)^2}\left(\frac{Q^2R^2}{4}-\frac{2-\frac{3}{2}\rho^2}{1+\frac{3}{2}\rho^2}\right) \quad (E.12)$$

$$G_M^p(Q^2)\Big|_{3q}^{NLO} = (b_2^B+b_3^B\varepsilon)\frac{m_B}{m_N}G_M^p(Q^2)\Big|_{3q}^{NLO} \qquad (E.13)$$

where

$$G_M^p(Q^2)\Big|_{3q}^{NLO} = \frac{2m_N \hat{m}^r \rho^2 R^2 e^{-\frac{Q^2 R^2}{4}}}{(1+\frac{3}{2}\rho^2)^2}\left(\frac{Q^2 R^2}{4} - \frac{2-\frac{3}{2}\rho^2}{1+\frac{3}{2}\rho^2}\right)$$

$$= G_M^p(Q^2)\Big|_{3q}^{LO} \hat{m}^r \frac{\rho R}{1+\frac{3}{2}\rho^2}\left(\frac{Q^2 R^2}{4} - \frac{2-3\rho^2}{1+\frac{3}{2}\rho^2}\right) \quad \text{(E.14)}$$

$$b_2^B = \langle B(\uparrow)|\sum_{i=1}^{3}\hat{\mathcal{Q}}(i)\sigma_3(i)|B(\uparrow)\rangle \quad \text{(E.15)}$$

$$b_3^B = \langle B(\uparrow)|\sum_{i=1}^{3}\mathcal{Q}_s(i)\sigma_3(i)|B(\uparrow)\rangle \quad \text{(E.16)}$$

E.2 Three-quark counterterm

$$\chi_{s'}^\dagger \frac{i\vec{\sigma}_B \times \vec{q}}{2m_B}\chi_s G_M^B(Q^2)\Big|_{CT} = \langle\phi_0|\int\delta(t)d^4x e^{-iq\cdot x}:\bar{\psi}(x)(Z-1)\vec{\gamma}\mathcal{Q}\psi(x):|\phi_0\rangle^B$$

$$= \langle\phi_0|b_0^\dagger\int d^3x e^{-i\vec{q}\cdot\vec{x}}(Z-1)\mathcal{Q}u_0^\dagger(\vec{x})\gamma^0\vec{\gamma}u_0(\vec{x})b_0|\phi_0\rangle^B$$

$$= i\langle B|\sum_{i=1}^{3}(Z_i-1)\mathcal{Q}(i)\vec{\sigma}(i)\times\vec{q}|B\rangle\frac{\rho R}{1+\frac{3}{2}\rho^2}\exp\left(-\frac{Q^2 R^2}{4}\right) \quad \text{(E.17)}$$

$$G_M^B(Q^2)\Big|_{CT} = \left[b_2^B(\hat{Z}-1)+b_3^B(Z_s-1)\right]G_M^p(Q^2)\Big|_{3q}^{LO} \quad \text{(E.18)}$$

E.3 Meson cloud diagram

$$\chi_{s'}^\dagger \frac{i\vec{\sigma}_B \times \vec{q}}{2m_B} \chi_s G_M^B(Q^2)\Big|_{MC} = 4\langle\phi_0| \frac{i^2}{2!} \int \delta(t)d^4x d^4x_1 d^4x_2 e^{-iq\cdot x}$$

$$\times : [-\bar{\psi}i\gamma^5 \frac{\lambda_k}{F}\underbrace{\Phi_k S\psi]_{x_1}[-\bar{\psi}i\gamma^5 \frac{\lambda_l}{F}\Phi_l S\psi]_{x_2}[(f_{3ij} + \frac{f_{8ij}}{\sqrt{3}})\Phi_i(-\vec{\nabla}\Phi_j)]_x} :$$

$$\times |\phi_0\rangle^B$$

$$= \frac{2}{F^2}\langle\phi_0|b_0^\dagger \int \delta(t)d^4x d^4x_1 d^4x_2 e^{-iq\cdot x}$$

$$\times \bar{u}_0(\vec{x}_1)e^{i\mathcal{E}_0 t_1}i\gamma^5 \lambda_k S(r_1)u_\alpha(\vec{x}_1)\bar{u}_\alpha(\vec{x}_2)e^{-i\mathcal{E}_\alpha(t_1-t_2)}\Theta(t_1 - t_2)$$

$$\times i\gamma^5 \lambda_l S(r_2)u_0(\vec{x}_2)e^{-i\mathcal{E}_0 t_2}(f_{3ij} + \frac{f_{8ij}}{\sqrt{3}})\delta_{ik} \int \frac{d^4k_1}{(2\pi)^4 i}\frac{e^{-ik_1(x_1-x)}}{M_{\Phi_i}^2 - k_1^2 - i\epsilon}$$

$$\times \vec{\nabla}\left\{\delta_{jl} \int \frac{d^4k_2}{(2\pi)^4 i}\frac{e^{-ik_2(x-x_2)}}{M_{\Phi_j}^2 - k_2^2 - i\epsilon}\right\} b_0|\phi_0\rangle^B$$

$$= \frac{-2i}{(2\pi)^8 F^2}\langle\phi_0|b_0^\dagger \int d^3x d^4x_1 d^4x_2 d^4k_1 d^4k_2 \Theta(t_1 - t_2)e^{-i(\mathcal{E}_\alpha - \mathcal{E}_0)(t_1-t_2)}$$

$$\times \int dt\delta(t)e^{-ik_2^0(t-t_2)-ik_1^0(t_1-t)-iq^0 t}\left[\bar{u}_0(\vec{x}_1)i\gamma^5 \lambda_i S(r_1)u_\alpha(\vec{x}_1)\right]$$

$$\times \left[\bar{u}_\alpha(\vec{x}_2)i\gamma^5 \lambda_j S(r_2)u_0(\vec{x}_2)\right](f_{3ij} + \frac{f_{8ij}}{\sqrt{3}})$$

$$\times \frac{\vec{k}_2 e^{-i\vec{q}\cdot\vec{x}+i\vec{k}_1\cdot(\vec{x}_1-\vec{x})+i\vec{k}_2\cdot(\vec{x}-\vec{x}_2)}}{[M_{\Phi_i}^2 + \vec{k}_1^2 - (k_1^0)^2 - i\epsilon][M_{\Phi_j}^2 + \vec{k}_2^2 - (k_2^0)^2 - i\epsilon]}b_0|\phi_0\rangle^B \tag{E.19}$$

$$\chi_{s'}^{\dagger} \frac{i\vec{\sigma}_B \times \vec{q}}{2m_B} \chi_s G_M^B(Q^2)\Big|_{MC}$$

$$= \frac{-2i}{(2\pi)^8 F^2} \langle\phi_0|b_0^{\dagger} \int d^3x_1 d^4x_2 d^4k_1 d^4k_2 \left[\int d^3x e^{i(\vec{q}-\vec{k}_1+\vec{k}_2)\cdot\vec{x}} \right]$$

$$\times \left[\int dt_1 e^{-i(k_1^0+\Delta\mathcal{E}_\alpha)t_1} \Theta(t_1-t_2) \right] \left[\bar{u}_0(\vec{x}_1) i\gamma^5 \lambda_i S(r_1) u_\alpha(\vec{x}_1) \right]$$

$$\times \left[\bar{u}_\alpha(\vec{x}_2) i\gamma^5 \lambda_j S(r_2) u_0(\vec{x}_2) \right] e^{i(k_2^0+\Delta\mathcal{E}_\alpha)t_2} (f_{3ij} + \frac{f_{8ij}}{\sqrt{3}})$$

$$\times \frac{e^{i\vec{k}_1\cdot\vec{x}_1}}{\left[M_{\Phi_i}^2 + \vec{k}_1^2 - (k_1^0)^2 - i\epsilon \right]} \frac{\vec{k}_2 e^{-i\vec{k}_2\cdot\vec{x}_2}}{\left[M_{\Phi_j}^2 + \vec{k}_2^2 - (k_2^0)^2 - i\epsilon \right]} b_0|\phi_0\rangle^B$$

$$= \frac{-2}{(2\pi)^5 F^2} \langle\phi_0|b_0^{\dagger} \int d^3x_1 d^3x_2 d^4k_2 dk_1^0 \left[\int dt_2 e^{i(k_2^0-k_1^0)t_2} \right]$$

$$\times \left[\bar{u}_0(\vec{x}_1) i\gamma^5 \lambda_i S(r_1) u_\alpha(\vec{x}_1) \right] \left[\bar{u}_\alpha(\vec{x}_2) i\gamma^5 \lambda_j S(r_2) u_0(\vec{x}_2) \right]$$

$$\times (f_{3ij} + \frac{f_{8ij}}{\sqrt{3}}) \left[\int d^3k_1 \frac{\delta^{(3)}(\vec{q}-\vec{k}_1+\vec{k}_2) e^{i\vec{k}_1\cdot\vec{x}_1}}{M_{\Phi_i}^2 + \vec{k}_1^2 - (k_1^0)^2 - i\epsilon} \right]$$

$$\times \frac{1}{[k_1^0 + \Delta\mathcal{E}_\alpha - i\eta]} \frac{\vec{k}_2 e^{-i\vec{k}_2\cdot\vec{x}_2}}{\left[M_{\Phi_j}^2 + \vec{k}_2^2 - (k_2^0)^2 - i\epsilon \right]} b_0|\phi_0\rangle^B$$

$$= \frac{-2}{(2\pi)^4 F^2} \langle\phi_0|b_0^{\dagger} \int d^3k_2 \vec{k}_2 \left[\int d^3x_1 \bar{u}_0(\vec{x}_1) i\gamma^5 S(r_1) u_\alpha(\vec{x}_1) e^{i\vec{k'}_2\cdot\vec{x}_1} \right]$$

$$\times \left[\int d^3x_2 \bar{u}_\alpha(\vec{x}_2) i\gamma^5 S(r_2) u_0(\vec{x}_2) e^{-i\vec{k}_2\cdot\vec{x}_2} \right] (f_{3ij} + \frac{f_{8ij}}{\sqrt{3}}) \lambda_i \lambda_j$$

$$\times \int dk_2^0 f_2(k_2^0) b_0|\phi_0\rangle^B \tag{E.20}$$

where

$$f_2(k_2^0) \;=\; \frac{1}{[k_2^0 + \Delta\mathcal{E}_\alpha - i\eta][(k_2^0)^2 - \omega_{\Phi_j}^2(\vec{k}_2^2) + i\epsilon][(k_2^0)^2 - \omega_{\Phi_i}^2(\vec{k'}_2^2) + i\epsilon]} \tag{E.21}$$

$$\int dk_2^0 f_2(k_2^0) = \frac{\pi i \left[1 + \frac{\Delta\mathcal{E}_\alpha}{\omega_{\Phi_j}(\vec{k}_2^2) + \omega_{\Phi_i}(\vec{k'}_2^2)} \right]}{\omega_{\Phi_j}(\vec{k}_2^2)\omega_{\Phi_i}(\vec{k'}_2^2) \left[\omega_{\Phi_j}(\vec{k}_2^2) + \Delta\mathcal{E}_\alpha \right] \left[\omega_{\Phi_i}(\vec{k'}_2^2) + \Delta\mathcal{E}_\alpha \right]} \tag{E.22}$$

After we substitute Eq.(E.22) into Eq.(E.20), the expression is given as

$$\chi_{s'}^\dagger \frac{i\vec{\sigma}_B \times \vec{q}}{2m_B} \chi_s G_M^B(Q^2) \Big|_{MC}^\alpha = \frac{1}{(2\pi)^3 F^2} \langle \phi_0 | b_0^\dagger \chi_{f'}^\dagger \chi_{s'}^\dagger \int d^3 k_2 \vec{k}_2$$

$$\times \frac{R_\alpha^\dagger(\vec{k'}_2) R_\alpha(\vec{k}_2)[-i(f_{3ij} + \frac{f_{8ij}}{\sqrt{3}})\lambda_i \lambda_j]\vec{\sigma} \cdot \vec{k'}_2 \vec{\sigma} \cdot \vec{k}_2}{\omega_{\Phi_j}(\vec{k}_2^2)\omega_{\Phi_i}(\vec{k'}_2^2)[\omega_{\Phi_j}(\vec{k}_2^2) + \Delta\mathcal{E}_\alpha][\omega_{\Phi_i}(\vec{k'}_2^2) + \Delta\mathcal{E}_\alpha]}$$

$$\times \left[1 + \frac{\Delta\mathcal{E}_\alpha}{\omega_{\Phi_j}(\vec{k}_2^2) + \omega_{\Phi_i}(\vec{k'}_2^2)} \right] \chi_f \chi_s b_0 |\phi_0\rangle^B$$

$$= \frac{1}{(2\pi F)^2} \langle \phi_0 | b_0^\dagger \chi_{f'}^\dagger \chi_{s'}^\dagger \int_0^\infty dp p^4 R_\alpha^\dagger(y) R_\alpha(p) \int_{-1}^1 dx \left[-i(f_{3ij} + \frac{f_{8ij}}{\sqrt{3}})\lambda_i \lambda_j \right]$$

$$\times \left[\frac{i}{2}(1 - x^2)(\vec{\sigma} \times \vec{q}) + x(p + Qx)\hat{q} \right] \mathcal{D}_{\alpha,\Phi_{ij}}(p^2, Q^2, x) \chi_f \chi_s b_0 |\phi_0\rangle^B \tag{E.23}$$

where we define $x = \cos\theta = \frac{\vec{q} \cdot \vec{k}_2}{|\vec{q}||\vec{k}_2|}$, $\hat{p} = \frac{\vec{k}_2}{|\vec{k}_2|}$, $p = |\vec{k}_2|$, $Q = |\vec{q}|$ and

$$y = |\vec{q} + \vec{k}_2| = \sqrt{p^2 + Q^2 + 2pQx}, \tag{E.24}$$

$$\int d^3 k_2 \vec{k}_2 = \int_0^\infty p^3 dp \int_{-1}^1 dx \int_0^{2\pi} d\phi \hat{p}, \tag{E.25}$$

$$\int_0^{2\pi} d\phi \hat{p} \left[\vec{\sigma} \cdot \vec{k'}_2 \vec{\sigma} \cdot \vec{k}_2 \right] = \int_0^{2\pi} d\phi \hat{p} \left[\vec{\sigma} \cdot (\vec{q} + \vec{k}_2)\vec{\sigma} \cdot \vec{k}_2 \right]$$

$$= 2\pi \left[\frac{i}{2} p(1 - x^2)(\vec{\sigma} \times \vec{q}) + x(p^2 + pQx)\hat{q} \right] \tag{E.26}$$

$$\mathcal{D}_{\alpha,\Phi_{ij}}(p^2,Q^2,x) \;=\; D^{11}_{0,\Phi_{ij}}(p^2,Q^2,x)D^{11}_{\alpha,\Phi_{ij}}(p^2,Q^2,x)\left[1+A_{\alpha,\Phi_{ij}}\right] \quad \text{(E.27)}$$

$$A_{\alpha,\Phi_{ij}}(p^2,Q^2,x) \;=\; \frac{\Delta\mathcal{E}_\alpha}{\omega_{\Phi_j}(p^2)+\omega_{\Phi_i}(p^2+Q^2+2pQ)} \quad \text{(E.28)}$$

By choosing $\vec{q}$ to piont in the y-direction and restricting the initial and final state to the spin-up state, then

$$\chi^\dagger_\uparrow \frac{i\vec{\sigma}_B\times\vec{q}}{2m_B}\chi_\uparrow = \frac{-iq}{2m_B}\hat{i}. \quad \text{(E.29)}$$

Thus, on the right-hand-side of Eq.(E.23) we need only to calculate the x-component.

$$\frac{-iq}{2m_B}G^B_M(Q^2)\Big|^\alpha_{MC} = -\frac{1}{(2\pi F)^2}\langle\phi_0|b_0^\dagger\chi_{f'}^\dagger\chi_{s'}^\dagger\int_0^\infty dp\,p^4 R_\alpha^\dagger(y)R_\alpha(p)\int_{-1}^1 dx$$

$$\times\left[(f_{3ij}+\frac{f_{8ij}}{\sqrt{3}})\lambda_i\lambda_j\right]\frac{q\sigma_3}{2}(1-x^2)\mathcal{D}_{\alpha,\Phi_{ij}}(p^2,Q^2,x)\chi_f\chi_s b_0|\phi_0\rangle^B \quad \text{(E.30)}$$

$$G^B_M(Q^2)\Big|^\alpha_{MC} = \frac{5m_B}{6(\pi F)^2}\int_0^\infty dp\,p^4 R_\alpha^\dagger(y)R_\alpha(p)$$

$$\times\int_{-1}^1 dx(1-x^2)t^B_m(p^2,Q^2,x)\Big|^\alpha_{MC} \quad \text{(E.31)}$$

where

$$t^B_M(p^2,Q^2,x)\Big|^\alpha_{MC} = \langle\phi_0|b_0^\dagger\chi_{f'}^\dagger\chi_{s'}^\dagger\left[\frac{-3i}{10}(f_{3ij}+\frac{f_{8ij}}{\sqrt{3}})\sigma_3\lambda_i\lambda_j\right]$$

$$\times\mathcal{D}_{\alpha,\Phi_{ij}}(p^2,Q^2,x)\chi_f\chi_s b_0|\phi_0\rangle^B$$

$$= \sum_{i,j=1}^8\sum_{k=1}^3 \mathcal{D}_{\alpha,\Phi_{i,j}}(p^2,Q^2,x)\langle B(\uparrow)|\frac{-3i}{10}(f_{3ij}+\frac{f_{8ij}}{\sqrt{3}})\sigma_3(k)\lambda_i(k)\lambda_j(k)|B(\uparrow)\rangle,$$

$$= b_4^B\mathcal{D}_{\alpha,\pi}(p^2,Q^2,x) + b_5^B\mathcal{D}_{\alpha,K}(p^2,Q^2,x) \quad \text{(E.32)}$$

If we restrict the quark propagator just only to the ground state($\alpha = 0$), the magnetic form factor from the meson-cloud diagram $G_M^B(Q^2)\big|_{MC}^{\alpha=0}$ is given by

$$G_M^B(Q^2)\bigg|_{MC}^{\alpha=0} = \frac{3m_B}{40}\left(\frac{g_A}{\pi F}\right)^2 \int_0^\infty dp\, p^4 \int_{-1}^1 dx(1-x^2)$$

$$\times \mathcal{F}_{\pi NN}(p^2, Q^2, x) t_M^B(p^2, Q^2, x)\bigg|_{MC}^{\alpha=0} \tag{E.33}$$

E.4 Vertex correction diagram

$$\chi_{s'}^{\dagger} \frac{i\vec{\sigma}_B \times \vec{q}}{2m_B} \chi_s G_M^B(Q^2)\Big|_{VC}^{\alpha\beta} = 2\langle\phi_0| \frac{i^2}{2!} \int \delta(t) d^4x d^4x_1 d^4x_2 e^{-iq\cdot x}$$

$$\times : [-\bar{\psi}i\gamma^5 \frac{\lambda_k}{F} \Phi_k S\psi]_{x_1} [-\bar{\psi}i\gamma^5 \frac{\lambda_l}{F} \Phi_l S\psi]_{x_2} [\mathcal{Q}\bar{\psi}\vec{\gamma}\psi]_x : |\phi_0\rangle^B$$

$$= \frac{-1}{F^2} \langle\phi_0| \int \delta(t) d^4x d^4x_1 d^4x_2 e^{-iq\cdot x} : b_0^{\dagger}$$

$$\times \bar{u}_0(\vec{x_1}) e^{i\mathcal{E}_0 t_1} i\gamma^5 \lambda_i S(r_1) u_\alpha(\vec{x_1}) \bar{u}_\alpha(\vec{x}) e^{-i\mathcal{E}_\alpha(t_1-t)} \Theta(t_1 - t)$$

$$\times \mathcal{Q}\vec{\gamma} u_\beta(\vec{x}) \bar{u}_\beta(\vec{x_2}) e^{-i\mathcal{E}_\beta(t-t_2)} \Theta(t - t_2) i\gamma^5 \lambda_j S(r_2)$$

$$\times b_0 u_0(\vec{x_2}) e^{-i\mathcal{E}_0 t_2} \delta_{ij} \int \frac{d^4k}{(2\pi)^4 i} \frac{e^{-ik\cdot(x_1-x_2)}}{[M_{\Phi_j}^2 - k^2 - i\epsilon]} : |\phi_0\rangle^B$$

$$= \frac{i}{(2\pi)^4 F^2} \langle\phi_0| b_0^{\dagger} \int dt_1 dt_2 d^4k \int \delta(t) e^{-i(q^0 + \Delta\mathcal{E}_{\alpha\beta})t} \Theta(t_1 - t)$$

$$\times \Theta(t - t_2) \left[\int d^3x_1 \bar{u}_0(\vec{x_1}) i\gamma^5 S(r_1) u_\alpha(\vec{x_1}) e^{i\vec{k}\cdot\vec{x_1}} \right] \lambda_i \mathcal{Q} \lambda_i$$

$$\times \frac{e^{-i(\Delta\mathcal{E}_\alpha + k^0)t_1} e^{i(\Delta\mathcal{E}_\beta + k^0)t_2}}{[M_{\Phi_i}^2 - k^2 - i\epsilon]} \left[\int d^3x \bar{u}_\alpha(x) \vec{\gamma} u_\beta(x) e^{-i\vec{q}\cdot\vec{x}} \right]$$

$$\times \left[\int d^3x_2 \bar{u}_0(\vec{x_2}) i\gamma^5 S(r_2) u_\beta(\vec{x_2}) e^{-i\vec{k}\cdot\vec{x_2}} \right] b_0 |\phi_0\rangle \tag{E.34}$$

$$\chi_{s'}^{\dagger}\frac{i\vec{\sigma}_B \times \vec{q}}{2m_B}\chi_s G_M^B(Q^2)\bigg|_{VC}^{\alpha\beta} = \frac{i}{(2\pi)^4 F^2}\langle\phi_0|b_0^{\dagger}\chi_{f'}^{\dagger}\chi_{s'}^{\dagger}\int d^4k$$

$$\times\left[\int dt_1 e^{-i(\Delta\mathcal{E}_\alpha+k^0)t_1}\Theta(t_1)\right]\left[\int dt_2 e^{i(\Delta\mathcal{E}_\beta+k^0)t_2}\Theta(-t_2)\right]$$

$$\times\frac{\lambda_i\mathcal{Q}\lambda_i R_\alpha^{\dagger}(p)\mathcal{V}_{\alpha\beta}(Q^2)R_\beta(p)(\vec{\sigma}\cdot\vec{k})(i\vec{\sigma}\times\vec{q})(\vec{\sigma}\cdot\vec{k})}{[M_{\Phi_i}^2 + \vec{k}^2 - (k^0)^2 - i\epsilon]}\chi_f\chi_s b_0|\phi_0\rangle^B$$

$$= \frac{-1}{(2\pi)^4 F^2}\langle\phi_0|b_0^{\dagger}\chi_{f'}^{\dagger}\chi_{s'}^{\dagger}\int d^3k R_\alpha^{\dagger}(p)\mathcal{V}_{\alpha\beta}(Q^2)R_\beta(p)\int dk^0$$

$$\times\frac{\lambda_i\mathcal{Q}\lambda_i(\vec{\sigma}\cdot\vec{k})(\vec{\sigma}\times\vec{q})(\vec{\sigma}\cdot\vec{k})}{(k^0 + \Delta\mathcal{E}_\alpha - i\eta')(k^0 + \Delta\mathcal{E}_\beta - i\eta)[(k^0)^2 - \omega_{\Phi_i}^2(\vec{k}^2) + i\epsilon]}\chi_f\chi_s b_0|\phi_0\rangle^B$$

$$= \frac{-1}{(2\pi)^4 F^2}\langle\phi_0|b_0^{\dagger}\chi_{f'}^{\dagger}\chi_{s'}^{\dagger}\int dk^3 R_\alpha^{\dagger}(p)\mathcal{V}_{\alpha\beta}(Q^2)R_\beta(p)\int dk^0 f_4(k^0)$$

$$\times\lambda_i\mathcal{Q}\lambda_i(\vec{\sigma}\cdot\vec{k})(\vec{\sigma}\times\vec{q})(\vec{\sigma}\cdot\vec{k})\chi_f\chi_s b_0|\phi_0\rangle^B \tag{E.35}$$

where

$$Q = |\vec{q}|, \qquad p = |\vec{k}|, \tag{E.36}$$

$$\int d^3x\,\bar{u}_\alpha(x)\vec{\gamma}u_\beta(x)e^{-i\vec{q}\cdot\vec{x}} = (i\vec{\sigma}\times\vec{q})\mathcal{V}_{\alpha\beta}(Q^2), \tag{E.37}$$

$$f_4(k^0) = \frac{1}{(k^0 + \Delta\mathcal{E}_\alpha - i\eta')(k^0 + \Delta\mathcal{E}_\beta - i\eta)[(k^0)^2 - \omega_{\Phi_i}^2(p^2) + i\epsilon]} \tag{E.38}$$

$$\int dk^0 f_4(k^0) = \frac{-\pi i}{\omega_{\Phi_i}(p^2)[\omega_{\Phi_i}(p^2) + \Delta\mathcal{E}_\alpha][\omega_{\Phi_i}(p^2) + \Delta\mathcal{E}_\beta]} = -i\pi W_{\Phi_i}^{\alpha\beta} \tag{E.39}$$

$$(\vec{\sigma}\cdot\vec{k})(\vec{\sigma}\times\vec{q})(\vec{\sigma}\cdot\vec{k}) = -(\vec{k}\cdot\vec{k})(\vec{\sigma}\times\vec{q}) + 2(\vec{k}\times\vec{q})(\vec{\sigma}\cdot\vec{k}) \tag{E.40}$$

Again, by putting $\vec{q}$ in the y-direction and restricting initial and final state to the spin-up state, on the left-hand side of Eq.(E.35) we have the result as in Eq.(E.29), but on the right-hand side depends on the term of Eq.(E.40). If we integrate Eq.(E.40) over the solid angle of k-space the second term vanishes, so that we can ignore this term and rewrite Eq.(E.35) as

$$\frac{-iq\hat{i}}{2m_B}G_M^B(Q^2)\bigg|_{VC}^{\alpha\beta} = \frac{q\hat{i}}{(2\pi F)^2}\langle\phi_0|b_0^\dagger\chi_{f'}^\dagger\chi_{s'}^\dagger\int_0^\infty dp\,p^4 R_\alpha^\dagger(p)\mathcal{V}_{\alpha\beta}(Q^2)R_\beta(p)W_{\Phi_i}^{\alpha\beta}(p^2)$$

$$\times\lambda_i\mathcal{Q}\lambda_i\sigma_3\chi_f\chi_s b_0|\phi_0\rangle^B \tag{E.41}$$

$$G_M^B(Q^2)\bigg|_{VC}^{\alpha\beta} = m_B\mathcal{V}_{\alpha\beta}(Q^2)\frac{1}{2(\pi F)^2}\int_0^\infty dp\,p^4 R_\alpha^\dagger(p)R_\beta(p)t_M^B(p^2)\bigg|_{VC}^{\alpha\beta} \tag{E.42}$$

where

$$t_M^B(p^2)\bigg|_{VC}^{\alpha\beta} = -\langle\phi_0|b_0^\dagger\chi_{f'}^\dagger\chi_{s'}^\dagger\lambda_i\mathcal{Q}\lambda_i\sigma_3 W_{\Phi_i}^{\alpha\beta}(p^2)\chi_f\chi_s b_0|\phi_0\rangle^B$$

$$= \sum_{i=1}^{8}\sum_{k=1}^{3}W_{\Phi_i}^{\alpha\beta}(p^2)\langle B(\uparrow)|[-\lambda_i\mathcal{Q}\lambda_i](k)\sigma_3(k)|B(\uparrow)\rangle,$$

$$= b_6^B W_\pi^{\alpha\beta}(p^2) + b_7^B W_K^{\alpha\beta}(p^2) + b_8^B W_\eta^{\alpha\beta}(p^2), \tag{E.43}$$

$$W_\Phi^{\alpha\beta}(p^2) = \frac{1}{\omega_\Phi(p^2)[\omega_\Phi(p^2)+\Delta\mathcal{E}_\alpha][\omega_\Phi(p^2)+\Delta\mathcal{E}_\beta]} \tag{E.44}$$

If we restrict the quark propagator only to the ground state $(\alpha=0,\beta=0)$ our expression is reduced to following form.

$$G_M^B(Q^2)\bigg|_{VC}^{00} = m_B G_M^B(Q^2)\bigg|_{3q}^{LO}\frac{9}{200}\left(\frac{g_A}{\pi F}\right)^2\int_0^\infty dp\,p^4 F_{\pi NN}^2(p^2)t_M^B(p^2)\bigg|_{VC}^{00} \tag{E.45}$$
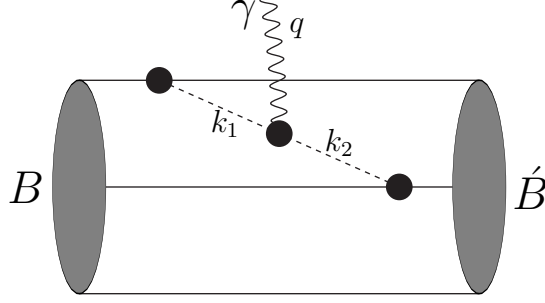
Figure E.1: The meson-in-flight diagram

where

$$\mathcal{V}_{00}(Q^2) = G_M^B(Q^2)\Big|_{3q}^{LO} \tag{E.46}$$

E.5   Meson-in-flight diagram

$$\chi_{s'}^\dagger \frac{i\vec{\sigma}_B \times \vec{q}}{2m_B} \chi_s G_M^B(Q^2)\Big|_{MF} = 2\langle\phi_0|\frac{i^2}{2!}\int \delta(t)d^4x d^4x_1 d^4x_2 e^{-iq\cdot x}$$

$$\times : [-\bar{\psi}i\gamma^5\frac{\lambda_k}{F}\Phi_k S\psi]_{x_1}[-\bar{\psi}i\gamma^5\frac{\lambda_l}{F}\Phi_l S\psi]_{x_2}[(f_{3ij} + \frac{f_{8ij}}{\sqrt{3}})\Phi_i(-\vec{\nabla}\Phi_j)]_x : |\phi_0\rangle^B$$

$$= \frac{1}{F^2}\langle\phi_0|b_0^{m\dagger}b_0^{n\dagger}\int \delta(t)d^4x d^4x_1 d^4x_2 e^{-iq\cdot x}\bar{u}_0(\vec{x}_1)e^{i\mathcal{E}_0 t_1}i\gamma^5\lambda_k S(r_1)u_0(\vec{x}_1)$$

$$\times e^{-i\mathcal{E}_0 t_1}\bar{u}_0(\vec{x}_2)e^{i\mathcal{E}_0 t_2}i\gamma^5\lambda_l S(r_2)u_0(\vec{x}_2)e^{-i\mathcal{E}_0 t_2}(f_{3ij} + \frac{f_{8ij}}{\sqrt{3}})\delta_{ik}\int \frac{d^4k_1}{(2\pi)^4 i}$$

$$\times \frac{e^{-ik_1(x_1-x)}}{M_{\Phi_i}^2 - k_1^2 - i\epsilon}\vec{\nabla}\left\{\delta_{jl}\int \frac{d^4k_2}{(2\pi)^4 i}\frac{e^{-ik_2(x-x_2)}}{M_{\Phi_j}^2 - k_2^2 - i\epsilon}\right\}b_0^m b_0^n|\phi_0\rangle^B \tag{E.47}$$

$$\chi_{s'}^\dagger \frac{i\vec{\sigma}_B \times \vec{q}}{2m_B} \chi_s G_M^B(Q^2)\bigg|_{MF}$$

$$= \frac{-i}{(2\pi)^8 F^2} \langle\phi_0|b_0^{m\dagger} b_0^{n\dagger} \int d^3x\, d^4x_1\, d^4x_2\, d^4k_1\, d^4k_2 \int dt\, \delta(t) e^{-ik_2^0(t-t_2)-ik_1^0(t_1-t)}$$

$$\times \left[\bar{u}_0(\vec{x}_1) i\gamma^5 S(r_1) u_0(\vec{x}_1) e^{i\vec{k}_1\cdot\vec{x}}\right] \left[\bar{u}_0(\vec{x}_2) i\gamma^5 \lambda_j S(r_2) u_0(\vec{x}_2) e^{-i\vec{k}_2\cdot\vec{x}}\right]$$

$$\times \frac{(f_{3ij} + \frac{f_{8ij}}{\sqrt{3}})\lambda_i \lambda_j \vec{k}_2 e^{-i(\vec{q}+\vec{k}_2-\vec{k}_1)\cdot\vec{x}}}{[M_{\Phi_i}^2 - k_1^2 - i\epsilon][M_{\Phi_j}^2 - k_2^2 - i\epsilon]} b_0^m b_0^n |\phi_0\rangle^B$$

$$= \frac{-i}{(2\pi)^8 F^2} \langle\phi_0|b_0^{m\dagger} b_0^{n\dagger} \int d^3x_1\, d^3x_2\, d^4k_1\, d^4k_2 \left[\int d^3x\, e^{-i(\vec{q}-\vec{k}_1+\vec{k}_2)\cdot\vec{x}}\right]$$

$$\times \left[\int dt_1 e^{-ik_1^0 t_1} \int dt_2 e^{ik_2^0 t_2}\right] \left[\bar{u}_0(\vec{x}_1) i\gamma^5 S(r_1) u_0(\vec{x}_1) e^{i\vec{k}_1\cdot\vec{x}_1}\right]$$

$$\times \left[\bar{u}_0(\vec{x}_2) i\gamma^5 S(r_2) u_0(\vec{x}_2) e^{-i\vec{k}_2\cdot\vec{x}_2}\right]$$

$$\times \frac{\vec{k}_2(f_{3ij} + \frac{f_{8ij}}{\sqrt{3}})\lambda_i \lambda_j}{\left[M_{\Phi_i}^2 + \vec{k}_1^2 - (k_1^0)^2 - i\epsilon\right]\left[M_{\Phi_j}^2 + \vec{k}_2^2 - (k_2^0)^2 - i\epsilon\right]} b_0^m b_0^n |\phi_0\rangle^B$$

$$= \frac{-i}{(2\pi)^3 F^2} \langle\phi_0|b_0^{m\dagger} b_0^{n\dagger} \int d^3x_1\, d^3k_1 \left[\int d^3x_2\, \bar{u}_0(\vec{x}_2) i\gamma^5 S(r_2) u_0(\vec{x}_2) e^{-i\vec{k}_2\cdot\vec{x}_2}\right]$$

$$\times \bar{u}_0(\vec{x}_1) i\gamma^5 S(r_1) u_0(\vec{x}_1) \lambda_i \lambda_j \left[\int dk_2^0 \frac{\vec{k}_2\, \delta(k_2^0)}{\left[(k_2^0)^2 - \omega_{\Phi_j}^2(\vec{k}_2^2) + i\epsilon\right]}\right]$$

$$\times \left[\int d^4k_1\, \delta(k_1^0) \frac{e^{i\vec{k}_1\cdot\vec{x}_1} \delta^{(3)}(\vec{q} - \vec{k}_1 + \vec{k}_2)}{\left[(k_1^0)^2 - \omega_{\Phi_i}^2(\vec{k}_1^2) + i\epsilon\right]}\right] (f_{3ij} + \frac{f_{8ij}}{\sqrt{3}}) b_0^m b_0^n |\phi_0\rangle^B \quad \text{(E.48)}$$

$$\chi_{s'}^\dagger \frac{i\vec{\sigma}_B \times \vec{q}}{2m_B} \chi_s G_M^B(Q^2)\Big|_{MF} = \frac{-i}{(2\pi)^3 F^2} \langle\phi_0|b_0^{m\dagger} b_0^{n\dagger} \chi_{f'}^{m\dagger} \chi_{s'}^{m\dagger} \int d^3k_2 R_0(\vec{k}_2)\vec{\sigma}_m \cdot \vec{k}_2$$

$$\times \left[\int d^3x_1 \bar{u}_0(\vec{x}_1) i\gamma^5 S(r_1) u_0(\vec{x}_1) e^{i\vec{k}_2 \cdot \vec{x}_1}\right] \frac{(f_{3ij} + \frac{f_{8ij}}{\sqrt{3}})\lambda_i \lambda_j}{\omega_{\Phi_j}^2(\vec{k}_2^2)\omega_{\Phi_j}^2(\vec{k'}_2^2)} \chi_f^m \chi_s^m b_0^m b_0^n |\phi_0\rangle^B$$

$$= \frac{-i}{(2\pi)^3 F^2} \langle\phi_0|b_0^{m\dagger} b_0^{n\dagger} \chi_{f'}^{m\dagger} \chi_{s'}^{m\dagger} \chi_{f'}^{n\dagger} \chi_{s'}^{n\dagger} \int d^3k_2 R_0^\dagger(\vec{k'}_2) R_0(\vec{k}_2)\vec{k}_2 \vec{\sigma}_m \cdot \vec{k}_2 \vec{\sigma}_n \cdot \vec{k'}_2$$

$$\times (f_{3ij} + \frac{f_{8ij}}{\sqrt{3}})\lambda_i \lambda_j \frac{1}{\omega_{\Phi_i}^2(\vec{k}_2^2)} \frac{1}{\omega_{\Phi_j}^2(\vec{k'}_2^2)} \chi_f^{m\dagger} \chi_s^{m\dagger} \chi_f^n \chi_s^n b_0^m b_0^n |\phi_0\rangle^B \tag{E.49}$$

To simplify the expression, we define $x = \cos\theta = \frac{\vec{q} \cdot \vec{k}_2}{|\vec{q}||\vec{k}_2|}$, $p = |\vec{k}_2|$, $Q = |\vec{q}|$ and

$$y = |\vec{k'}_2| = |\vec{q} + \vec{k}_2| = \sqrt{p^2 + Q^2 + 2pQx}, \tag{E.50}$$

$$\int d^3k_2 \vec{k}_2 = \int_0^\infty p^3 dp \int d\hat{p}\, \hat{p}, \tag{E.51}$$

$$\int d\hat{p}\, \hat{p}(\vec{\sigma}_m \cdot \vec{k}_2)(\vec{\sigma}_n \cdot \vec{k'}_2) = \int d\hat{p}\, \hat{p}\, (\vec{\sigma}_m \cdot \vec{k}_2)\{\vec{\sigma}_n \cdot (\vec{q} + \vec{k}_2)\}$$

$$= \int d\hat{p}\, \hat{p}\, (\vec{\sigma}_m \cdot \vec{k}_2)(\vec{\sigma}_n \cdot \vec{k}_2) + (\vec{\sigma}_n \cdot \vec{q}) \int d\hat{p}\, \hat{p}\, (\vec{\sigma}_m \cdot \vec{k}_2) \tag{E.52}$$

$$\int d\hat{p}\, \hat{p}\, (\vec{\sigma}_m \cdot \vec{k}_2) = \pi p \int_{-1}^1 dx \left\{(1 - x^2)[\sigma_m^1 \hat{i} + \sigma_m^2 \hat{j}] + x^2 \sigma_m^3 \hat{k}\right\} \tag{E.53}$$

The first term on the right hand side of Eq.(E.52) depends on the pair of two-body operators, $\sigma_m^3 \sigma_n^i$, $i = 1, 2, 3$. For this operator the result vanishes, so that we can keep only the second term. We do the same process as we have done for Eq.(E.30)

then the expression is shown as

$$\frac{-iq}{2m_B}G_M^B(Q^2)\Big|_{MF} = \frac{-iq}{8(\pi F)^2}\langle\phi_0|b_0^{m\dagger}b_0^{n\dagger}\chi_{f'}^{m\dagger}\chi_{s'}^{m\dagger}\chi_{f'}^{n\dagger}\chi_{s'}^{n\dagger}\int_0^\infty dp\ p^4\int_{-1}^1 dx(1-x^2)$$

$$\times R_0^\dagger(p)R_0(y)\sigma_m^1\sigma_n^2(f_{3ij}+\frac{f_{8ij}}{\sqrt{3}})\lambda_i\lambda_j D_{\Phi_{i,j}}^{22}\chi_f^{m\dagger}\chi_s^{m\dagger}\chi_f^n\chi_s^n b_0^m b_0^n|\phi_0\rangle^B \qquad (E.54)$$

$$G_M^B(Q^2)\Big|_{MF} = m_B\frac{9}{400}\left(\frac{g_A}{\pi F}\right)^2\int_0^\infty dp\ p^4\int_{-1}^1 dx(1-x^2)$$

$$\times\mathcal{F}_{\pi NN}(p^2,Q^2,x)t_M^B(p^2,Q^2,x)\Big|_{MF} \qquad (E.55)$$

where

$$t_M^B(p^2,Q^2,x)\Big|_{MF} = \langle\phi_0|b_0^{m\dagger}b_0^{n\dagger}\chi_{f'}^{m\dagger}\chi_{s'}^{m\dagger}\chi_{f'}^{n\dagger}\chi_{s'}^{n\dagger}[\frac{1}{4}(f_{3ij}+\frac{f_{8ij}}{\sqrt{3}})\lambda_i\lambda_j\sigma_m^1\sigma_n^2]$$

$$\times D_{\Phi_{i,j}}^{22}(p^2,Q^2,x)\chi_f^m\chi_s^m\chi_f^n\chi_s^n b_0^m b_0^n|\phi_0\rangle^B$$

$$= \sum_{i\neq j}\sum_{k\neq l}D_{\Phi_{i,j}}^{22}(p^2,Q^2,x)\langle B(\uparrow)|$$

$$\times\frac{1}{4}(f_{3ij}+\frac{f_{8ij}}{\sqrt{3}})\lambda_i(k)\lambda_j(l)\sigma_1(k)\sigma_2(l)|B(\uparrow)\rangle,$$

$$= b_9^B D_\pi^{22}(p^2,Q^2,x)+b_{10}^B D_K^{22}(p^2,Q^2,x) \qquad (E.56)$$

Curriculum Vitae

FIRST NAME: Sampart   LAST NAME: Cheedket

GENDER: Male   NATIONALITY: Thai

DATE OF BIRTH: June 7, 1975

EDUCATIONAL BACKGROUND:

- B. Sc. (Physics) 1998, Mahidol University, Thailand.

SCHOLARSHIPS:

- A four-year scholarship from the Royal Golden Jubilee Ph.D. Program, Thailand Research Fund, 1999 - 2003.

- A five-month fellowship from the European Graduate School Basel-Tübingen, funding by the Deutsche Forschungsgemeinschaft (DFG), 2002.

- A one-year fellowship from the German Academic Exchange Service (DAAD), 2000 - 2001.

- A five-year scholarship from Development and Promotion of Science and Technology talents project of Thailand (DPST), 1994 - 1998.

PUBLICATIONS:

- Cheedket, S., Lyubovitskij, V.E., Gutsche, Th., Faessler, A., Pumsa-ard, K., and Yan, Y. Electromagnetic form factors of the baryon octet in the perturbative chiral quark model. **European Physical Journal A** (accepted).

- Pumsa-ard, K., Lyubovitskij, V.E., Gutsche, Th., Faessler, A., and Cheedket, S. (2003). Electromagnetic nucleon-delta transition in the perturbative chiral quark model. **Physical Review C.** 68: 015205.